PNNL-27023

Pacific Northwest NATIONAL LABORATORY

Proudly Operated by Battelle Since 1965

A New Dose Calculation Methodology for New PNAD and FNAD Designs at PNNL

October 2017

BA Rathbone

U.S. DEPARTMENT OF ENERGY

Prepared for the U.S. Department of Energy under Contract DE-AC05-76RL01830

PACIFIC NORTHWEST NATIONAL LABORATORY
operated by
BATTELLE
for the
UNITED STATES DEPARTMENT OF ENERGY
under Contract DE-AC05-76RL01830

Printed in the United States of America

Available to DOE and DOE contractors from the
Office of Scientific and Technical Information,
P.O. Box 62, Oak Ridge, TN 37831-0062;
ph: (865) 576-8401
fax: (865) 576-5728
email: reports@adonis.osti.gov

Available to the public from the National Technical Information Service
5301 Shawnee Rd., Alexandria, VA 22312
ph: (800) 553-NTIS (6847)
email: orders@ntis.gov <http://www.ntis.gov/about/form.aspx>
Online ordering: http://www.ntis.gov

This document was printed on recycled paper.
(8/2010)

PNNL-27023

A New Dose Calculation Methodology for New PNAD and FNAD Designs at PNNL

BA Rathbone

October 2017

Prepared for
the U.S. Department of Energy
under Contract DE-AC05-76RL01830

Pacific Northwest National Laboratory
Richland, Washington 99352

Abstract

The Pacific Northwest National Laboratory (PNNL) participated in a criticality accident dosimetry intercomparison exercise held at the Nevada National Security Site (NNSS) May 24-27, 2016. The exercise was administered by Lawrence Livermore National Laboratory (LLNL) and utilized the Godiva-IV critical assembly housed in the Device Assembly Facility (DAF) situated on the NNSS site. The exercise allowed participants to test the ability of their nuclear accident dosimeters to meet the performance criteria in ANSI/HPS N13.3-2013, *Dosimetry for Criticality Accidents* and to obtain new measurement data for use in revising dose calculation methods where appropriate. PNNL participated with new prototype Personal Nuclear Accident Dosimeter (PNAD) and Fixed Nuclear Accident Dosimeter (FNAD) designs as well as the existing historical PNAD design. The results indicated that the effective cross sections and/or dose conversion factors used historically for calculation of neutron dose from activation foils in PNADs and FNADs needed to be updated to effectively measure the operational quantities recommended for nuclear accident dosimetry in ANSI/HPS N13.3-2013 and to ensure that performance meets the performance criteria given in the standard. The measurement results obtained during the exercise are used in this report to establish a new dose calculation methodology to be used with PNNL's new PNAD and FNAD designs. The report describes the methods used to derive new cross sections, dose conversion factors and a new dose calculation algorithm. The report also describes the algorithm used to calculate gamma and neutron dose from OSL and OSLN elements in the PNAD and FNADs. The report demonstrates that the new methodology provides accurate dose results that meet the performance criteria in ANSI/HPS N13.3-2013 when applied to the dosimeters exposed during the exercise.

Executive Summary

The Pacific Northwest National Laboratory (PNNL) participated in a criticality accident dosimetry intercomparison exercise held at the Nevada National Security Site (NNSS) May 24-27, 2016. The exercise was administered by Lawrence Livermore National Laboratory (LLNL) and consisted of three exposures performed using the Godiva-IV critical assembly which is part of the Nuclear Criticality Experimental Research Center (NCERC) situated on the NNSS site (Hutchinson et. al. 2012). The exercise allowed participants to test the ability of their nuclear accident dosimeters to meet the performance criteria in ANSI/HPS N13.3-2013, *Dosimetry for Criticality Accidents* and to obtain new measurement data for use in revising dose calculation methods. PNNL participated with new Personal Nuclear Accident Dosimeter (PNAD) and Fixed Nuclear Accident Dosimeter (FNAD) designs. as well as the historical Hanford PNAD design. The new PNNL designs incorporate optically stimulated luminescence (OSL) dosimeters in place of thermoluminescence dosimeters (TLDs), among other design changes, while retaining the same set of activation foils used historically. The dosimeter designs, exercise measurement data, calculated doses and dosimeter performance using historical dose calculation methodology are documented in detail in PNNL 26497 *PNNL Measurement Results for the 2016 Criticality Accident Dosimetry Exercise at the Nevada National Security Site (IER-148)* (Rathbone et. al. 2017). The results indicated that the dose calculation methodology used historically needed to be revised to accurately measure the operational quantities recommended for nuclear accident dosimetry in ANSI/HPS N13.3-2013.

The current report documents the new PNAD and FNAD designs used at PNNL, the new dose calculation methodology developed for use with them, and the performance of the new dosimeter designs in the 2016 criticality accident exercise at NNSS when the new dose calculation methodology is applied to the measurement data obtained in the exercise. The new methodology provides for calculation of neutron dose from OSL/OSLN elements as well as activation foils in the dosimeter. For neutron dose calculated from foil activity, the new methodology provides for calculation of both fluence and dose in each of five energy regions, thus providing a spectral distribution for the calculated fluence and dose. The new energy regions were chosen to be contiguous, covering the neutron energy spectrum from 0.001 eV to 20 MeV without overlap or gaps. Thus the fluence or dose from each region can be summed to obtain the total measured fluence or dose. One of the design objectives was to develop a dose calculation methodology that would be intuitive and provide quantitative information on the spectral distribution of the measured absorbed dose. These features were lacking in the previous methodology.

The basic approach taken in developing the new calculation methodology was to use the foil activity measurements documented in PNNL 26497, in conjunction with the reference values for total delivered fluence and delivered dose provided by LLNL, and the Godiva-IV fluence energy spectrum characterization performed by the United Kingdom’s Atomic Weapons Establishment (AWE) to empirically determine the appropriate restricted energy effective cross section and activity to fluence conversion factor for each energy region. The AWE spectrum data (Wilson et. al, 2014) was folded with the fluence to absorbed dose conversion factors in ANSI/HPS N13.3-2013, to determine the delivered dose in each energy region and the appropriate fluence to absorbed dose conversion factor for each energy region.

For the dosimeters exposed in the Godiva-IV exercise, the new methodology for calculating neutron dose from foil activity provides fluence results and dose results for each of the five energy regions represented and accurate neutron dose results overall. When calculated using the new methodology, the neutron dose result for every dosimeter exposed in air or on phantom in normal AP geometry during the Godiva-IV exercise was within ± 25% of the delivered dose.

The OSL/OSLN response data obtained during the exercise were used to develop corrections for neutron influence on the OSL gamma dose response in PNADs and FNADs. Without correction for the neutron influence, the gamma dose calculated from the OSL element in PNADs exposed on phantom, was on average 2.6 times the actual delivered gamma dose. Similarly, without correction the gamma dose calculated from the OSL element in the outer dosimetry package of FNADs was on average 1.31 times the actual delivered gamma dose. The revised gamma dose calculation methodology now provides gamma dose results for FNADs exposed in air and for PNADs exposed either on phantom ***or*** in air, that are within ± 25% of the delivered gamma dose for 28 of the 33 dosimeters tested.

When the new methodology for calculating neutron dose from foils and the new methodology for calculating gamma dose from OSL elements are used together, the total (gamma + neutron) absorbed dose result for every PNAD exposed in normal AP geometry either in air or on phantom during the exercise meets the ANSI/HPS N13.3-2013 ± 25% accuracy requirement for total gamma+neutron dose.

The OSLN neutron response data for PNADs and FNADs obtained during the exercise were used to calculate Godiva-IV spectrum specific neutron dose calibration factors for use with PNADs and FNADs. For PNADs exposed on phantom in normal AP geometry, use of a single factor provided OSLN albedo neutron dose results within ± 25% of the delivered neutron dose at 2.0 m, 2.5 m, 3.0 m and 4.0 m distances. For FNADs, use of the PNNL default neutron calibration factor based on the FNAD response to ^{252}Cf provided OSLN neutron dose results within ± 25% of the delivered neutron dose at the single 4.0 m distance used for FNAD exposures.

This report demonstrates that the new dose calculation methodology provides satisfactory gamma and neutron dose results for the new PNNL dosimeters tested in the 2016 Godiva-IV exercise.

Acknowledgments

The author would like to thank PNNL Radiation Protection Division Manager, Richard Pierson, for making funding available for this report and implementing improved nuclear accident dosimeter designs at PNNL. In addition, the author would like to thank to Larry Greenwood and Andrey Mozhayev for their modeling calculations and expert advice on a number of technical issues related to gamma spectroscopy and neutron activation. The author would like to acknowledge team members Shannon Morley and John Stephens who assisted with measurements at NNSS during the exercise. Finally, the author would like to thank David Heinrichs and David Hickman at LLNL for organizing and hosting the 2016 intercomparison exercise at NNSS, and ultimately making the measurements used in this report possible.

Acronyms and Abbreviations

ABS	acrylonitrile butadiene styrene
ANSI	American National Standards Institute
AWE	Atomic Weapons Establishment (U.K.)
BOMAB	BOttle MAnnikin Absorber
DAF	device assembly facility
EOB	end of burst
EPD	electronic personal dosimeter
FNAD	fixed nuclear accident dosimeter
FWHM	full width at half maximum
GM	Geiger-Mueller tube
HD	high dose
HPGe	high purity germanium
HPRR	Health Physics Research Reactor
HPS	Health Physics Society
IAEA	International Atomic Energy Agency
ICRP	International Commission on Radiation Protection
LANL	Los Alamos National Laboratory
LCD	liquid crystal display
LD	low dose
LED	light emitting diode
LLNL	Lawrence Livermore National Laboratory
MCA	multi-channel analyzer
mil	one thousandth of an inch
NAD	nuclear accident dosimeter
NCERC	Nuclear Criticality Experimental Research Center
NNSS	Nevada National Security Site
NRC	Nuclear Regulatory Commission (U.S.)
OSL	optically stimulated luminescence
OSLN	optically stimulated luminescence (neutron sensitive)
PMMA	polymethylmethacrylate
PNAD	personal nuclear accident dosimeter
PBSS	passive bonner sphere spectrometer
TLD	thermoluminescence dosimeter

Contents

Appendices

1.0 INTRODUCTION

PNNL participated in an international nuclear accident dosimetry exercise was conducted at the Nevada National Security Site (NNSS) on May 24-27, 2016 using the Godiva-IV critical assembly. The experimental design for the exercise is described in *LLNL-TR-661851, Final Design for an International Intercomparison Exercise for Nuclear Accident Dosimetry at the DAF Using GODIVA-IV (IER-148 CED-2 Report),* (Heinrichs, D. et. al, 2014) . The primary purpose of the exercise was to allow participants to test the ability of their criticality accident dosimetry systems to meet the performance criteria in ANSI/HPS N13.3-2013. The exercise also afforded participants the opportunity to evaluate their measurement methods and collect measurement data for use in revising dose calculation methodology where appropriate. For PNNL, the exercise presented an opportunity to test prototypes of new personal nuclear accident dosimeter (PNAD) and fixed nuclear accident dosimeter (FNAD) designs planned for implementation at PNNL in 2018. The new designs were developed to address a number of issues with the historical dosimeter design and to capitalize on the transition of PNNL from a TLD based external dosimetry program with its associated infrastructure to an OSL based external dosimetry program. Among other things, the new designs incorporate optically stimulated luminescence (OSL) dosimeters in place of thermoluminescence dosimeters (TLDs), activation foils and sulfur pellets with larger mass to increase sensitivity, and sealed sulfur pellet packets with sufficient mass to allow direct beta counting without the need for melting, crushing or handling of dispersible activity.

The measurements made by the PNNL team during the exercise, the doses calculated from the measurement data using default calibration factors and historical dose calculation formulae, and the resulting dosimeter performance with respect to ANSI/HPS N13.3-2013 criteria are documented in detail in *PNNL 26497, Measurement Results for the 2016 Criticality Accident Dosimetry Exercise at the Nevada National Security Site (IER-148)* (Rathbone et. al. 2017). In general, neutron absorbed dose results calculated from foil activity were consistently low while gamma absorbed dose results from OSL dosimeters were consistently high. These results indicated that the effective cross sections and dose conversion factors used historically to calculate dose from foil activity, needed to be revised to accurately measure the operational quantities recommended for nuclear accident dosimetry in ANSI/HPS N13.3-2013. The operational quantities recommended for nuclear accident dosimetry are personal absorbed dose, Dp(10), and ambient absorbed dose, D*(10).

The purpose of the current report is to document the finalized design of the new PNAD and FNAD dosimeters, the new dose calculation methodology and the methods by which the new cross sections and fluence to dose conversion factors used in that methodology were arrived at. This report also documents the performance of the new designs in the 2016 criticality accident exercise at NNSS when the new dose calculation methodology is applied to the measurement data obtained in the exercise with prototypes of the new design. The new methodology provides for calculation of neutron dose from OSL/OSLN elements as well as activation foils in the dosimeter. For neutron dose calculated from foil activity, the new methodology provides for calculation of both fluence and dose in each of five energy regions, thus providing a spectral distribution for the calculated fluence and dose. The new energy regions were chosen to be contiguous, covering the neutron energy spectrum from 0.001 eV to 20 MeV without overlap or gaps. Thus the fluence or dose from each region can be summed to obtain the total measured fluence or dose. The objective was to develop a dose calculation methodology that would be intuitive and provide quantitative information on the spectral distribution of the measured absorbed dose. These features were lacking in the previous methodology.

2.0 MATERIALS AND METHODS

2.1 PNNL PNAD Design

The PNNL PNAD consists of metal foils and sulfur pellets housed inside a Landauer InLight® Model 2 dosimeter clear polycarbonate shell together with an InLight® Model 2 OSLN dosimeter case ("BA" type case) and slide ("N" type slide). The six sulfur pellets are sealed in a polyethylene bag for direct beta counting on a standard 50 mm planchet with commonly available beta counting equipment. The InLight® OSLN dosimeter is read on a Landauer microStar® reader specially modified with a neutral density filter for readout of accident level dosimeters. The InLight® OSLN dosimeters may also be read on an unmodified microStar® reader without neutral density filter if the dose is sufficiently low. Both readers must be set up and specifically calibrated for nuclear accident dosimeter readout. The InLight® OSLN dosimeter provides the primary gamma dose to be used for the PNAD and an albedo neutron dose value that can be used as an initial estimate of neutron dose. The albedo neutron dose response is highly energy dependent and not suitable for final reporting of neutron dose. Photos of the front and back side of an assembled PNNL PNAD are shown in **Figure 1** and **Figure 2**. **Appendix A** contains detailed design information for the PNNL PNAD. Components of a disassembled PNNL PNAD are shown in **Figure A.1** and an exploded view of the dosimeter is shown in **Figure A.2**. Component dimensions and composition are given in **Table A.1**. A simplified listing of the detector dimensions for the PNNL PNAD is provided below in **Table 1**.

Figure 1. PNNL PNAD front side

Figure 2. PNNL PNAD back side

Table 1. PNNL PNAD Detector Dimensions and Composition

PNNL PNAD Activation Detectors				
detector name	A	B	C	D
detector description	sulfur pellet (sixpack)	10 mil copper foil (Cd covers)	10 mil indium foil (Cd covers)	10 mil indium foil (bare)
detector composition	S	Cu	In	In
detector thickness (mm)	1.91	0.254	0.254	0.254
detector mass (g)	2.61	0.281	0.236	0.236
detector density thickness (g/cm^2)	0.343	0.228	0.186	0.186
detector diameter (cm)	n/a	1.27	1.27	1.27
detector L (cm) x W (cm)	3.81 x 2.54	n/a	n/a	n/a
filter composition	none	Cd	Cd	none
filter thickness (mm)	none	0.533	0.533	none

2.2 PNNL FNAD Design

The PNNL FNAD design is based on the Hanford FNAD which has been used since the 1960s at both Hanford and PNNL. The historical Hanford FNAD is described in Hanford historical documents (Bramson 1963, Glen and Bramson 1977). The most recent iteration of that design, currently in use at PNNL as of this writing, is documented in the PNNL Nuclear Accident Dosimetry Technical Basis Manual, Rev 0.1, April 2017. The PNNL FNAD design uses the same types of neutron activation detectors, and activation reactions for neutron dose assessment as the Hanford FNAD. The new design differs from the old design primarily in the replacement of TLDs with OSL dosimeters. Landauer OSL and OSLN nanoDots have replaced the TLD 700 and TLD 600 chips respectively, and are read on the same modified Landauer microStar® reader used for reading the InLight® dosimeters in the PNNL PNADs. The new design also differs in the dimensions of foils used, in the packaging used, and in the arrangement of foils within the packaging (metal foils are no longer stacked on top of each other). The PNNL FNAD inner and outer dosimetry packages have been re-designed for easier loading and unloading. The PNNL FNAD is described in greater detail in **Appendix B**. An exploded view of the dosimeter is shown in **Figures B.1** through **B.5**. Component dimensions and composition are given in **Table B.1**. **Figure 3** shows an assembled FNAD.

Figure 3 PNNL FNAD

2.3 Dosimeter Irradiations

The source used for the intercomparison exercise was the Godiva-IV critical assembly. The assembly consists of enriched U-235 concentric metal cylinders. The exercise consisted of three bursts from the unmoderated Godiva-IV critical assembly, each being administered on a separate day with a new set of dosimeters being exposed each day. The reactor was operated in the pulse mode and the burst intensity was varied on each day to achieve the desired range of doses at dosimeter locations in the DAF. Each pulse consisted of a super-prompt-critical excursion lasting approximately 50 microseconds (pulse FWHM $\approx$ 25 microseconds). The exact dimensions of the room in which the reactor is housed and the irradiations took place were not provided to participants. However, it was revealed that the room is heavily shielded with concrete walls, floor and ceiling. Dosimeters were irradiated either in air or on phantom. To simulate irradiations in air, PNADs were mounted on thin aluminum plates suspended on portable racks called "trees", or in the case of the FNADs, placed on low mass stands. The phantoms used were saline filled Bottle Manikin Absorption (BOMAB) phantoms and 30 x 30 x 15 cm polymethyl methacrylate (PMMA) slab phantoms. PNADs were mounted on the front and back of the phantoms. For the third pulse, one BOMAB was placed in a lateral orientation with respect to the source with PNADS mounted on the front and back of the phantom to provide lateral irradiation geometry. For each pulse, the phantoms, dosimeter trees, and FNAD stands were placed at designated locations numbered 1 through 12, having distances of either 2 meters, 2.5 meters, 3 meters, 4 meters or 9 meters. The single location at 9 meters (location 10) was described as an "alcove" location. Maps of the locations and types of phantoms/trees at each location for each pulse are shown in **Appendix C**, **Figures C.1-C.3**. The identities of the individual dosimeters placed on each phantom or tree are also documented in **Appendix C**, in **Table C.1**. The BOMAB phantoms complied with the standard dimensions and fill volumes documented ANSI/HPS N13.35-2009 (HPS 2009) for a phantom representing a contemporary adult male. The cylinders in each phantom were filled with Ringer's lactate solution.

2.4 Delivered Fluence and Dose

Prior to the exercise, each designated test location (except for the alcove location, no. 10) had been characterized for neutron fluence as a function of ΔT in the Godiva-IV core, neutron energy spectrum, and the operational quantities including personal absorbed dose from neutrons, $D_p(10)_n$ and ambient absorbed dose from neutrons, $D^*(10)_n$ which are recommended operational quantities to use for calibration of PNADs and FNADs respectively. Gamma doses at each location except the alcove location had also been characterized. Preliminary reference fluence and dose information provided by LLNL (Hickman, 2017) is shown in **Appendix D**, **Tables D.1.1-D.3.3**. The reference data for location 10 was not used in this report because the position distance and delivered dose data were not finalized as of this writing and dosimeter response data for this location were significant outliers.

2.5 Delivered Neutron Energy Spectrum

Prior to the exercise, each designated test location (except for the alcove location, no. 10) had been characterized for neutron energy spectrum by the Atomic Weapons Establishment (AWE) of the United Kingdom (U.K.). Characterization was accomplished in two phases. In the first phase, the Godiva-IV critical assembly was operated in a subcritical mode at steady state with a ^{252}Cf source providing neutrons multiplied by the assembly. During this phase, a series of active Bonner sphere spectrometer and RoSpec measurements were made. In the second phase, "passive" spectrometry techniques involving materials sensitive to neutron activation were used to measure the leakage spectrum from a super-prompt-critical excursion of the Godiva reactor. A passive Bonner sphere spectrometer (PBSS) system using gold foils as detectors was used in conjunction with NADs to characterize the neutron energy spectrum at each test location. Spectral data (fluence per unit lethargy) at each test location are given in Annex F of the AWE phase 2 characterization report (Wilson et. al. 2014). These data are used in the present report to establish activity to fluence conversion factors and fluence to dose conversion factors for the energy regions relevant to the neutron activation reactions used in the PNNL PNAD and FNAD detectors. The AWE data (given in fluence per unit lethargy) have been converted to fluence and listed in **Appendix E** of this report for convenience. The original AWE fluence per unit lethargy data were normalized to the fluence resulting from a burst producing a 70°C temperature rise in the Godiva-IV core, and the data in **Appendix E** retain that normalization. Two noteworthy conclusions from the Godiva-IV phase 2 characterization report by AWE are: 1) The neutron energy spectrum did not vary significantly as a function of radial distance from the core. 2) The neutron energy spectrum varied significantly as a function of height above the floor. To the extent practicable, PNNL dosimeters were placed at a uniform height across locations, matching as closely as possible the height of the Godiva-IV core and the PBSS spheres during phase 2 measurements.

2.6 Foil Activity Measurements

The activation reactions and product radionuclides utilized for the purpose of determining dose in PNNL PNADs and FNADS are summarized in **Table 2**. Participants in the IER-148 International Intercomparison Exercise for Nuclear Accident Dosimetry at the DAF Using Godiva-IV were required to bring their own counting equipment for analyzing the foils in their nuclear accident dosimeters. For PNNL, this meant bringing gamma counting equipment, beta counting equipment, and associated shielding. The equipment used, how it was calibrated, the analytical methods used to measure the activity, and the measurement results are documented in detail in **PNNL 26497** (Rathbone et. al. 2017). The mean measured activity per unit delivered fluence for each combination of exposure distance and exposure geometry are also provided in the current report in **Appendix F**, **Table F.1** and **Table F.2**.

Table 2. Activation Reactions Used in FNADs and PNADs

Energy range	Reaction	Effective Threshold or resonance energy (approx.) [1]	Filter	Product half-life	Principal radiations for assay (MeV)	Other principle radiations (MeV)
Thermal	$^{197}Au(n,\gamma)^{198}Au$	-	-	2.696 d	$\gamma(0.412)$	β^- (0.961)
	$^{115}In(n,\gamma)^{116m}In$	-	-	54.2 m	$\gamma(0.417)$ $\gamma(1.097)$ $\gamma(1.294)$	β^- (0.189 avg) β^- (0.294 avg) β^- (0.351 avg)
Intermediate	$^{63}Cu(n,\gamma)^{64}Cu$	580 eV	Cd	12.701 h	$\gamma(0.511)$ [2]	β^- (0.578)
Fast	$^{32}S(n,p)^{32}P$	3.16 MeV	-	14.29 d	β^- (1.711)	-
	$^{115}In(n,n')^{115m}In$	1.25 MeV	-	4.486 h	$\gamma(0.336)$	ce (0.308) [3]

1. from Delafield, 1988. (Resonance energy for intermediate range. Threshold energy for fast range)
2. annihilation photon
3. conversion electron

2.7 Energy Regions for Fluence and Dose Calculation

For each reaction shown in **Table 2,** the foil combinations used and the neutron energy regions predominantly contributing to activity, are shown in **Table 3**.

Table 3. Neutron Energy Regions Contributing to Activity in Foils

Energy Region	Reaction	Foil Combination
< 0.464 eV	$^{197}Au(n,\gamma)^{198}Au$	Au(bare) - Au(Cd)
< 0.464 eV	$^{115}In(n,\gamma)^{116m}In$	In(bare) - In(Cd)
0.464 eV – 0.1 MeV	$^{63}Cu(n,\gamma)^{64}Cu$	Cu(Cd)
> 1.25 MeV	$^{115}In(n,n')^{115m}In$	In(Cd) or In(bare)
> 3.16 MeV	$^{32}S(n,p)^{32}P$	S (pellet)

Because of a practical limit to the number of detectors and reactions that can be used for fluence and dose measurement in PNADs, the number of energy bins available for fluence and dose calculation is also limited and thus the quality of energy spectrum information obtainable is inherently limited. A simplified energy bin scheme involving five energy regions was chosen for use in the current analysis for the new PNAD and FNAD designs. The bin boundaries were chosen based on the following considerations:

1) the location of resonances or thresholds in cross section plots,
2) the location of the region of constant lethargy and the fission peak in neutron energy spectra,
3) the shape of the fluence to dose conversion factor curve ,
4) the energy regions used with NAD foils at other DOE facilities,
5) the desire to align bin boundaries with the bin structure of ANSI/HPS N13.3,
6) the advantages of a straightforward and intuitive dose calculation methodology

The simplified energy bin scheme is shown in **Table 4.**

2.8 Re-binning of AWE Energy Spectrum Data

To allow the fluence to absorbed dose conversion factors from ANSI/HPS N13.3 to be folded with the AWE energy spectrum data it was necessary to re-bin the AWE data to match the energy bin scheme used in Table B.1 of that standard. A spectrum average for each irradiation distance used in the exercise (2.0 m, 2.5 m, 3.0 m and 4.0 m) was calculated in the original AWE 66 energy bin structure. Then each average spectrum was re-binned in the 53 bin structure matching ANSI/HPS N13.3. The re-binned fluence data for each distance are given in tabular form in **Appendix G, Table G.1**. The color shading indicates the energy regions chosen for fluence and dose calculation with PNAD and FNAD foils. The normalized fluence falling within each energy region was calculated for each irradiation distance and is shown in **Table 4** below. The values were calculated by summing fluence from the 53 bin normalized fluence data across the bins representing the energy region of interest. The values represent the fraction of total fluence falling within the designated energy region.

Table 4. Normalized Fluence Within Selected Energy Regions

Distance (m)	Normalized Bin Fluence Φ_{bin} / Φ_{tot}					
	0.001 eV - 0.464 eV	0.464 eV - 100 keV	100 keV - 1.25 MeV	1.25 MeV - 20 MeV	1.25 MeV - 3.16 MeV	3.16 MeV - 20 MeV
2.0 m	0.11	0.28	0.38	0.23	0.18	0.04
2.5 m	0.12	0.34	0.37	0.17	0.14	0.03
3.0 m	0.13	0.33	0.36	0.18	0.15	0.03
4.0 m	0.14	0.37	0.34	0.15	0.13	0.03

The average energy spectrum at each distance from Godiva-IV, are plotted as fluence per unit lethargy in **Figures 4** through **7**. The normalized fluence is plotted in both 5 bin and 53 bin formats.

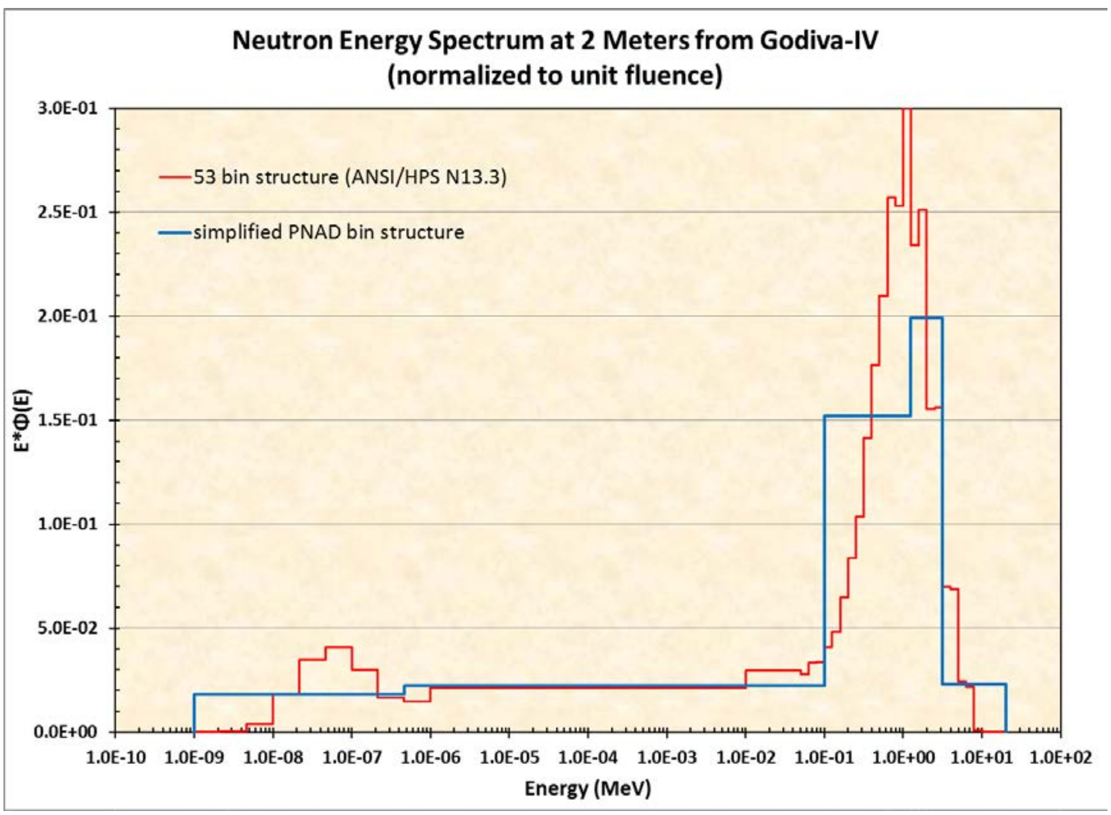

Figure 4. Neutron energy spectrum at 2.0 m from Godiva-IV

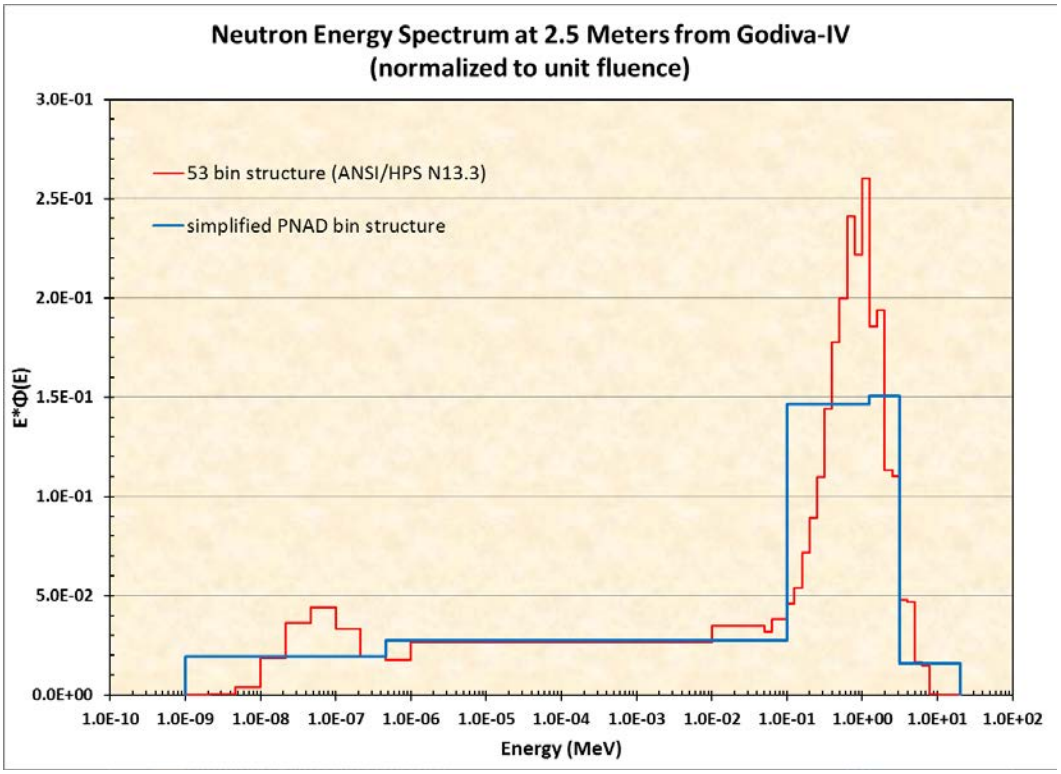

Figure 5. Neutron energy spectrum at 2.5 m from Godiva-IV

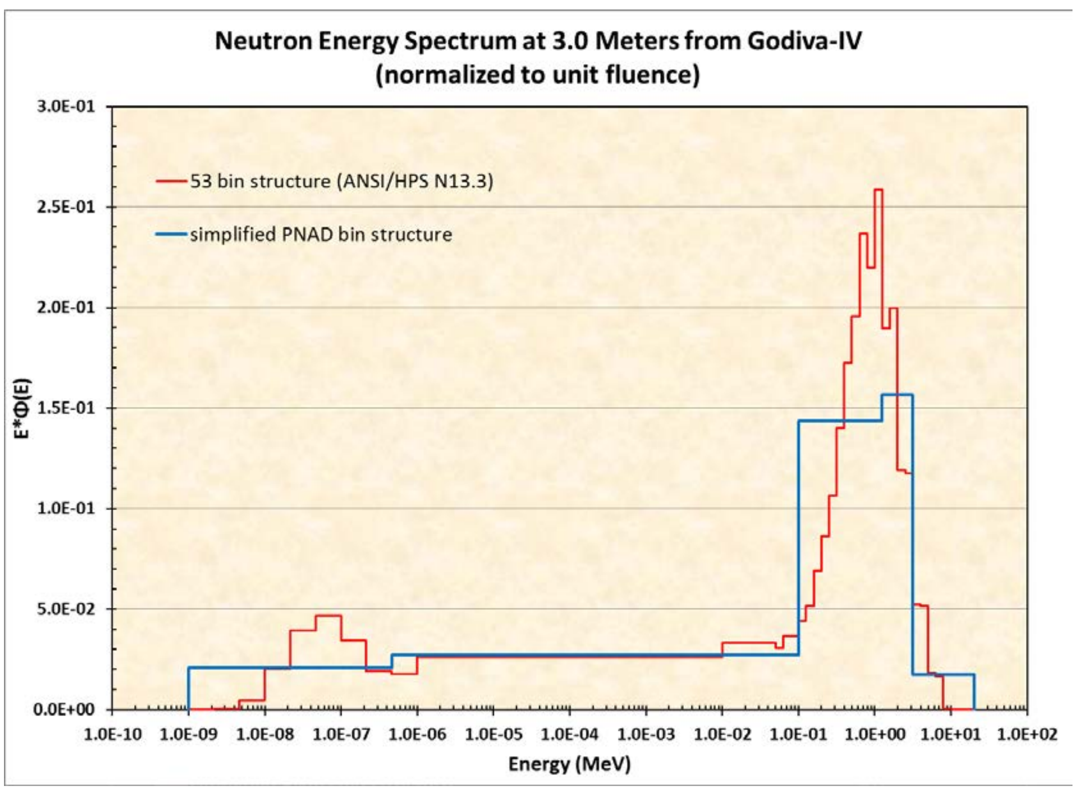

Figure 6. Neutron energy spectrum at 3.0 m from Godiva-IV

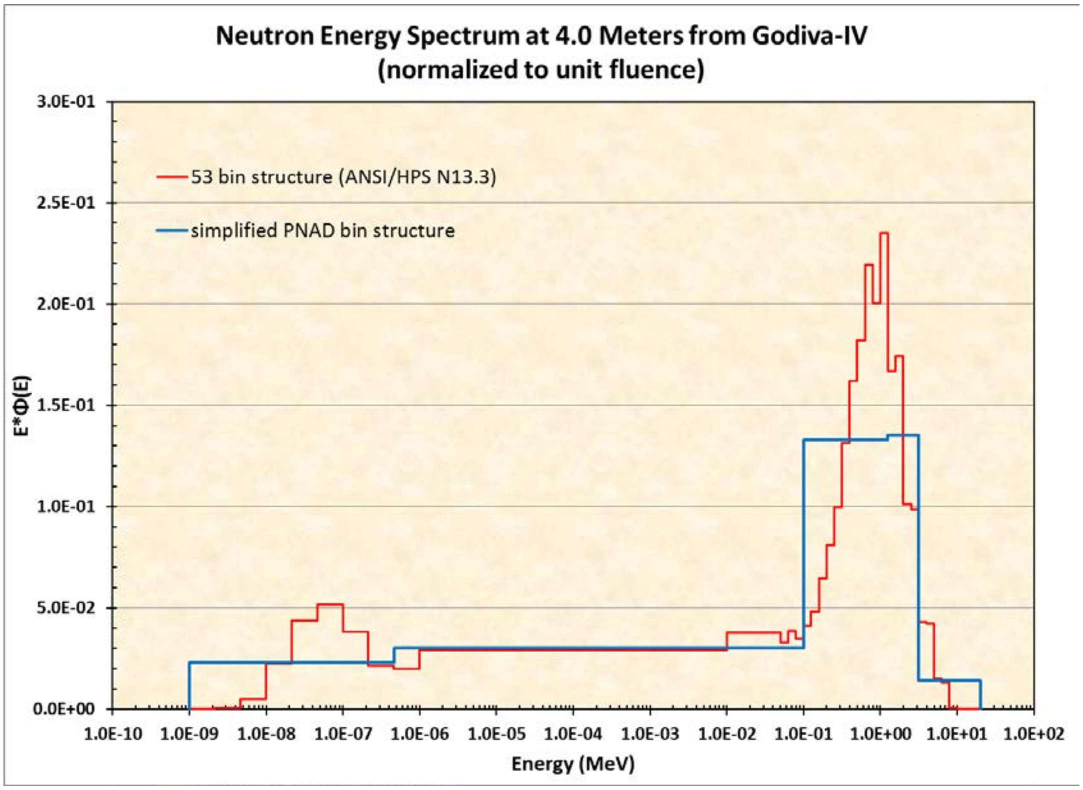

Figure 7. Neutron energy spectrum at 4.0 m from Godiva-IV

2.9 Determining Activity-to-Fluence Conversion Factors

Fluence within a given region can be directly measured from foil activity if an activity to fluence conversion factor, C_x, has been determined for the reaction based on the restricted fluence falling only within that energy region. For dosimeters exposed by Godiva-IV, the fluence falling within each energy region is known from the normalized neutron energy spectrum data in **Appendix G** and **Table 3**, combined with the reference values for total delivered fluence in **Appendix D**. The reaction product activity per unit delivered fluence is known from the activity measurement data in **Appendix F.** Therefore, it is possible to empirically determine a C_x for each reaction and associated energy region using this data. The C_x thus determined will be somewhat dependent on the energy spectrum used.

The average data for measured activity per unit delivered fluence for dosimeters exposed in normal geometry are summarized in **Appendix F** in **Table F.3** The averages shown in the table do not include dosimeters with 5 mil thick foils, or dosimeters exposed on the back or side of a phantom. The activity data for ^{32}P, ^{64}Cu, ^{115m}In, and ^{116m}In are from PNAD measurements. The activity data for ^{198}Au is from FNAD measurements. The net activity for bare -Cd covered foil pairs is also shown.

The average measured activity per unit delivered fluence *within in each relevant energy bin* was calculated as follows:

$$A_o / \Phi_{bin} = (A_o / \Phi_{tot}) / (\Phi_{bin} / \Phi_{tot}) \qquad \text{Eq. 1}$$

where:

A_o	=	measured specific activity decay corrected to end of burst
Φ_{tot}	=	reference value for total delivered fluence
Φ_{bin} / Φ_{tot}	=	fraction of total fluence in region of interest (from **Table 4**)

These results are shown in **Table 5**. The indium and sulfur data for the 2.5 meter distance in air were rejected as outliers and not used. The reciprocal of each value in **Table 5** was used as a direct measure of the activity to fluence conversion factor, C_x, for each distance and exposure geometry. The measured C_x values are shown in **Table 6**.

Albedo neutrons produced by a phantom heavily influence the measured foil activity for thermal and epithermal reactions. The reference values for delivered fluence at each location and the measured energy spectra at each location were measured without a phantom present. As such, the ^{198}Au, ^{116m}In and ^{64}Cu activities from foils exposed on phantom were not included in the calculated average C_x factors for the associated reactions. The albedo neutrons have less effect on the fast reactions so the ^{115m}In and ^{32}P activities from foils exposed on phantom *were* included in the calculated average C_x factors. These choices were made with the understanding that as a result, PNADs mounted on phantom or body will tend to overestimate the incident thermal and epithermal neutron fluence while PNADs exposed in air will tend to provide unbiased estimates of thermal and epithermal fluence. The effect on dose accuracy is considerably less because the fluence to dose conversion factors for neutron energies less 100 keV are considerably smaller than for neutron energies greater than 100 keV.

Table 5. Average Activity per Unit Delivered Bin Fluence

Irradiaton Geometry	Irradiation Distance	Average Specific Activity Per Bin Fluence A_o / Φ_{bin} (cm^2 g^{-1} min^{-1})				
		0.001 eV - 0.464 eV	0.001 eV - 0.464 eV	0.464 eV - 100 keV	1.25 MeV - 20 MeV	3.16 MeV - 20 MeV
		Au (bare) - Au (Cd)	In (bare) - In (Cd)	Cu (Cd)	In (Cd)	S
		Au-198	I-116m	Cu-64	I-115m	P-32
on phantom	2.0 m		2.02E-02	2.65E-06	4.82E-06	3.39E-07
	2.5 m					
	3.0 m		1.84E-02	2.10E-06	4.13E-06	3.11E-07
	4.0 m		1.85E-02	2.02E-06	4.56E-06	3.49E-07
in air	2.0 m		6.00E-03	1.70E-06	4.58E-06	3.21E-07
	2.5 m		7.13E-03	1.65E-06	5.07E-06	3.83E-07
	3.0 m					
	4.0 m	5.46E-05	8.42E-03	1.76E-06	4.25E-06	2.99E-07

Table 6. Measured Values for Activity to Fluence Conversion Factors, C_x

Irradiaton Geometry	Irradiation Distance	Average Activity to Fluence Conversion Factors, C_x $C_x = \Phi_{bin} / A_o$ (min g cm^{-2})				
		0.001 eV - 0.464 eV	0.001 eV - 0.464 eV	0.464 eV - 100 keV	1.25 MeV - 20 MeV	3.16 MeV - 20 MeV
		Au (bare) - Au (Cd)	In (bare) - In (Cd)	Cu (Cd)	In (Cd)	S
		Au-198	I-116m	Cu-64	I-115m	P-32
on phantom	2.0 m				2.08E+05	2.95E+06
	2.5 m					
	3.0 m				2.42E+05	3.22E+06
	4.0 m				2.19E+05	2.87E+06
in air	2.0 m		1.67E+02	5.89E+05	2.18E+05	3.11E+06
	2.5 m		1.40E+02	6.08E+05		
	3.0 m					
	4.0 m	1.83E+04	1.19E+02	5.69E+05	2.35E+05	3.35E+06
	avg	1.83E+04	1.42E+02	5.88E+05	2.25E+05	3.10E+06

2.10 Determining Effective Cross Sections

The effective cross section, σ_{eff} for each reaction was determined using data for measured specific activity per bin fluence, A_o / Φ_{bin} , from **Table 5**. As with the calculation of C_x factors, the ^{115m}In and ^{32}P data for 2.5 m exposures in air were not used. The effective cross section was calculated using the following relationship:

$$\sigma_{eff} = A_o / (\lambda n \Phi_{bin}) \qquad \text{Eq. 2}$$

where:

λ	=	product radionuclide decay constant (min^{-1})
n	=	number of target atoms per gram in the foil
Φ_{bin}	=	fluence within restricted energy region (cm^{-2})
A_o	=	initial activity as dpm *per gram* (min^{-1} g^{-1})

The number of target atoms per gram of foil, n, was calculated using the following equation:

$$n = [\text{A.N.} / \text{A.W.}] \cdot \chi \cdot P \qquad \text{Eq. 3}$$

where:

A.N.	=	Avogadro's number = 6.0221409 x 10^{23} (atoms/mole)
χ	=	abundance of target isotope in target element (target atoms / element atoms)

P	=	elemental abundance in activation foil or sample (purity)
A.W.	=	atomic weight for target *element* (grams/mole)

Table 7. Measured Values for Effective Cross Sections

Irradiation Geometry	Irradiation Distance	Energy Restricted Effective Cross Section, σ_{eff} (barns) $\sigma_{eff} = A_o / (\lambda n \Phi_{bin})$				
		0.001 eV - 0.464 eV	0.001 eV - 0.464 eV	0.464 eV - 100 keV	1.25 MeV - 20 MeV	3.16 MeV - 20 MeV
		Au (bare) - Au (Cd)	In (bare) - In (Cd)	Cu (Cd)	In (Cd)	S
		Au-198	I-116m	Cu-64	I-115m	P-32
on phantom	2.0 m				0.373	0.565
	2.5 m					
	3.0 m				0.319	0.517
	4.0 m				0.352	0.581
in air	2.0 m		93.5	0.285	0.354	0.535
	2.5 m		111	0.276	0.392	0.638
	3.0 m					
	4.0 m	100	131	0.295	0.329	0.498
	avg.	100	112	0.285	0.346	0.539

The physical data used to calculate *n* are given in **Appendix H**. Foil purities were all 99.9% or better so a value of 1.0 was assumed for P in the calculations. The empirically derived values for effective cross section, σ_{eff} , are shown in **Table 7**. These effective cross sections may be thought of as energy restricted effective cross sections, and are somewhat dependent on the energy spectrum used. It should be noted that the cross sections shown for the ^{198}Au, ^{116m}In and ^{64}Cu reactions in the above table are apparent cross sections for the foil thickness used. No correction was made for neutron attenuation by absorption within the foils which can be significant for gold, indium, and copper foils (IAEA 1982). The cross sections for infinitely dilute foils would be larger.

2.11 Determining a Method for Estimating Fluence between 100 keV and 1.25 MeV

As can be seen from the data in **Table 4**, between 34% and 38% of the delivered fluence at Godiva-IV dosimeter irradiation locations falls between 100 keV and 1.2 MeV. Unfortunately, none of the reactions in the PNAD and FNAD foils that have a significant cross section for neutrons in this energy range. Therefore, the fluence in this region must be inferred from the fluence measured in adjacent regions and a knowledge of typical energy spectrum shape. Through an iterative process of successive approximation, it was found that by using a weighted combination of the copper measured fluence in the 0.464 eV – 100 keV region and the indium measured fluence in the 1.25 MeV –20 MeV region, satisfactory estimates of the known fluence in the 100 keV – 1.25 MeV region could be obtained for dosimeters exposed both in air and on phantom. The measured fluences were determined, using the activity measurements from the Godiva-IV irradiations and the empirically established C_x in **Table 6.** Fluence in the 100 keV – 1.25 MeV region can be satisfactorily estimated using the following relationship:

$$\Phi_a = W_{Cu}\,\Phi_{Cu} + W_{In}\,\Phi_{In} \qquad \text{Eq. 4}$$

where:

W_{Cu} = weighting factor for copper measured fluence = 0.48
Φ_{Cu} = fluence in 0.464 eV – 100 keV region measured with copper foil
W_{In} = weighting factor for indium measured fluence = 1.12
Φ_{In} = fluence in 1.25 MeV –20 MeV region measured with indium foil

2.12 Determining Fluence-to-Dose Conversion Factors for Energy Regions

Although fluence-to-dose conversion factors exist for a 53 bin structure, the PNAD and FNAD measure fluence in a simplified 5 bin structure. Therefore it was necessary to calculate a fluence-to-dose conversion factor to be used with each of those 5 bins. To accomplish this, the 53 bin normalized fluence data for each dosimeter irradiation distance were folded with the 53 bin dose conversion factor data from ANSI/HPS N13.3. The dose in groups of bins corresponding to each of the 5 larger energy bins used by PNADs and FNADs was summed and divided by the summed fluence delivered to the same bins. The results are shown in **Table 8**.

Table 8. Fluence to Dose Conversion Factors for NAD Energy Bins

Irradiation Geometry	Irradiation Distance	Fluence to Dose Conversion Factors [delivered dose per bin fluence] D_{bin} / Φ_{bin} (cGy - cm^2)				
		0.001 eV - 0.464 eV	0.464 eV - 100 keV	100 keV - 1.25 MeV	1.25 MeV - 3.16 MeV	3.16 MeV - 20 MeV
		$D_p(10)_{n,bin} / \Phi_{bin}$ (cGy - cm^2)				
on phantom	2.0 m	2.98E-10	3.83E-10	2.13E-09	3.62E-09	5.27E-09
	2.5 m	3.00E-10	3.81E-10	2.08E-09	3.61E-09	5.27E-09
	3.0 m	2.99E-10	3.81E-10	2.09E-09	3.62E-09	5.27E-09
	4.0 m	2.99E-10	3.79E-10	2.08E-09	3.61E-09	5.27E-09
	avg * 1.1	3.29E-10	4.19E-10	2.31E-09	3.98E-09	5.79E-09
		$D^*(10)_{n,bin} / \Phi_{bin}$ (cGy - cm^2)				
in air	2.0 m	2.84E-10	3.20E-10	2.04E-09	3.57E-09	5.12E-09
	2.5 m	2.84E-10	3.17E-10	1.99E-09	3.56E-09	5.12E-09
	3.0 m	2.84E-10	3.17E-10	2.00E-09	3.56E-09	5.12E-09
	4.0 m	2.84E-10	3.15E-10	1.99E-09	3.56E-09	5.12E-09
	avg * 1.1	3.12E-10	3.49E-10	2.21E-09	3.92E-09	5.63E-09

In **Table 8**, the average of each column has been multiplied by a factor 1.1. This was done to better align the dose results obtained for PNADs and FNADs exposed during the exercise, with the reference doses given in **Appendix D**. The reasons for this are not clear, but may include use of different (i.e. updated) energy spectrum data and/or dose conversion factors to calculate the reference doses.

At each irradiation distance, the fraction of the total dose falling in each energy region was also calculated. The results are shown in **Table 9**.

Table 9. Fraction of Total Dose by Energy Region

Irradiation Geometry	Irradiation Distance	Delivered Dose Distribution D_{bin} / D_{tot}					
		0.001 eV - 0.464 eV	0.464 eV - 100 keV	100 keV - 1.25 MeV	1.25 MeV - 20 MeV	1.25 MeV - 3.16 MeV	3.16 MeV - 20 MeV
		$D_p(10)_n$					
on phantom	2.0 m	0.02	0.06	0.44	0.48	0.36	0.12
	2.5 m	0.02	0.08	0.48	0.41	0.32	0.10
	3.0 m	0.02	0.08	0.47	0.43	0.32	0.10
	4.0 m	0.03	0.10	0.47	0.40	0.31	0.09
		$D^*(10)_n$					
in air	2.0 m	0.02	0.05	0.44	0.49	0.37	0.12
	2.5 m	0.02	0.07	0.48	0.42	0.33	0.10
	3.0 m	0.02	0.07	0.47	0.44	0.33	0.11
	4.0 m	0.03	0.08	0.48	0.41	0.32	0.10

2.13 Methodology for Calculating PNAD and FNAD Neutron Dose from Foil Activity

The activity-to-fluence conversion factors and fluence to dose conversion factors established for use with PNADs and FNADs in the preceding sections are summarized in **Table 10**.

Table 10. Conversion Factors for use with PNADs and FNADs

Energy Bin	Fluence Symbol	Foil Combination	Reaction	Activity to Fluence Conversion Factor, C_x $C_x = \Phi_{bin} / A_o$ (min g cm^{-2})		Fluence to Dose Conversion Factor [delivered dose per bin fluence] D_{bin} / Φ_{bin} (cGy - cm^2)			
						$D_p(10)_n / \Phi_{bin}$ (cGy - cm^2)		$D^*(10)_n / \Phi_{bin}$ (cGy - cm^2)	
				symbol	value	symbol	value	symbol	value
0.001 eV - 0.464 eV	$\Phi_{th\text{-}Au}$	Au(bare) - Au(Cd)	$^{197}Au(n,\gamma)^{198}Au$	$C_{th\text{-}Au}$	1.83E+04	K_{th}	3.29E-10	L_{th}	3.12E-10
0.001 eV - 0.464 eV	$\Phi_{th\text{-}In}$	In(bare) - In(Cd)	$^{115}In(n,\gamma)^{116m}In$	$C_{th\text{-}In}$	1.42E+02	K_{th}	3.29E-10	L_{th}	3.12E-10
0.464 eV - 100 keV	Φ_{Cu}	Cu(Cd)	$^{63}Cu(n,\gamma)^{64}Cu$	C_{Cu}	5.88E+05	K_{Cu}	4.19E-10	L_{Cu}	3.49E-10
1.25 MeV - 20 MeV	Φ_{In}	In(Cd) or In(bare)	$^{115}In(n,n')^{115m}In$	C_{In}	2.25E+05				
3.16 MeV - 20 MeV	Φ_S	S (pellet)	$^{32}S(n,p)^{32}P$	C_S	3.10E+06	K_S	5.79E-09	L_S	5.63E-09
100 keV - 1.25 MeV	Φ_a					K_a	2.31E-09	L_a	2.21E-09
1.25 MeV - 3.16 MeV	Φ_b					K_b	3.98E-09	L_b	3.92E-09

2.13.1 Calculating Neutron Fluence from Foils

The neutron fluences are calculated from the decay corrected activities, A_o, (dpm/g) of the foils using the activity to fluence conversion factors, C_x, given in **Table 10**. The measured activity, A_o must be expressed as specific activity (i.e. dpm/g) and decay corrected to the end of the burst. If multiple excursions are involved, then activity should be decay corrected to the end of the last excursion.

Using the foil activity at time zero, $\mathbf{A_0}$ (dpm/g), and the activity to fluence conversion factor $\mathbf{C_x}$, from **Table 10**, a fluence, Φ, for each of the first five energy regions in **Table 10** is calculated using the following general relationship.

$$\Phi = C_x A_o \qquad \text{Eq. 5}$$

where:

Φ = fluence (cm^{-2})
C_x = activity-to-fluence conversion factor (min g cm^{-2})
A_o = initial activity as dpm *per gram* (min^{-1} g^{-1})

The steps and specific equations used for calculating fluence (cm^{-2}) for each region are described below. Calculations are performed in logical sequence . The equations involving gold foil activities are used only for the FNAD.

<u>0.001 eV to 0.464 eV (thermal region)</u>

<u>For FNADs</u>, the difference between the ^{198}Au activity in the bare gold foil (**E**), and the ^{198}Au activity in the cadmium covered gold foil (**F**) is used to calculate the neutron fluence as follows:

$$\Phi_{th} = C_{th\text{-}Au} \; [\, A_o \text{ (bare gold)} \; - \; A_o \text{ (cadmium covered gold)} \,] \qquad \text{Eq. 6}$$

<u>For PNADs</u>, the difference between the ^{116m}In activity in the bare indium foil (**D**) and the ^{116m}In activity in the cadmium covered indium foil (**C**) is used to calculate the neutron fluence as follows:

$$\Phi_{th} = C_{th\text{-}In} \; [\, A_o \text{ (bare indium)} \; - \; A_o \text{ (cadmium covered indium)} \,] \qquad \text{Eq. 7}$$

<u>For FNADs</u>, **equation 7** can also be used to calculate the neutron fluence. **Equations 6** and **7** provide two independent measurements of the fluence in this energy region, one (the indium) being more sensitive but decaying away much more rapidly.

<u>0.464 eV to 100 keV (epithermal region of constant lethargy)</u>

Fluence for this energy region can be calculated from the ^{64}Cu in the cadmium covered copper foil (**B)**, as follows:

$$\Phi_{Cu} = C_{Cu} \; A_o \text{ (cadmium covered copper).} \qquad \text{Eq. 8}$$

<u>1.25 MeV to 20 MeV</u>

Fluence for this energy region can be calculated from the ^{115m}In activity in the cadmium covered indium foil (**C**) as follows:

$$\Phi_{In} = C_{In} \; A_o \text{ (cadmium covered indium).} \qquad \text{Eq. 9}$$

<u>3.16 MeV to 20 MeV</u>

The fluence in this energy region can be calculated from the ^{32}P activity in the sulfur pellet pack (**A**) as follows:

$$\Phi_S = C_S \; A_o \text{ (sulfur pellet pack } \mathbf{A}\text{).} \qquad \text{Eq. 10}$$

<u>100 keV to 1.25 MeV</u>

Calculation of the fluence in this energy region is based on the above calculated results for Φ_{Cu} and Φ_{In}. Fluence for this energy region is calculated as follows:

$$\Phi_a = 0.48 * \Phi_{Cu} + 1.12 * \Phi_{In} \qquad \text{Eq. 11}$$

1.25 MeV to 3.16 MeV

Calculation of the fluence in this energy region is based on the previously calculated results for Φ_{In} and Φ_S. Fluence for this energy region is calculated as follows:

$$\Phi_b = \Phi_{In} - \Phi_S \qquad \text{Eq. 12}$$

2.13.2 Calculating Neutron Dose from Foils

For PNADs, the personal absorbed dose from neutrons, $D_p(10)_n$, is calculated from energy bin fluence as follows:

$$D_p(10)_n = \Phi_{th\text{-}In} K_{th} + \Phi_{Cu} K_{Cu} + \Phi_a K_a + \Phi_b K_b + \Phi_S K_S \qquad \text{Eq. 13}$$

where $\Phi_{th\text{-}In}$, Φ_{Cu}, Φ_a, Φ_b and Φ_S are the values of neutron fluence within designated energy bins in **Table 10**, and K_{th}, K_{Cu}, K_a, K_b and K_S are the corresponding fluence-to-dose conversion factors listed in **Table 10**. The calculated value for $D_p(10)_n$ has units of cGy.

For FNADs, the ambient absorbed dose from neutrons, $D^*(10)_n$, is calculated from energy bin fluence as follows:

$$D^*(10)_n = \Phi_{th\text{-}Au} L_{th} + \Phi_{Cu} L_{Cu} + \Phi_a L_a + \Phi_b L_b + \Phi_S L_S \qquad \text{Eq. 14}$$

where $\Phi_{th\text{-}Au}$, Φ_{Cu}, Φ_a, Φ_b and Φ_S are the values of neutron fluence within designated energy bins in **Table 10**, and L_{th}, L_{Cu}, L_a, L_b and L_S are the corresponding fluence-to-dose conversion factors listed in **Table 10**. The calculated value for $D^*(10)_n$ has units of cGy.

For FNADs, the ambient absorbed dose from neutrons is ***also*** calculated from the ^{198}Au activity in the bare gold foil (**G**) located in the *inner dosimetry package* using the following empirically derived formula:

$$D^*(10)_n = k A_o \qquad \text{Eq. 15}$$

where D*(10)n is the ambient absorbed dose in cGy, A_o is the decay corrected ^{198}Au activity in dpm/g, and the activity-to-dose conversion factor $k = 5.97 \times 10^{-5}$ (cGy g min). This relationship is based on the $A_o / D^*(10)_n$ data for ^{198}Au in gold foil **G**, in **Appendix F**, **Table F.2**.

For FNADs, the calculation of $D^*(10)_n$ from activity on gold foil (**G**) using **equation 15** is used as the primary value for $D^*(10)_n$ because it is less influenced by variations in neutron energy spectrum.

For PNADs, a first-approximation of $D_p(10)_n$, can be made using the ^{115m}In specific activity in either the bare or cadmium covered indium foil as follows:

$$D_p(10)_n = k A_o \qquad \text{Eq. 16}$$

where A_o is the decay corrected ^{115m}In activity in dpm/g, $k = 2.28 \times 10^{-3}$ (cGy g min), and $D_p(10)_n$ is the personal absorbed dose in units of cGy. This relationship is based on the $A_o / D_p(10)_n$ data for ^{115m}In in **Appendix F**, **Table F.1**.

A similar but less accurate first-approximation of $D_p(10)_n$, can be made using the ^{32}P specific activity in the sulfur pellets as follows:

$$D_p(10)_n = k A_o \qquad \text{Eq. 17}$$

where A_o is the decay corrected ^{32}P activity in dpm/g, $k = 1.74 \times 10^{-1}$ (cGy g min), and $D_p(10)_n$ is the personal absorbed dose in units of cGy. This relationship is based on the $A_o / D_p(10)_n$ data for ^{32}P in **Appendix F**, **Table F.1**.

The approximation of dose using ^{32}P activity is less accurate than the approximation using ^{115m}In activity because the energy range for which the $^{32}S(n,p)^{32}P$ reaction has significant cross section encompasses a smaller percentage of the dosimetrically significant fluence than the energy range for the $^{115}In(n,n')^{115m}In$ reaction.

2.14 Methodology for Calculating PNAD Gamma and Neutron Dose from InLight® Readings

The Landauer InLight® OSLN dosimeter is used in the PNNL PNAD to provide the primary gamma dose information and supplemental neutron dose information used in the event of a criticality. Because of the highly energy dependent nature of the albedo neutron response, the neutron dose result from the InLight® OSLN dosimeter is suitable for use only as an initial estimate (i.e. first approximation) of neutron dose until the results of foil analysis become available. The OSL technology allows repeated readout of the InLight® dosimeter with minimal signal loss (< 0.5% per reading with strong beam). The InLight® OSLN dosimeter used in the PNNL PNAD consists of a BA-type case loaded with an N-type slide containing three gamma sensitive OSL elements (E1, E3, E4) and one gamma + neutron sensitive OSLN element (E2). The BA case filtration in front of and behind each element is symmetrical and consists of an open window (E1), plastic filter (E2), copper filter (E3), and aluminum filter (E4). The InLight® OSLN dosimeter is described in greater detail in **Appendix A** and in Landauer internal documentation (Landauer, 2010). For accident level doses, the InLight® OSLN dosimeters are read first on the accident level Landauer microStar® reader (a reader that has been modified with a neutral density filter to extend the dynamic range to 20,000 cGy). Using the microStar® 5.0 software serving this reader, the dosimeters are read in a reader environment named "PNAD" that has been set up and calibrated specifically for readout of high dose InLight® dosimeters retrieved from PNNL PNADs. After initial readout on the accident level modified reader, InLight® OSLN dosimeters may be read on the unmodified microStar® protection level reader in the "PNAD LD" reader environment for more accurate readings *if the dose is sufficiently low* (E2 < 3000 cGy and E1, E3 and E4 less than 1000 cGy). This limit is necessary to avoid damage to the unmodified reader's one inch diameter PM tube and to avoid PM tube saturation. *Both readers must have been specifically set up and calibrated for readout of nuclear accident dosimeters*. When using either reader, each dosimeter is read three times and the dose result is generally based on the average of the three readings.

For the purpose of reading InLight® OSLN dosimeters exposed in PNADs, the microStar® readers are calibrated using sets of InLight® reader calibration dosimeters (CC-type case with A-type slide) that have been exposed to protection and accident level doses using a ^{60}Co beam irradiator at PNNL. The CC type dosimeter contains four OSL gamma sensitive elements, with equal amounts of ABS plastic filtration (178 mg/cm^2) covering each element front and back. The CC calibration dosimeters are exposed on 30 cm x 30 cm x 15 cm PMMA slab phantoms with 30 cm x 30 cm x 3.2 mm thick PMMA cover plates covering the dosimeters and front faces of the phantoms. The calibration dosimeters are irradiated to known levels of personal absorbed dose, $D_p(10)_\gamma$. During readout, the microStar® readers use two different power levels for optical stimulation of OSL elements with green colored LEDs. The two beams of light (weak and strong) are optimized to provide a large dynamic range for the system (5 mrad to 1000 rad ^{60}Co equivalent signal for the unmodified reader and 100 mrad to 20,000 rad for the modified reader). Both beams are calibrated using OSL elements exposed to a known dose from a ^{60}Co photon source. Thus, the reader calibration factors nominally have units of counts/cGy. Typical reader calibration factors that are applied by the reader software are shown in **Appendix I, Table I.1**.

NOTE: The suffix HD (high dose) is used in Table I.1 and Table I.2 after the PNAD and FNAD reader environment names to indicate the accident level reader. However when using the microStar® 5.0 software serving the accident level reader, the environments are referred to as PNAD and FNAD. The HD is implicit. For the protection level reader, the LD (low dose) nomenclature in **Table I.1** and **Table I.2** is consistent with the microStar® reader software environment names.

In the data files exported form the microStar® Reader database, dosimeter element readings are recorded as both raw readings (in units of "counts" from the PM tube), and as "converted values". Element converted values are readings that have been corrected for element sensitivity and have had the reader calibration factor applied. On the two dedicated microStar® readers specially calibrated for accident dosimetry, an InLight® element converted value of 1 cGy results from an element light output (measured as PMT counts) equal to that from an OSL element exposed in a CC case to 1 cGy of ^{60}Co gamma radiation, on phantom, under CPE conditions. Element readings expressed as converted values may thus be thought of as ^{60}Co cGy equivalent signal.

The microStar® software nominally reports the calculated reader calibration factors in units of counts/cGy during the reader calibration process. However, when reading BA type dosimeters, *the "converted values" for E1, E2, E3 and E4 that are recorded in the microStar® database are actually given in units of **mrad**. In the formulas below, it is assumed that E1, E2, E3 and E4 converted values exported from the microStar® database have been properly converted to units of cGy by dividing each value by 1000.* <u>The gamma absorbed dose calibration factors and neutron absorbed dose calibration factors used in the formulas below require "converted values" that are expressed in units of cGy</u>.

2.14.1 Calculating Gamma Dose from InLight® Readings

For each PNAD, the personal absorbed dose from photons, $D_p(10)_\gamma$ is calculated in using the E1, E2, E3 and E4 converted values (cGy) in a two-step process as follows:

<u>Step1</u>: Calculate the gamma signal with neutron influence on gamma signal subtracted.

$$x = ([(E3 + E4) / 2] - [R * (E2 - E1) / C_n]) \qquad \text{Eq. 18}$$

where

x is the OSL measured personal absorbed dose from photons (in cGy) without correction for photon energy dependence or supralinearity of dose response.

E1, E2, E3 and E4 are the element converted values in cGy

R is a dimensionless factor to estimate the fraction of delivered neutron absorbed dose that appears as apparent gamma signal on the gamma dose elements E3 and E4.

R = 0.165 (default) This value is based on dosimeters exposed on phantom in unmoderated fields with n/γ dose ratio = 8.

C_n is a dimensionless neutron absorbed dose calibration factor.

C_n = 2.90 (default) This value is based on dosimeters exposed at 50 cm on phantom to bare ^{252}Cf.

C_n = 6.19 (optimum C_n for Godiva-IV irradiations in DAF) This value is based on the response of dosimeters exposed at 2m, 3m and 4m distances on phantom from unshielded Godiva-IV bursts in DAF, with the average response at each distance given equal weighting.

<u>Step 2</u>: Calculate the personal absorbed dose from photons with corrections for photon energy and supralinearity applied.

$$D_p(10) = x / (S_{\gamma 34} * C_\gamma * RRF) \qquad \text{Eq. 19}$$

where

$D_p(10)_\gamma$ is the OSL measured personal absorbed dose from photons in cGy

x is the personal absorbed dose from photons (in cGy) without correction for gamma energy or supralinearity, as determined in Step 1 above.

$S_{\gamma 34}$ is the gamma supralinearity factor calculated from the average of E3 and E4 converted values ***after subtraction of the neutron response***. $S_{\gamma 34}$ is dimensionless.

$$S_{\gamma 34} = 9.8283E\text{-}13x^3 - 2.7185E\text{-}08x^2 + 2.0069E\text{-}04x + 1.0000E\text{+}00 \qquad \text{Eq. 20}$$

C_γ is a dimensionless gamma absorbed dose calibration factor. It adjusts for any differences in element response to the photon energies used to calibrate the dosimetry system in the lab (^{60}Co) and the energies encountered in an actual criticality.

C_γ = 1.00 default for prompt and delayed gamma from unshielded criticalities

RRF is the ^{60}Co relative response factor which is the ratio of OSL element response when exposed to ^{60}Co in the geometry used to calibrate the reader (inside CC case mounted on phantom with 3.2 mm PMMA cover plate) relative to the response when exposed to ^{60}Co in the geometry used to measure personal absorbed dose (inside BA case inside a PNAD assembly mounted on phantom. RRF is dimensionless.

RRF = relative response factor = 1.00 for E3 and E4 in the PNAD. (This preliminary value may need revision after more thorough response characterization is completed).

2.14.2 Calculating Neutron Dose from InLight® Readings

For each dosimeter, the personal absorbed dose from neutrons, $D_p(10)_n$, is calculated in a two-step process using E1 and E2 converted values (cGy) as follows:

<u>Step 1</u>: Calculate the gamma supralinearity correction factor for the E1 converted value reading

$$S_{\gamma 1} = 9.8283E\text{-}13z^3 - 2.7185E\text{-}08z^2 + 2.0069E\text{-}04z + 1.0000E{+}00 \qquad \text{Eq. 21}$$

where

z = E1 converted value (cGy)

<u>Step 2</u>: Calculate the personal absorbed dose from neutrons, $D_p(10)_n$ as follows:

$$D_p(10)_n = [E2 - E1/(S_{\gamma 1})^{0.8}] / C_n \qquad \text{Eq. 22}$$

where

C_n = neutron absorbed dose calibration factor

C_n = 2.90 for dosimeters exposed at 50 cm on phantom to bare ^{252}Cf (default)

C_n = 6.19 for dosimeters exposed at 2 m, 3 m and 4 m distances on phantom from unshielded Godiva-IV in DAF (optimum C_n for Godiva-IV irradiations in DAF)

The appropriate values for C_n are unique to each radiation field and highly dependent on neutron energy spectrum. The default value of C_n = 2.90, based on PNAD response to unmoderated ^{252}Cf neutrons at 50 cm, is expected to provide a conservative result for a solution type criticality. For more accurate albedo neutron dose results, the neutron calibration factor C_n should be evaluated for BA cases in fully loaded

PNAD holders mounted on phantom a neutron field more closely simulating the anticipated spectrum from a criticality in PNNL facilities where the dosimeter is used.

Correction factors for non-linearity of element dose response have been developed for use with converted value element readings from InLight® and nanoDot® dosimeters. OSL dose response linearity from 10 cGy to 10,000 cGy for gamma radiation was determined using the accident level reader to read sets of reader calibration dosimeters exposed on phantom covered with 3.2 mm PMMA plate, using a ^{60}Co beam irradiator to deliver 12 dose levels equally distributed across six decades. The OSL dose response to gamma radiation was shown to be supralinear above 100 cGy with a maximum response of 1.44 observed at 4000 cGy delivered dose. The empirically derived function for calculating the supralinearity correction factor, S_γ for an InLight® OSL element converted value reading is shown in **Appendix J, Figure J.1.** The nearly identical supralinearity correction function empirically derived in the same manner for OSL nanoDots is shown in **Appendix J, Figure J.2**.

OSLN unmoderated neutron dose response linearity was determined using the accident level reader to read sets of specially prepared dosimeters (CC-type case with N-type slide) that had been exposed to a moderated ^{252}Cf source to produce readings equivalent to an absorbed dose between 10 cGy and 1000 cGy from an unmoderated ^{252}Cf source. The "simulated" fast neutron response thus measured was essentially linear from 10 cGy to 1000 cGy simulated dose from an unmoderated ^{252}Cf source. Dosimeters were then given additional gamma dose from a ^{60}Co gamma source, and read again, to simulate neutron response in mixed neutron/gamma fields in which the gamma component comprised more than half of the total absorbed dose. Under these conditions, the neutron response became non-linear, decreasing as gamma/neutron ratio increases. The neutron dose response data are shown graphically in **Appendix J, Figure J.3**. The value $C_n = 4.27$ is shown on the data plots because this is the neutron calibration factor for unmoderated ^{252}Cf neutrons that was measured with the experimental dosimeter configuration used to generate the neutron linearity data (N-type slide in CC-type case, covered with3.2 mm PMMA). Because the dose response, and the associated non-linearity correction functions will vary as a function of gamma/neutron dose ratio, it is not possible to accurately calculate the non-linearity correction factor for every situation unless the gamma/neutron dose ratio is known. Instead, a general neutron non-linearity correction is applied in **equation 22** which provides an acceptable compromise between over response and under response under varying dose levels and gamma/neutron dose ratios. The improved accuracy in calculated neutron doses after applying this simple correction to the data used to generate **Figure J.3** is shown graphically in **Appendix J, Figure J.4.** The accuracy in calculated total dose (gamma+neutron) over a large dynamic range is shown graphically in **Figure J.5**.

For dosimeters exposed in the Godiva-IV exercise, the delivered gamma doses were less than 100 cGy and calculated corrections for gamma dose response non-linearity were < 3% . Calculated corrections for neutron dose response non-linearity were also < 3% because the gamma/neutron absorbed dose ratio in Godiva-IV fields varies between 7 and 9 depending on distance, (i.e.gamma component of absorbed dose comprised 11% - 14% of the total).

2.15 Methodology for Calculating FNAD Gamma and Neutron Dose from nanoDot® Readings

Landauer OSL and OSLN nanoDots are used in the PNNL FNAD to provide the primary gamma dose information and supplemental neutron dose information. Primary neutron dose information for the PNNL FNAD is provided by the activation foils. The sensitive elements in the OSL and OSLN nanoDots are the same composition and thickness as the OSL and OSLN elements on the N-type slide in the InLight® BA type case described in **Section 2.14**. The OSL and OSLN nanoDots are first read on the modified microStar® reader in a reader environment named "FNAD" which is specifically configured and calibrated for reading high dose nanoDots retrieved from FNADs. The reader calibration factors for this environment are determined from the response of OSL nanoDots that have been exposed on PMMA slab phantoms with 30 cm x 30 cm x 3.2 mm thick PMMA cover plates covering the dosimeters and front faces of the phantoms. The nanoDot dosimeters used to calibrate the reader are exposed to ^{60}Co photons from a beam irradiator to achieve a known delivered personal absorbed dose, $D^*(10)_\gamma$. Reader calibration factors thus nominally have units of counts/cGy. After initial readout on the accident level modified reader, nanoDot dosimeters may be read on the unmodified microStar® protection level reader in the "FNAD LD" reader environment for more accurate readings *if the dose is sufficiently low* (OSLN nanoDot < 3000 cGy and OSL nanoDot < 1000 cGy). This limit is necessary to avoid damage to the unmodified reader's one inch diameter PM tube and to avoid PM tube saturation. When using either reader, all the nanoDots from a given FNAD should be read and each nanoDot read three times. The dose result is generally based on the average of the three readings.

The unmodified microStar® reader environment named "FNAD LD" is configured and calibrated in the same manner as "FNAD". As with the reader calibrations performed for the PNAD and PNAD LD reader environments, the weak beam and strong beams are calibrated independently. OSL nanoDots given doses larger than 100 cGy are not used, so as to ensure that reader calibration factors are determined based on linear response of the OSL elements. As with the PNAD environments, the crossover point for the FNAD LD reader environment is set to correspond to doses of approximately 10 cGy. For the FNAD reader environment, the crossover point is set to correspond to a dose of approximately 75 cGy. The reader calibration factors for the FNAD and FNAD LD reader environments are shown in **Appendix I, Table I.2**.

NOTE: The suffix HD (high dose) is used in **Table I.1** and **Table I.2** after the PNAD and FNAD reader environment names to identify the accident level reader. However when using the microStar® 5.0 software serving the accident level reader, the environments will be displayed as "PNAD" and "FNAD" in the user interface. The HD suffix is implicit. For the protection level reader, the LD (low dose) nomenclature in **Table I.1** and **Table I.2** is consistent with the microStar® reader software environment names.

In the data files exported form the microStar® Reader database, dosimeter element readings are recorded as both raw readings (in units of "counts" from the PM tube), and as "converted values". Element converted values are readings that have been corrected for element sensitivity and have had the reader calibration factor applied. On the two dedicated microStar® readers specially calibrated for accident dosimetry, a nanoDot element converted value of 1 cGy results from an element light output (measured as PMT counts) equal to that from an OSL element exposed in a nanoDot case to 1 cGy of ^{60}Co gamma radiation, on phantom, under CPE conditions (i.e. with PMMA cover plate). Element readings expressed as converted values may thus be thought of as ^{60}Co cGy equivalent signal.

The microStar® software nominally reports the calculated reader calibration factors in units of counts/cGy during the reader calibration process. However, when reading nanoDot® dosimeters, *the "converted value" for E1 recorded in the microStar® database is actually given in units of **mrad**. In the formulas below, it is assumed that E1 converted values exported from the microStar® database have been properly converted to units of cGy by dividing each value by 1000.* <u>The formulas below assume that the "converted values" have units of cGy</u>.

2.15.1 Calculating Gamma Dose from nanoDot® Readings

The outer dosimetry package of the PNNL FNAD is used to measure gamma dose from criticality accidents. It includes an OSL nanoDot (dot1) paired with an OSLN nanoDot (dot2). Each nanoDot is read three times and the average reading used in the formulas below. For the purpose of the exercise, the ambient absorbed dose from photons $D^*(10)_\gamma$ is calculated from the OSL / OSLN nanoDot pair in the outer dosimetry package as follows:

<u>Step1</u>: Calculate the gamma signal with neutron influence on gamma signal subtracted.

$$x = [\text{dot1} - R\,(\text{dot2} - \text{dot1})] \qquad \text{Eq. 23}$$

where

x is the photon dose (^{60}Co cGy equivalent signal) after correction for neutron influence but without correction for photon energy dependence or supralinearity of dose response.

dot1 and dot2 are the E1 converted value <u>readings in cGy</u> for nanoDot 1 (OSL) and nanoDot 2 (OSLN) in the outer dosimetry package. Element converted value readings for nanoDots are always recorded as E1 in the microStar® database, with units of mrad and must be converted to cGy for use with the formulas in this section.

R is a dimensionless factor to estimate the fraction of delivered neutron absorbed dose that appears as apparent gamma signal on the gamma detector, dot1.

R = 0.0086 (default) This value is based on FNADs exposed to unmoderated fields from Godiva-IV with n/γ dose ratio = 8. Unlike PNADs, R for FNADs is <u>not</u> used in conjunction with C_n.

<u>Step 2</u>: Calculate the ambient absorbed dose from photons, $D^*(10)_\gamma$, with corrections for photon energy dependence and supralinearity applied.

$$D^*(10)_\gamma = x / (S_\gamma * C_\gamma * RRF) \qquad \text{Eq. 24}$$

where

$D^*(10)_\gamma$ is the measured ambient absorbed dose from photons in cGy x is the dose from photons (in cGy) without correction for gamma energy or supralinearity, as determined in Step 1 above.

S_γ is the gamma supralinearity factor calculated using x as determined in Step 1 above. S_γ is dimensionless.

$S_\gamma = 1.2251E\text{-}12x^3 - 3.1340E\text{-}08x^2 + 2.1261E\text{-}04x + 1.0000E\text{+}00$

C_γ is a dimensionless gamma absorbed dose calibration factor. It adjusts for any differences in element response to the photon energies used to calibrate the dosimetry system in the lab (^{60}Co) and the energies encountered in an actual criticality.

C_γ = 1.00 default for prompt and delayed gamma from unshielded criticalities

RRF is the ^{60}Co relative response factor which is the ratio of OSL element response when exposed to ^{60}Co in the geometry used to calibrate the reader (inside nanoDot case mounted on phantom with 3.2 mm thick PMMA cover plate) relative to the response when exposed to ^{60}Co in the geometry used to measure personal absorbed dose (in outer dosimetry package mounted on candle exposed in air). RRF is dimensionless.

RRF = 1.00 for dots in the outer dosimetry package of the FNAD. (This preliminary value may need revision after more thorough response characterization is completed).

2.15.2 Calculating Neutron Dose from nanoDot® Readings

The ambient absorbed dose from neutrons $D^*(10)_n$ is calculated from the nanoDots in the inner dosimetry package as follows:

Step 1: Calculate the gamma supralinearity correction factor for the dot3 converted value reading

$$S_\gamma = 1.2251E\text{-}12z^3 - 3.1340E\text{-}08z^2 + 2.1261E\text{-}04z + 1.0000E\text{+}00 \qquad \text{Eq. 25}$$

where

z = dot3 converted value (cGy)

Step 2: Calculate the ambient absorbed dose from neutrons, $D^*(10)_n$ as follows:

$$D^*(10)_n = [\,(dot4 + dot5 + dot6) / 3 - dot3 / (S_\gamma)^{0.8}\,] / C_n \qquad \text{Eq. 26}$$

where

dot3 is the inner dosimetry package OSL nanoDot converted value reading (^{60}Co cGy equivalent signal)

dot4, dot5 and dot6 are the inner dosimetry package OSLN nanoDot converted value readings (^{60}Co cGy equivalent signal)

C_n = neutron absorbed dose calibration factor (dimensionless)

C_n = 12.89 (default). This value is based on calibration of the FNAD with an unmoderated ^{252}Cf source at a distance of 1 meter. This value also provided unbiased neutron absorbed dose results for FNADs exposed at a distance of 4.0 meters from Godiva-IV.

3.0 RESULTS and DISCUSSION

3.1 Neutron Fluence and Dose Results for PNADs Calculated from Foil Activity

Using **equations 5 – 13** in conjunction with **Table 10**, neutron fluence and neutron absorbed dose were calculated for each PNAD exposed in the IER-148 exercise with Godiva-IV. This includes the six Hanford PNADs and 46 PNNL PNADs exposed in the exercise. For each dosimeter, neutron fluence and absorbed dose were calculated for individual NAD energy regions and summed to obtain values for total fluence and total dose. The calculated values are compared against delivered values and presented in **Appendix K. Table K.1** shows the results for PNADs exposed in air and **Table K.2** shows the results for PNADs exposed on phantom. The results show that the dose calculation methodology developed in **Section 2** provides accurate dose results for each energy region and accurate results for total neutron dose that are within ± 25% of the delivered value *for every dosimeter exposed either in air or in AP geometry on phantom*. The relative standard deviation of results for each combination of distance and geometry show good measurement precision. As expected, dosimeters exposed on the back side of a phantom under respond significantly. The two dosimeters mounted on phantoms irradiated in lateral geometry produced inconsistent results. The results for dosimeters exposed in air or in AP geometry on phantom are summarized by distance for fluence in **Table 11** and by distance for dose in **Table 12** below. Data for 3 Hanford PNADs containing 5 mil thick foils are shown on the second row All other data are for 10 mil foils . The values for Φ_{th} and Φ_{Cu} on phantom in **Table 11** and the values for D_{th} and D_{Cu} in **Table 12** over respond due to the additional fluence from albedo neutrons not accounted or in the reference values for fluence an dose. The effective cross sections and activity to fluence conversion factors for these two energy regions were based only on measured foil activity and known fluence for foils exposed in air and thus correctly measure the 4π fluence seen by the foils which includes albedo neutrons. Although the calculated dose from thermal neutrons shows a significant over response for dosimeters mounted on phantom, the relative contribution to total dose from thermal neutrons is small (2-3 %).

Table 11. Accuracy of Calculated Fluence Using Foil Activity in PNADs.

	distance (m)	phantom type	Measured Φ_{bin} /Given Φ_{bin}						
			Φ_{th}	Φ_{Cu}	Φ_{a}	Φ_{In}	Φ_{b}	Φ_{S}	Φ_{total}
			0.001 eV - 0.464 eV	**0.464 eV - 100 keV**	**100 keV - 1.25 MeV**	**1.25 MeV - 20 MeV**	**1.25 MeV - 3.16 MeV**	**3.16 MeV - 20 MeV**	**0.001 eV - 20 MeV**
	2.0	air	0.85	1.00	1.03	1.03	1.04	1.00	**1.00**
*	2.0	air	0.76	1.08	1.03	1.00	1.01	0.97	**1.01**
	2.5	air	1.01	0.97	1.01	1.14	1.13	1.19	**1.02**
	4.0	air	1.19	1.03	1.03	0.96	0.96	0.93	**1.02**
	3.0	BOMAB	2.61	1.23	1.05	0.93	0.92	0.96	**1.29**
	4.0	BOMAB	2.85	1.17	1.14	1.03	1.01	1.09	**1.37**
	2.0	PMMA	2.86	1.56	1.26	1.08	1.09	1.05	**1.48**
	4.0	PMMA	2.40	1.21	1.16	1.02	1.01	1.07	**1.33**

* **5 mil foils**

Table 12. Accuracy of Calculated Neutron Dose, $D_p(10)_n$, Using Foil Activity in PNADs.

	distance (m)	phantom type	Reported D_{bin} / Given D_{bin}						B
			D_{th}	D_{Cu}	D_a	D_b	D_S	D_{total}	
			0.001 eV - 0.464 eV	0.464 eV - 100 keV	100 keV - 1.25 MeV	1.25 MeV - 3.16 MeV	3.16 MeV - 20 MeV	0.001 eV - 20 MeV	
	2.0	air	0.82	0.95	0.97	0.99	0.96	0.97	**-0.03**
*	2.0	air	0.73	1.02	0.97	0.96	0.92	0.96	**-0.04**
	2.5	air	0.95	0.91	0.96	1.07	1.12	1.01	**0.01**
	4.0	air	1.13	0.98	0.98	0.91	0.87	0.95	**-0.05**
	3.0	BOMAB	2.48	1.17	1.00	0.87	0.91	1.00	**0.00**
	4.0	BOMAB	2.65	1.09	1.06	0.94	1.01	1.07	**0.07**
	2.0	PMMA	2.77	1.50	1.19	1.05	1.01	1.16	**0.16**
	4.0	PMMA	2.23	1.13	1.08	0.94	0.99	1.07	**0.07**

* **5 mil foils**

3.2 Neutron Fluence and Dose Results for FNADs Calculated from Foil Activity

Using **equations 5 – 15** in conjunction with **Table 10**, neutron fluence and neutron absorbed dose were calculated for each FNAD exposed in the IER-148 exercise with Godiva-IV. For each dosimeter, neutron fluence and absorbed dose were calculated for individual NAD energy regions and summed to obtain values for total fluence and total dose. The calculated values are compared against delivered values and presented in **Appendix K, Table K.3.** With the FNAD, thermal fluence and thermal dose can be calculated from either the indium foil activity in the outer dosimetry package or the gold foil activity in the outer dosimetry package. Fluence and dose results were calculated from foil activities in the outer dosimetry package using both options. The results show that the dose calculation methodology developed in **Section 2** provides generally accurate dose results for each energy region and *accurate results for total neutron dose that are within ± 25% of the delivered value for every dosimeter.* Neutron absorbed dose can also be calculated directly from the activity of the gold foil in the inner dosimetry package using **equation 15**. The results for this method are also presented in **Table K.3**. The results indicate *accurate results for total neutron dose that are within ± 25% of the delivered value for every dosimeter.* The relative standard deviation of dose results indicate satisfactory precision of measurement. The results are summarized for fluence in **Table 13** and for dose in **Table 14** below.

Table 13. Accuracy Of Calculated Neutron Fluence Using Foil Activity in FNADs.

distance (m)	Foil Used for Φ_{th}	Measured Φ_{bin} /Given Φ_{bin}						
		Φ_{th}	Φ_{Cu}	Φ_a	Φ_{In}	Φ_b	Φ_S	Φ_{total}
		0.001 eV - 0.464 eV	0.464 eV - 100 keV	100 keV - 1.25 MeV	1.25 MeV - 20 MeV	1.25 MeV - 3.16 MeV	3.16 MeV - 20 MeV	0.001 eV - 20 MeV
4.0	In	1.41	1.20	1.14	1.00	1.02	0.90	**1.18**
4.0	Au	1.00	1.20	1.14	1.00	1.02	0.90	**1.12**

Table 14. Accuracy of Calculated Neutron Dose, $D^*(10)_N$ Using Foil Activity in FNADs.

distance (m)	Foil Used for Φ_{th}	Reported D_{bin} / Given D_{bin}						B
		D_{th}	D_{Cu}	D_a	D_b	D_S	D_{total}	
		0.001 eV - 0.464 eV	0.464 eV - 100 keV	100 keV - 1.25 MeV	1.25 MeV - 3.16 MeV	3.16 MeV - 20 MeV	0.001 eV - 20 MeV	
4.0	In	1.33	1.13	1.08	0.96	0.84	1.01	**0.01**
4.0	Au	0.94	1.13	1.08	0.96	0.84	1.02	**0.02**

3.3 Gamma and Neutron Dose Results for PNADs Calculated from InLight® Dosimeter Readings

Using the equations and methodology described in **Section 2.14**, gamma absorbed dose and neutron absorbed dose were calculated for the 46 PNNL PNADs exposed in the IER-148 exercise using the InLight® dosimeter's element readings. The results are presented in **Appendix L, Table L.1**. The gamma dose results show that for PNADs exposed in air and in AP geometry on phantom, the applied corrections for neutron influence on gamma response were reasonably effective. Previously, without correction, the reported gamma dose for dosimeters exposed on phantom was on average, 2.59 times the given gamma dose. Similarly, without correction, the reported gamma dose for dosimeters exposed in air was on average, 1.31 times the given gamma dose. On average, the reported gamma dose is now within 5% of the given dose. The neutron dose results show that for dosimeters exposed on phantom in AP geometry, the dosimeters generally reported neutron dose that was within ±25% of the given dose. The one dosimeter not meeting this criteria had a reported dose that was 1.31 times the given dose. The dosimeters exposed on phantom in AP geometry generally reported total absorbed dose from neutrons and gamma that met the ±25% total dose accuracy criteria of ANSI/HPS N13.3 – 2013. The one dosimeter not meeting this total dose criteria was the same dosimeter not meeting the criteria for neutron dose. This dosimeter had a reported total dose that was 1.28 times the given total dose.

3.4 Gamma and Neutron Dose Results for FNADs Calculated from nanoDot® Dosimeter Readings

Using the equations and methodology described in **Section 2.15**, gamma absorbed dose and neutron absorbed dose were calculated for the 3 PNNL FNADs exposed in the IER-148 exercise using the nanoDot dosimeter readings. The results are presented in **Appendix M, Table M.1 and Table M.2**. The gamma dose results in **Table M.1** show that the applied corrections for neutron influence on gamma response of nanoDots in the outer dosimetry package were reasonably effective. Previously, without correction, the reported gamma dose for FNADs exposed at 4.0 meters from Godiva-IV was on average, 1.31 times the given gamma dose. With the corrections applied, the reported gamma dose is now within 6% of the given dose. The neutron dose results in **Table M.2** show that for FNADs exposed at a distance of 4.0 meters, the dosimeters reported neutron dose that was within ±5% of the given dose. These neutron dose results were calculated using the default calibration factor determined from ^{252}Cf irradiations at PNNL. The use of a generic rather than site specific neutron calibration factor is possible because, unlike the InLight® albedo neutron dosimeter, the FNAD enjoys the flattened energy response characteristic of a detector inside a 23 cm diameter cylindrical paraffin moderator.

3.5 Dosimeter Performance Evaluation

The primary purpose of this section is to consolidate the dose results obtained from different detectors and analyze dosimeter performance against the performance criteria in ANSI/HPS N13.3-2013. According to the standard, performance is to be evaluated for the total (gamma + neutron) absorbed dose on an individual dosimeter basis using the performance statistic P which is calculated as follows:

$$P = (\text{Measured Dose} - \text{Delivered Dose}) / \text{Delivered Dose} \qquad \text{Eq. 27}$$

Consistent with established nomenclature in personnel and environmental dosimeter performance test standards the symbol P is used in this report to represent the *performance quotient* for an individual dosimeter and the symbol B is used to represent the average value of P for a group of dosimeters (referred to as “bias”). ANSI/HPS N13.3-2013 used the symbol B to represent the performance quotient for an individual dosimeter. The performance testing criteria for PNADs and FNADs are given in ANSI/HPS N13.3 are shown in **Table 15**. The operational quantity recommended for use with PNADs is personal absorbed dose, $D_p(10)$. The operational quantity recommended for use with FNADs is ambient absorbed dose D*(10). All PNNL dosimeters exposed in the exercise received a total dose between 100 cGy and 1000 cGy. Thus <u>the ±25% criterion applies to all dosimeters in the study</u>.

Table 15. ANSI/HPS N13.3 Performance Test Criteria for Criticality Accident Dosimetry Systems

Total absorbed dose range	P
10 to 100 cGy (10 to 100 rad)	-0.50 < P < 0.50
100 to 1000 cGy (100 to 1000 rad)	-0.25 < P < 0.25
> 1000 cGy (1000 rad)	indication of dose > 1000 cGy (1000 rad)

3.5.1 PNAD Performance

The gamma+neutron total dose performance for PNNL PNADs when neutron dose is calculated from foil activity and gamma dose is calculated from the InLight® element readings is shown in **Appendix N, Table N.1.** The performance of dosimeters exposed on phantom in AP geometry as well as dosimeters exposed in air meets ANSI/HPS N13.3-2013 criteria applicable to the range of doses delivered. Dosimeters exposed on phantom in PA geometry measured only 64% of the delivered dose on average. The two dosimeters exposed on phantom in LAT geometry gave inconsistent results.

The gamma+neutron total dose performance for PNNL PNADs when both neutron dose and gamma dose are calculated from InLight® OSLN dosimeter readings is shown in **Appendix N, Table N.2.** The performance of dosimeters exposed on phantom in AP geometry meets ANSI/HPS N13.3-2013 criteria applicable to the range of doses delivered for all but one dosimeter. The failing dosimeter had a performance quotient, $P_i = 0.28$ which lies marginally outside the ANSI/HPS N13.3-2013 acceptable range, $-0.25 < P_i < 0.25$. Dosimeters exposed on phantom in PA geometry generally failed the test with a group bias of -0.33. Interestingly, the two dosimeters mounted on the backside of PMMA slab phantoms passed. The two dosimeters exposed on phantom in LAT geometry gave inconsistent results with one passing and one failing. As expected for an albedo neutron dosimeter, all of the dosimeters exposed in air all failed the test, with performance quotients varying between -0.36 and -0.65 as an inverse function of distance, and with a group bias of -0.52.

PNAD performance for exposures on phantom in AP geometry are shown in **Table 16** for foil based neutron dose results and **Table 17** for OSLN based neutron dose results.

Table 16. PNAD Performance on Phantom in AP Geometry (neutron dose from foils)

Irradiation Data				PNAD Performance with foil calculated neutron dose				
PNAD No.	Distance (m)	phantom type	dosimeter location on phantom	OSL Gamma R/G	Foil Neutron R/G	PNAD γ + n R/G	P_i	Pass or Fail
45	2	PMMA	front	1.17	1.16	1.16	0.16	Pass
5	3	BOMAB	front	1.07	0.99	0.99	-0.01	Pass
7	3	BOMAB	front	1.05	0.93	0.94	-0.06	Pass
21	3	BOMAB	front	1.25	1.05	1.07	0.07	Pass
23	3	BOMAB	front	1.07	1.00	1.01	0.01	Pass
34	3	BOMAB	front	1.24	1.02	1.05	0.05	Pass
13	4	PMMA	front	0.59	1.04	0.99	-0.01	Pass
25	4	PMMA	front	0.72	1.09	1.05	0.05	Pass
38	4	BOMAB	front	1.02	1.07	1.06	0.06	Pass

Table 17. PNAD Performance on Phantom in AP geometry (neutron dose from InLight® OSLN)

Irradiation Data				PNAD Performance with InLight calculated neutron dose (C_n = 6.19)				
PNAD No.	Distance (m)	phantom type	dosimeter location on phantom	OSL Gamma R/G	OSLN Neutron R/G	PNAD γ + n R/G	P_i	Pass or Fail
45	2	PMMA	front	1.17	0.81	0.85	-0.15	Pass
5	3	BOMAB	front	1.07	1.00	1.00	0.00	Pass
7	3	BOMAB	front	1.05	0.94	0.95	-0.05	Pass
21	3	BOMAB	front	1.25	0.94	0.98	-0.02	Pass
23	3	BOMAB	front	1.07	1.05	1.05	0.05	Pass
34	3	BOMAB	front	1.24	0.99	1.02	0.02	Pass
13	4	PMMA	front	0.59	1.22	1.15	0.15	Pass
25	4	PMMA	front	0.72	1.08	1.04	0.04	Pass
38	4	BOMAB	front	1.02	1.31	1.28	0.28	Fail

3.5.2 FNAD Performance

The gamma+neutron total dose performance for PNNL FNADs when neutron dose is calculated from foil activity and gamma dose is calculated from the nanoDot dosimeter readings is shown in **Appendix O, Table O.1.** The performance is well within ANSI/HPS N13.3-2013 criteria. The gamma+neutron total dose performance for PNNL FNADs when both neutron and gamma dose are calculated from nanoDot dosimeter readings is shown in **Appendix O, Table O.2.** The performance is well within ANSI/HPS N13.3-2013 criteria. For the OSL gamma dose calculations and the OSLN neutron dose calculations, the PNNL default calibration factors were used.

3.6 Dependence of Foil Calculated Neutron Dose on Neutron Energy Spectrum

The energy regions, restricted energy effective cross sections and associated activity to fluence conversion factors for the new methodology were developed empirically from the measured activity on dosimeters exposed at Godiva-IV and the reference values for delivered fluence, dose, and neutron energy spectrum. The methodology was designed to give dose results that are accurate for test dosimeters exposed in Godiva-IV radiation fields while being as independent as possible of the shape of the neutron energy spectrum to which the dosimeter are exposed. However, some dependence of dosimeter response on neutron energy spectrum is unavoidable. In particular, the fluence in the energy region from 100 keV to 1.25 MeV is not directly measurable with the neutron reactions available in the PNAD and FNAD foil set. Fluence in this region must be inferred from the fluence measured in adjacent regions, using an assumption about the shape of the neutron energy spectrum. For the methodology described in this report, the Godiva-IV spectrum was used. Thus, the weighting factors in **equation 4** are somewhat specific to the shape of the Godiva-IV spectrum and may need to be adjusted for spectra that differ significantly from Godiva-IV. For the Godiva-IV neutron fields, the neutron fluence in the 100 keV – 1.25 MeV energy region accounts for approximately 36% of the total fluence and approximately 47% of the total dose. Thus the accuracy of fluence assessment in this region has a potentially large impact on the accuracy of total measured dose. To some extent, the fluence-to-absorbed-dose conversion factors $\mathbf{K_a}$ and $\mathbf{L_a}$ for this energy region (given in **Table 10)** are also dependent on the shape of the neutron energy spectrum in this region.

3.7 Dependence of InLight® OSLN Measured Neutron Dose on Neutron Energy Spectrum

The OSLN element in the InLight dosimeter does not have a cadmium filter in front of it, so the influence of incident thermal neutrons on dose response is larger than a typical albedo dosimeter with cadmium filter in front of the neutron sensitive element. The neutron dose response of InLight OSLN component of the PNNL PNAD is strongly influenced by neutrons backscattered from walls, floors and other building materials ("room return") and thus dependent on the size of the room and distance of the dosimeter from the source. For example, the measured neutron calibration factor, C_n, for PNADs exposed on phantom with Godiva-IV was 5.03 at 2 meters, 6.09 at 3 meters and 7.46 at 4 meters. For PNADs exposed in air, the measured C_n factors were 1.78 at 2 meters, 2.53 at 2.5 meters and 3.69 at 4 meters.).

Figure 8 shows the measured InLight® OSLN neutron calibration factor on phantom as a function of distance. The data in **Figure 8** suggests that the OSLN neutron dose response for dosimeters worn on the chest and exposed in normal AP geometry may vary by a factor of 2 depending on distance from the source. The factor $C_n = (E2\text{-}E1)/D_p(10)_n$ where $D_p(10)_n$ is the delivered dose. The net neutron signal (E2-E1) and delivered dose $D_p(10)_n$ both have units of cGy, thus C_n is dimensionless. In essence, the coefficient C_n may be thought of as the dose "response" of the dosimeter as defined by ISO 8529-1 (ISO, 2001).

In addition to room size and distance from the source, the dose response is highly dependent on the degree to which the fission spectrum has been moderated by intervening materials. Response data from TLD based personnel dosimeters of similar design with a single unfiltered neutron sensitive element have shown that scatter in air and moderation in intervening materials can potentially produce a variation in dose response by a factor of 10 (Rathbone, 2011). Other variables such as orientation of the individual with respect to the source can produce a factor of 2 variation in response. Given the above considerations, the neutron results obtained from the InLight® should be considered preliminary dose estimates to be used only until neutron dose results from foils become available.

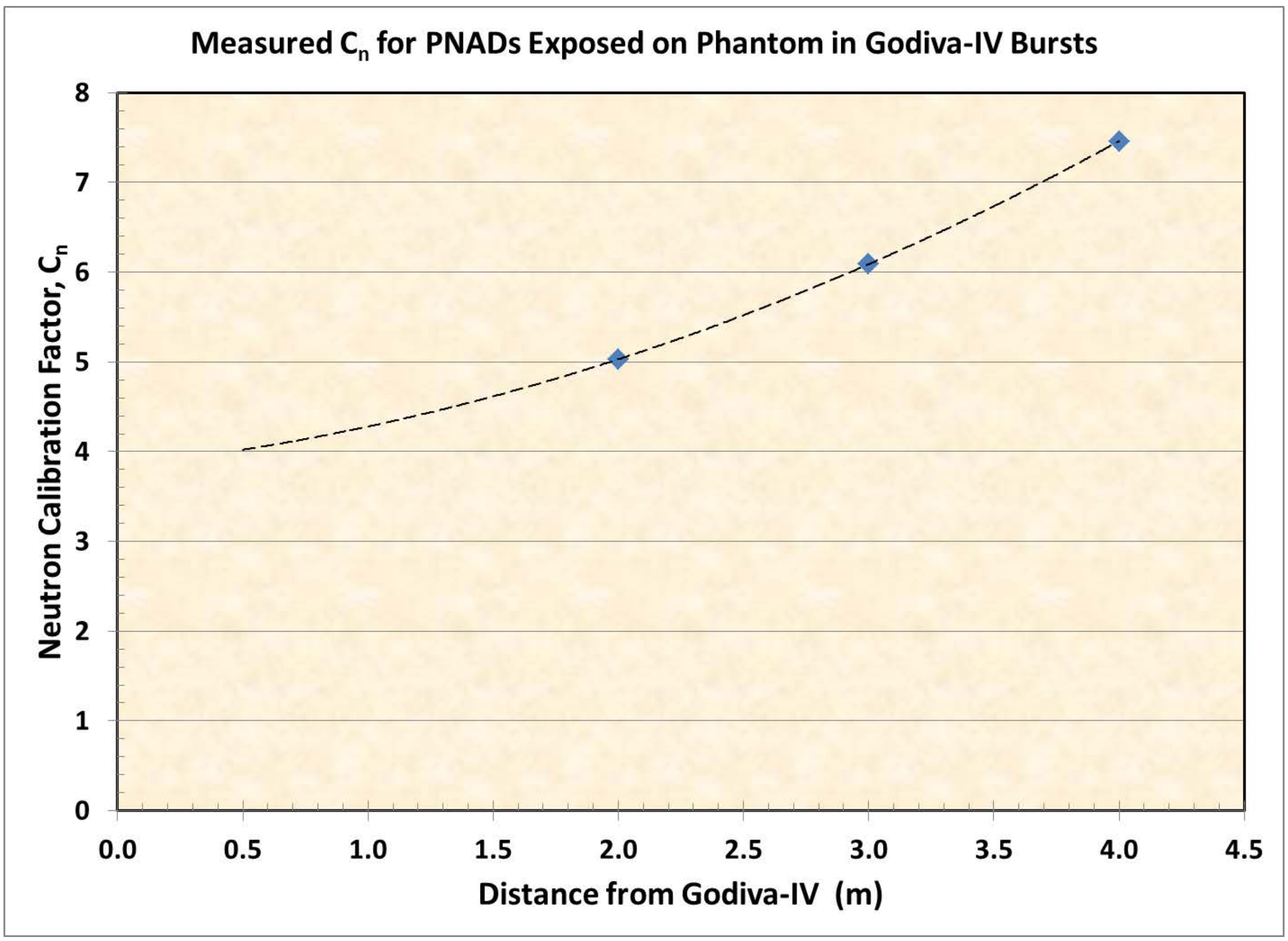

Figure 8. InLight® OSLN neutron response in PNADs exposed on phantom with Godiva-IV

3.8 Additional DOE Accuracy Requirements for FNADs

In addition to the accuracy requirements given in ANSI/HPS N13.3-2013, the Department of Energy Standard, DOE-STD-1098-2008 *Radiological Control*, contains the following requirements in Article 515 *Nuclear Accident Dosimeters*:

Fixed nuclear accident dosimeters should:

a. Be capable of determining the neutron dose from 10 rads to approximately 10,000 rads with an accuracy of ± 25%

b. Be capable of measuring fission gamma radiation from 10 rads to approximately 10,000 rads in the presence of neutron radiation with an accuracy of approximately ± 25%.

c. Be capable of measuring the approximate neutron energy spectrum

The separate gamma and neutron response data in **Table O.1** and **Table O.2** demonstrate that the accuracy requirements of ± 25% for gamma dose and ± 25% for neutron dose can be met by the FNAD over the range of doses delivered in the exercise. The ability to meet the gamma accuracy requirement for doses up to 10,000 cGy is supported by the incorporation of corrections for OSL gamma response supralinearity (**Appendix J, Figure J.2**) and the modification of the accident level microStar® reader with a neutral density filter to provide an extended dynamic range with linear response up to10,000 cGy ^{60}Co equivalent OSL element signal. For neutron dose determined from foil activity measurements, the activities resulting from a 10,000 cGy dose can be readily accommodated with existing instrumentation through a combination of extended decay time and/or use of counting geometries calibrated at larger source-detector distances and/or with source attenuators in place (e.g. beta attenuation). The measured specific activity per unit ambient absorbed dose values in **Appendix F, Table F.2** for FNAD foils exposed by Godiva-IV support this conclusion. The ability to measure the approximate neutron energy spectrum is supported by the data in **Table 11** and **Table 12** above.

4.0 CONCLUSIONS

A new dose calculation methodology has been developed for use with the new PNAD and FNAD designs planned for implementation at PNNL in 2018. The methodology is described in detail in this report. The ability of this methodology to meet the accuracy requirements of ANSI/HPS N13.11-2013 is demonstrated in this report using test data obtained from prototype dosimeters exposed in the *2016 Criticality Accident Dosimetry Exercise at the Nevada National Security Site (IER-148)*

The methodology for calculating dose from foil activity provides neutron fluence and neutron dose information for each of five energy regions between 0.001 eV and 20 MeV as well as total neutron fluence and total neutron dose information. This report demonstrates that the methodology provides accurate neutron dose results for FNADs exposed in air and for PNADs exposed either in air or on phantom in normal AP geometry.

The methodology for calculating gamma dose from OSL elements incorporates corrections for supralinearity of gamma dose response, and corrections for the influence of neutrons on gamma dose response. This report demonstrates that with the corrections applied, accurate gamma dose results are obtained in radiation fields with neutron / gamma ratios as large as 8:1.

The methodology for calculating neutron dose from OSLN elements incorporates corrections for non-linearity of neutron dose response. Data is provided to show that accurate OSLN neutron dose results can be obtained with PNADs over a wide range of neutron/gamma dose mixture ratios and dose levels. This report demonstrates that with the use of a source specific neutron calibration factor, OSL/OSLN gamma+neutron total dose results that meet the performance criteria of ANSI/HPS N13.3 – 2013 are obtained with PNADs at varying distances from the source. This report also demonstrates that accurate neutron dose results are obtained with FNADs using the default ^{252}Cf neutron calibration factor applied to the OSLN element inside the cylindrical paraffin moderator.

When neutron dose results calculated from foil activity are combined with gamma dose from OSL elements, total reported dose meets the accuracy requirements of ANSI/HPS N13.3-2013. This is true for both PNADs and FNADs. Total dose results that comply with ANSI/HPS N13.3 -2013 are also obtained for PNADs when OSLN neutron dose is combined with the OSL gamma dose. This however requires that the proper neutron calibration factor is applied. Total dose results that comply with ANSI/HPS N13.13.2013 are obtained for FNADS when OSLN neutron dose is combined with OSL gamma dose. For FNADs, this accuracy is achieved with the use of a single default neutron calibration factor.

Dose results that meet the accuracy requirements of ANSI/HPS N13.3-2013 can be obtained under the conditions of performance testing. Dose results under actual criticality accident conditions will likely be less accurate, and vary depending on how much is known about the critical configuration, the intervening materials between source and exposed individuals, the room size and location of exposed individuals within the room, the dosimeter location on the exposed individuals and their orientation with respect to the source.

5.0 REFERENCES

Bramson, P.E. 1963. *Hanford Criticality Dosimeter*. HW-71710 Revised 2-8-63, General Electric Hanford Atomic Products Operation, Richland, Washington.

Glenn, R. D. and P. E. Bramson 1977 *The Hanford Critical Radiation Dosimeter* PNL-2276, Pacific Northwest National Laboratory, November 1997.

Health Physics Society (HPS) 2009. ANSI/HPS N13.35-2009 *Specifications for the Bottle Manikin Absorption Phantom*, Health Physics Society, 2009.

Health Physics Society (HPS) 2013, ANSI/HPS N13.3 – 2013, *Dosimetry For Criticality Accidents*, Health Physics Society, 1313 Dolley Madison Blvd. Suite 402, McLean, VA

Heinrichs, D. et. al, 2014 *Final Design for an International Intercomparison Exercise for Nuclear Accident Dosimetry at the DAF Using GODIVA-IV (IER-148 CED-2 Report).* LLNL-TR-661851, Lawrence Livermore National Laboratory, September 30, 2014.

Hickman, David P, 2017 (Personal email communication, from D.P. Hickman to B.A. Rathbone, Subject: *RE: Element 57 dose and IAEA 211 dose* , dated March 27, 2017)

Hutchinson, J. D., D. K. Hayes and W. L. Myers 2012 *National Criticality Experiments Research Center: Capabilities and Experiments*, LA-UR-20701 Los Alamos National Laboratory 2012.

International Atomic Energy Agency (IAEA). 1982. *Dosimetry for Criticality Accidents, a Manual*. Technical Report Series No. 211, IAEA, Vienna, Austria.

International Organization for Standardization (ISO), 2001 *ISO 8529-1 Reference neutron radiations – Part 1: Characteristics and methods of production.*

Knolls Atomic Power Laboratory, *Chart of the Nuclides*, Naval Reactors, U.S. Department of Energy, 16th Edition-Revised to 2002

Rathbone, B. A. 2011. *Hanford External Dosimetry Technical Basis Manual PNL-MA-842* . PNNL-15750 Rev. 1.2, Pacific Northwest National Laboratory, Richland, WA.

Rathbone , B. A. et. al. 2017 *Measurement Results for the 2016 Criticality Accident Dosimetry Exercise at the Nevada National Security Site (IER-148) PNNL 26497.* Pacific Northwest National Laboratory, May 2017.

Wilson, C., Leo Clark, and Phil Angus 2014 *Neutron spectrometry results from phase two of the Godiva-IV characterization*. AWE Report No. 880/14 AWE/NAS/RPG/ADS/CRIT/TR/004 issue 5.

Appendix A

PNNL PNAD Design Features

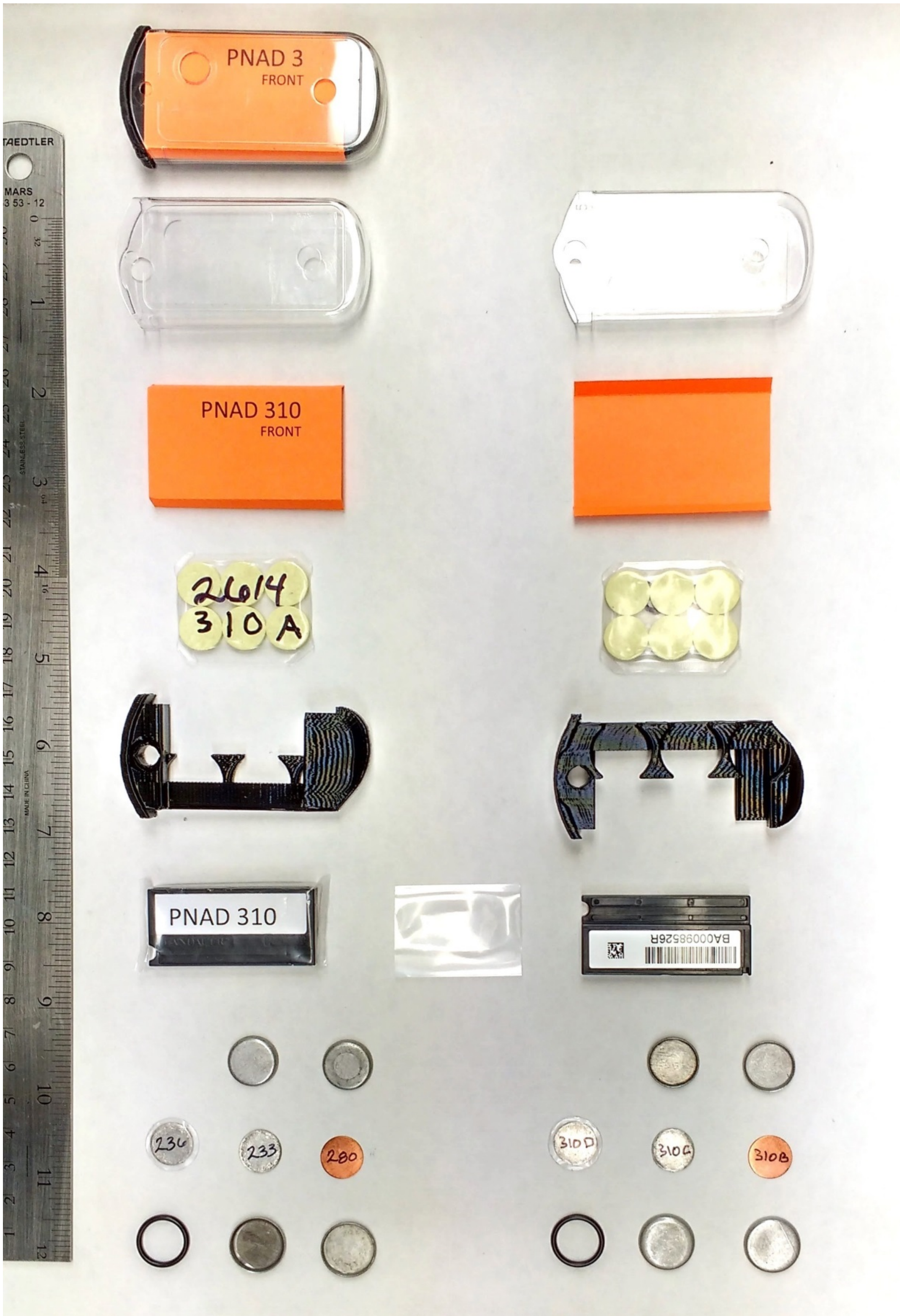

Figure A.1. Disassembled PNNL PNADs with components viewed from front and back sides

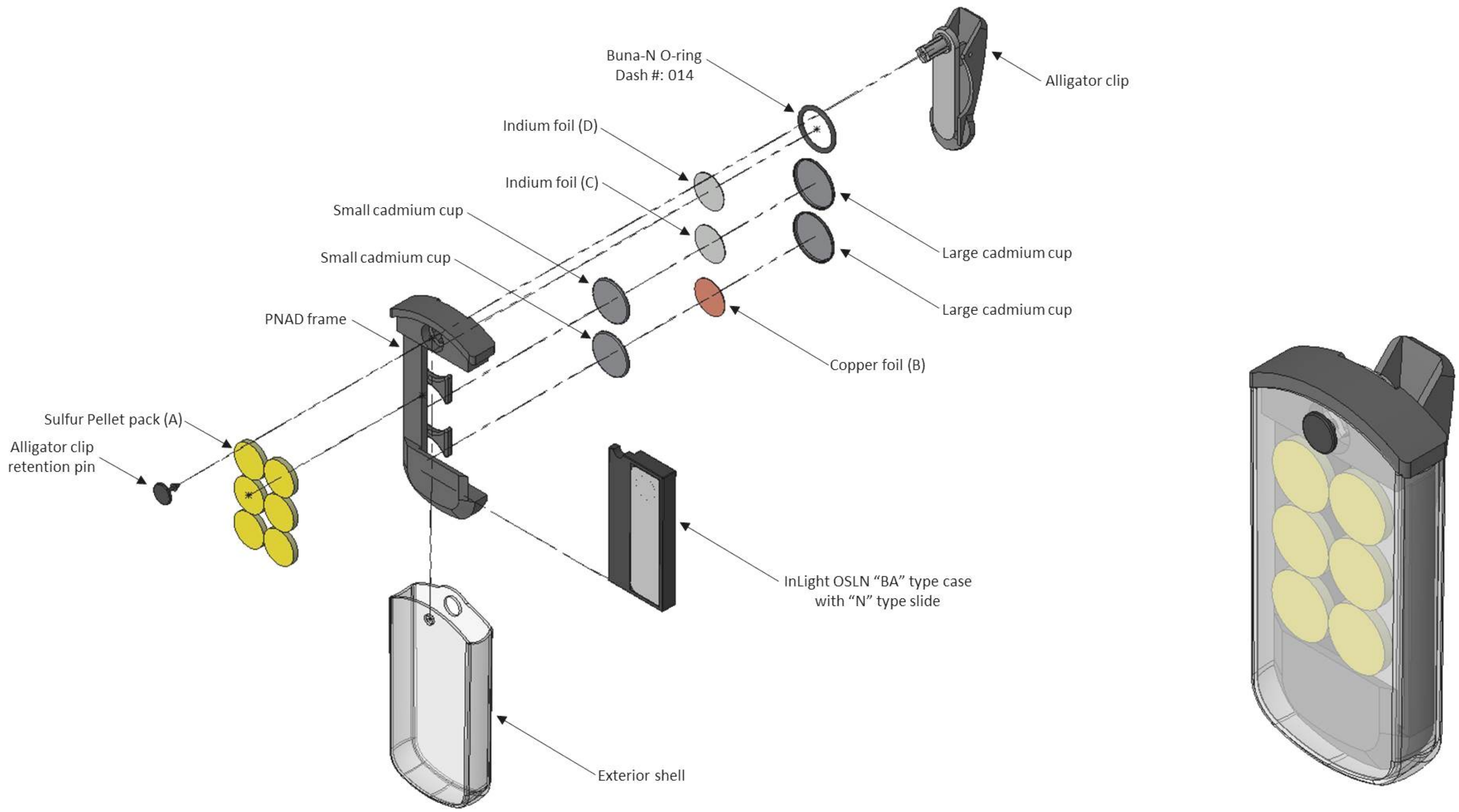

Figure A.2 PNNL PNAD Exploded View

Table A.1 PNNL PNAD Component Dimensions and Composition

Description	Detector	Composition	nominal density (g/cm^3)	diameter (cm)	length (cm)	Width (cm)	Nominal Thickness (cm) **	Nominal Mass (g)	nominal density thickness (g/cm^2)**
clear tape cover on exterior shell (3M 8412)		PF	1.34	n/a	5.51	2.54	0.015	0.286	0.020
exterior clear plastic shell		PC	1.2	n/a	7.1	3.6	0.089	5.62	0.107
orange cardstock label		paper	0.77	n/a	5.56	4.13	0.023	0.404	0.018
heat sealed bag for sulfur pellets		LDPE	0.902	n/a	3.81	2.9	0.010	n/a	0.00917
sulfur pellet (single) 0.5" dia. x 0.075" thick		S	1.8	1.27	n/a	n/a	0.191	0.435	0.343
sulfur pellet six pack (1" x 1.5" x 0.075")	A	S	1.8	n/a	3.81	2.54	0.191	2.61	0.343
black plastic PNAD frame (overall)		PET	1.15	n/a	n/a	n/a	n/a	4.86	n/a
black plastic PNAD frame (thick section)		PET	1.15	n/a	n/a	n/a	0.508	n/a	0.584
black plastic PNAD frame (thin section)		PET	1.15	n/a	n/a	n/a	0.292	n/a	0.336
lip of black plastic InLight Case		ABS	1.06	n/a	n/a	n/a	0.292	n/a	0.310
small cadmium cup		Cd	8.69	1.52	n/a	n/a	0.051	1.15	0.441
copper foil (inside Cd cups)	B	Cu	8.96	1.27	n/a	n/a	0.025	0.281	0.228
indium foil (inside Cd cups)	C	In	7.31	1.27	n/a	n/a	0.025	0.236	0.186
large cadmium cup		Cd	8.69	1.68	n/a	n/a	0.051	1.22	0.441
Indium foil (bare)	D	In	7.31	1.27	n/a	n/a	0.025	0.236	0.186
clear tape covering on foils (3M 142)		polyester	1.14	1.27	n/a	n/a	0.006	n/a	0.00723
black plastic InLight OSLN case		ABS plastic, Toyolac 10081 black, aluminum filter, copper filter,	1.06	n/a	4.91	2.30	0.554	n/a	n/a
"N" type slide		ABS plastic, black	1.06	n/a	4.70	1.18	0.191	n/a	n/a
Al2O3:C detectors on "N" type slide		Al_2O_3:C, $^6Li_2CO_3$	3.95	0.724	n/a	n/a	0.028	0.021	0.051
Heat sealed bag for InLight BA case		LDPE	1.04	n/a	5.72	2.86	0.004	n/a	0.0040

NOTES:

**	for clear plastic PNAD outer shell and for polyethylene heat sealed bags (sulfur pellet bag and InLight bag), the listed thickness or density thickness is the wall thickness. For adhesive tape, the listed thickness or density thickness is for a single layer and includes the adhesive.
LDPE	low density polyethylene
PET	polyethylene terephthalate
PC	polycarbonate
PF	3M 8412 polyester film tape
S	sulfur pellet
Cu	copper metal
In	indium metal
Cd	cadmium metal
air	dry air at STP

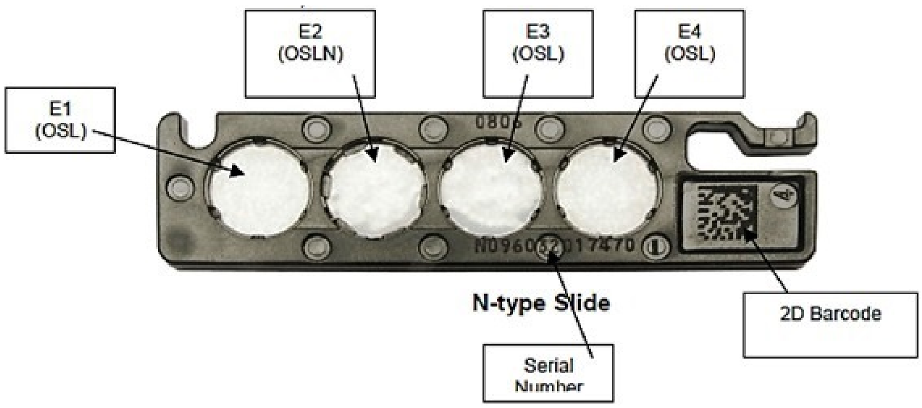

Figure A.3 N-type slide for InLight® OSLN "BA" type case

Figure A.4 InLight® OSLN "BA" type case

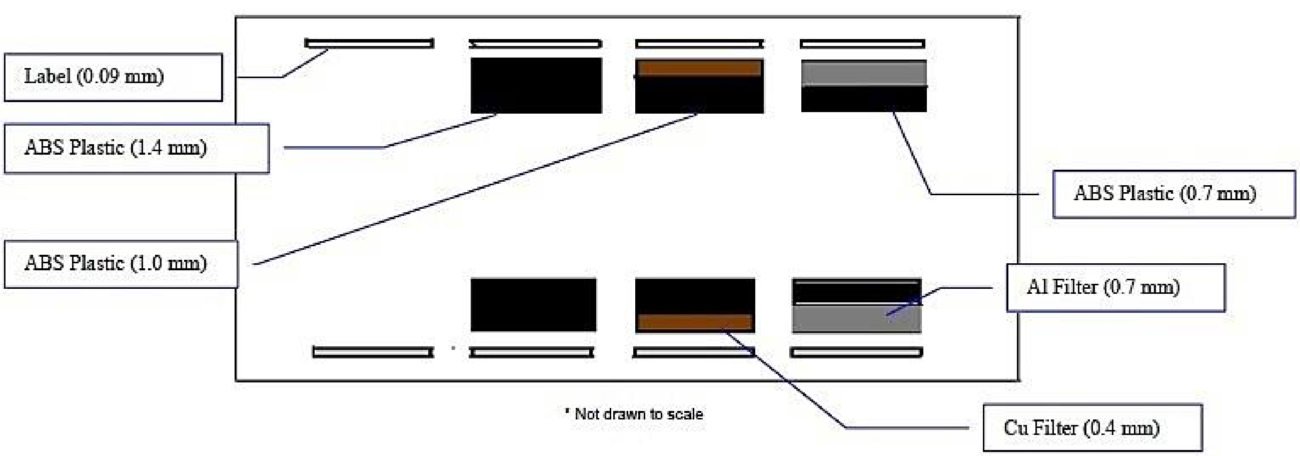

Figure A.4 InLight® OSLN BA case filtration

Table A.2 PNAD Filtration in front of and behind OSL/OSLN elements

	Material	Density (g/cm^3)	Thickness (mm)	Density Thickness (mg/cm^2)			
				Element 1 (E1)	Element 2 (E2)	Element 3 (E3)	Element 4 (E4)
FRONTSIDE	clear polyester film tape (3M 8412)	1.34	0.152	20.4	20.4	20.4	20.4
	clear polycarbonate Shell	1.21	0.76	-	92.2	92.2	92.2
	orange cardstock paper label	0.77	0.23	17.6	17.6	17.6	17.6
	polyethylene bag (wall)	0.90	0.10	9.17	9.17	9.17	9.17
	sulfur pellet	1.8	1.91	343	343	343	343
	polyethylene bag (wall)	0.90	0.10	9.17	9.17	9.17	9.17
	BA case paper label (PNAD number)	0.77	0.10	7.82	7.8	7.8	7.8
	BA filter cover label (blank) - polyester	1.01	0.09	9.09	9.09	9.09	9.09
	(ABS) plastic case - E2	1.26	0.70	-	88.2	-	-
	(ABS) plastic case - E3	1.26	1.00	-	-	126	-
	(ABS) plastic case - E4	1.26	0.70	-	-	-	88.2
	ABS plastic filter - E2	1.26	0.70	-	88.2	-	-
	Cu filter - E3	8.96	0.40	-	-	358	-
	Al filter - E4	2.7	0.70	-	-	-	189
	total in front of OSL or OSLN detector			416	685	993	786
OSL	Al_2O_3:C dots on "N" type slide	3.95	0.28	51.0	-	51.0	51.0
OSLN	Al_2O_3:C - $^6Li_2CO_3$ dot on "N" type slide	3.95	0.28	-	51.0	-	-
BACKSIDE	Al filter - E4	2.7	0.70	-	-	-	189
	Cu filter - E3	8.96	0.40	-	-	358	-
	ABS plastic filter - E2	1.26	0.70	-	88.2	-	-
	(ABS) plastic case - E4	1.26	0.70	-	-	-	88.2
	(ABS) plastic case - E3	1.26	1.00	-	-	126	-
	(ABS) plastic case - E2	1.26	0.70	-	88.2	-	-
	InLight barcode label - polyester	1.01	0.09	9.09	9.09	9.09	9.09
	clear polycarbonate shell	1.21	0.76	92.2	92.2	92.2	92.2
	total behind OSL or OSLN detector			101	278	586	378

Appendix B

PNNL FNAD Design Features

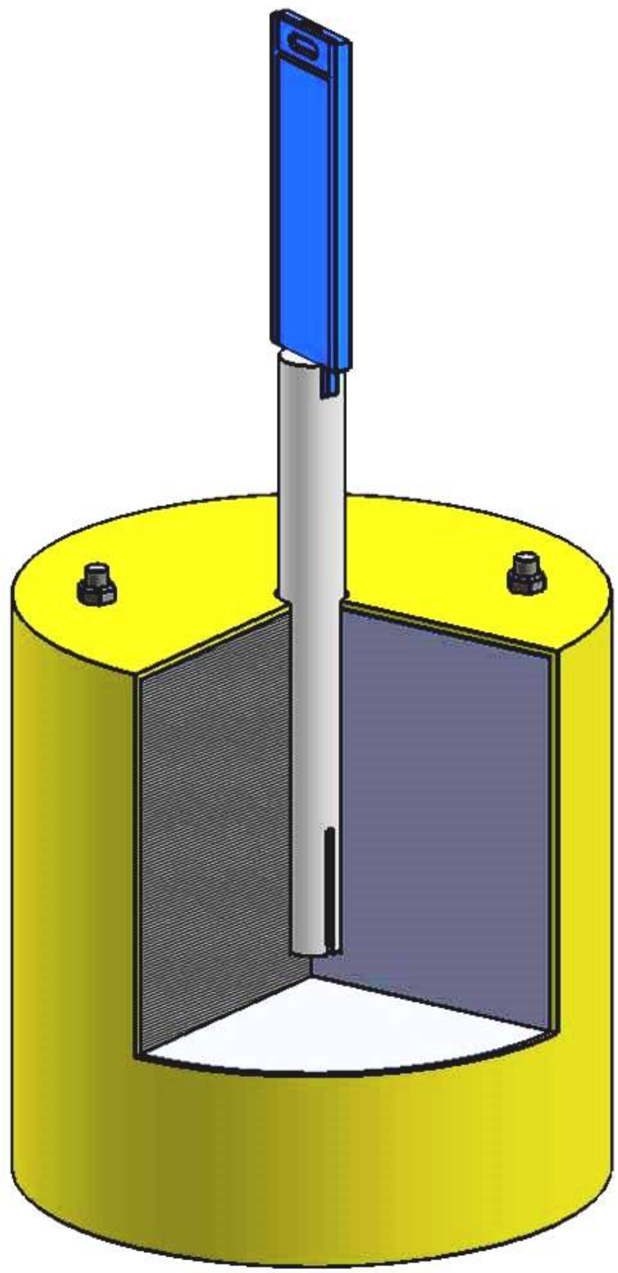

Figure B.1 PNNL FNAD

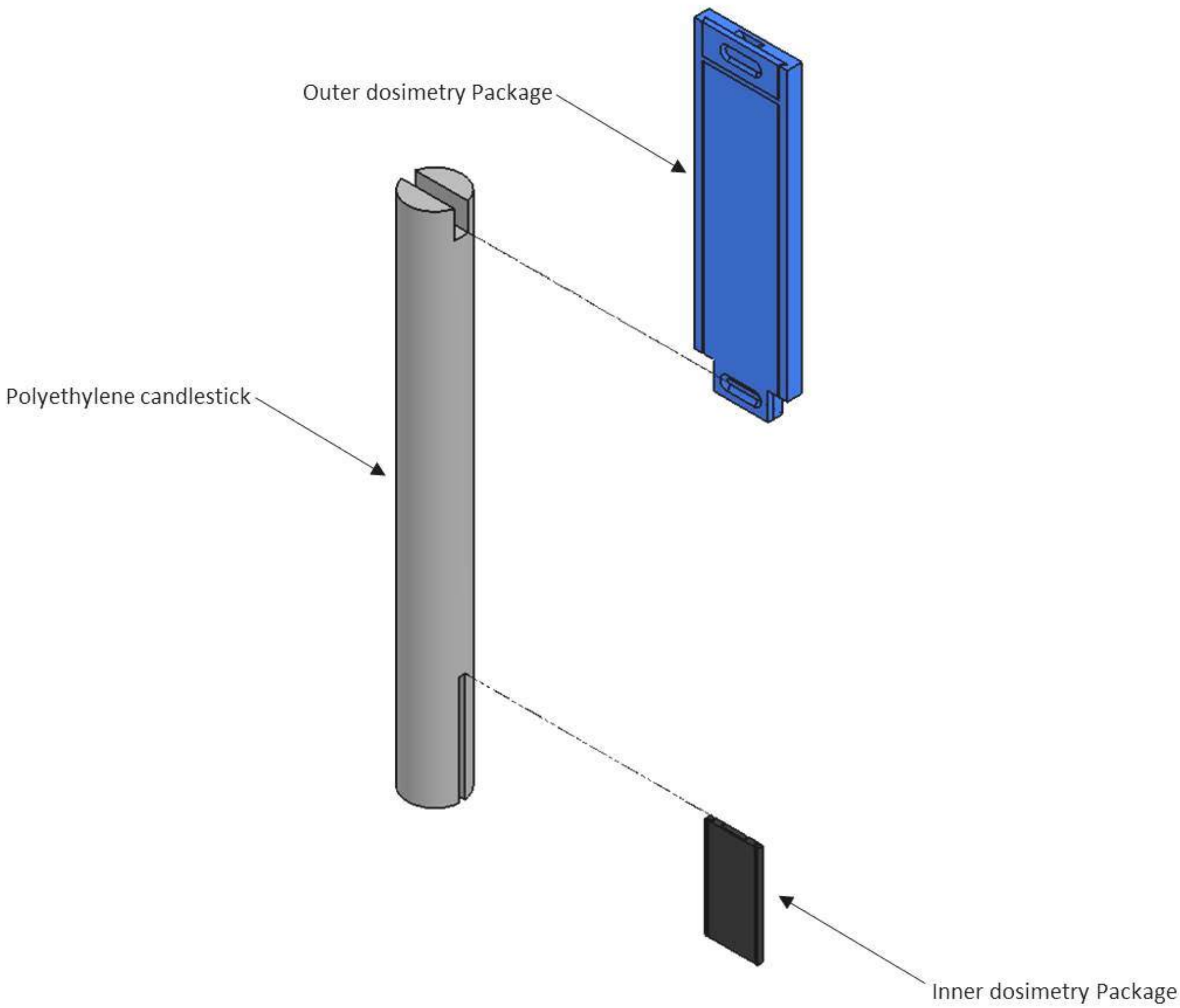

Figure B.2 PNNL FNAD “Candle” Assembly with Inner and Outer Dosimetry Packages

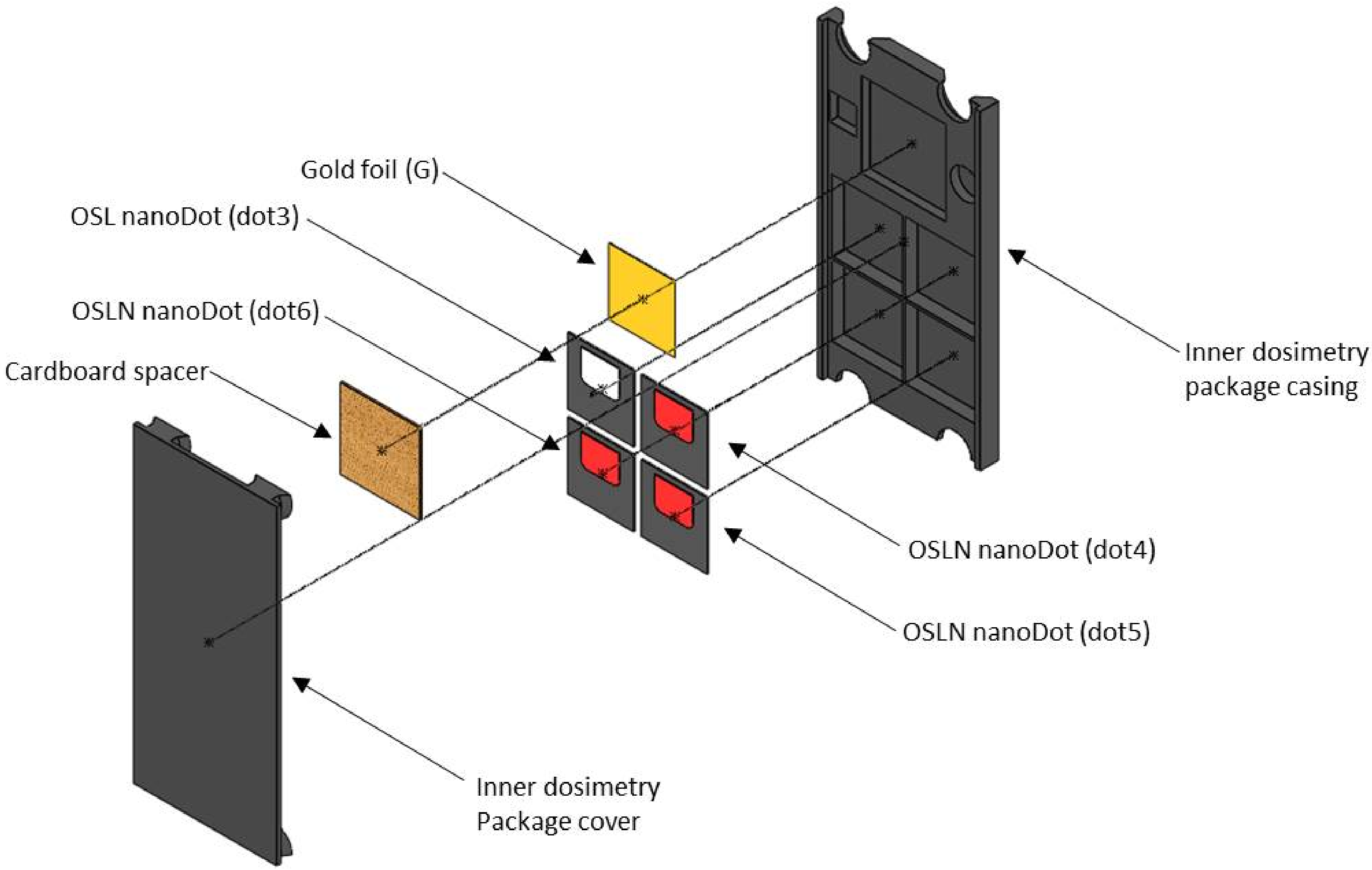

Figure B.3 PNNL FNAD Inner Dosimetry Package (exploded view)

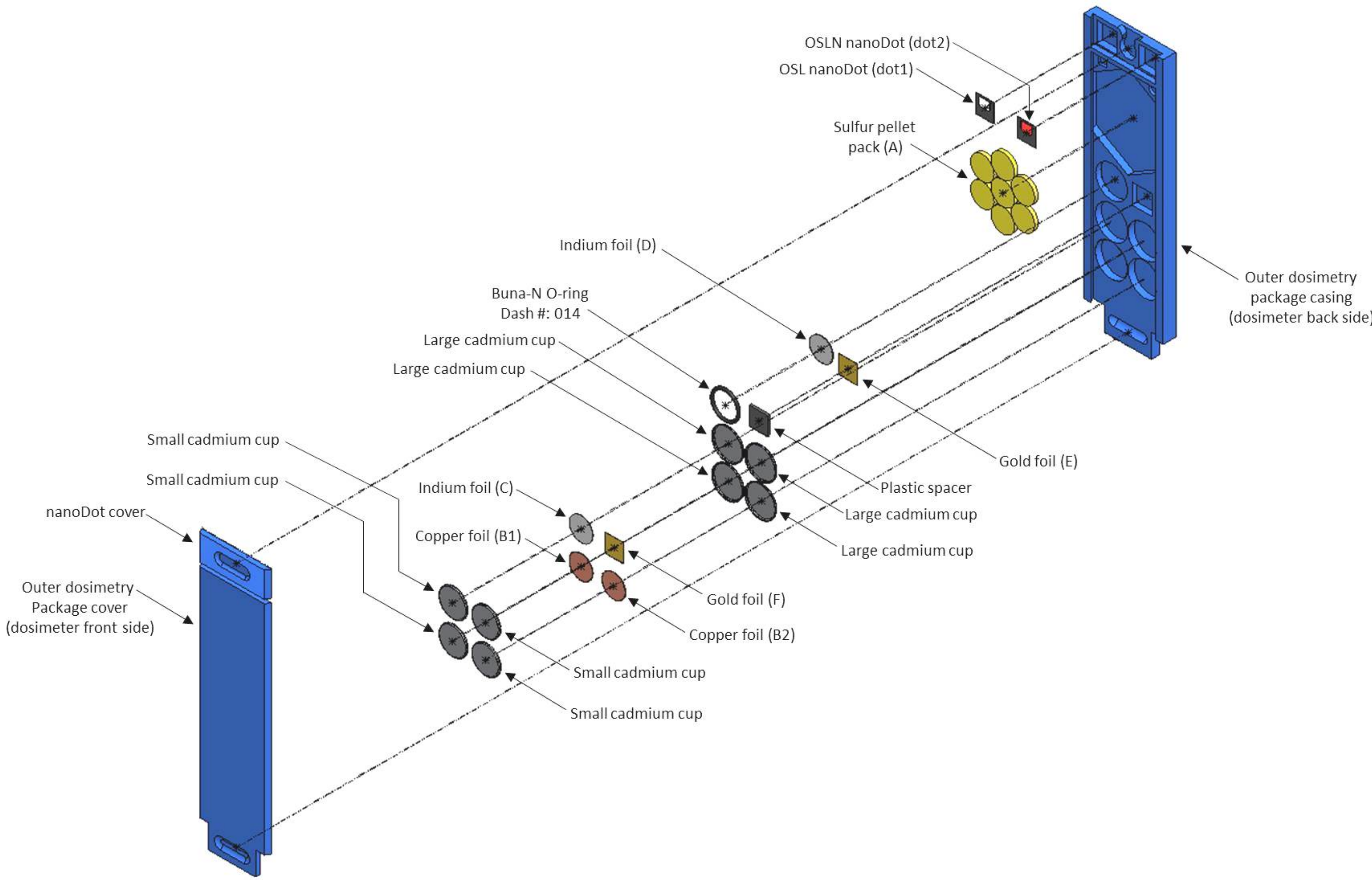

Figure B.4 PNNL FNAD Outer Dosimetry Package (exploded view)

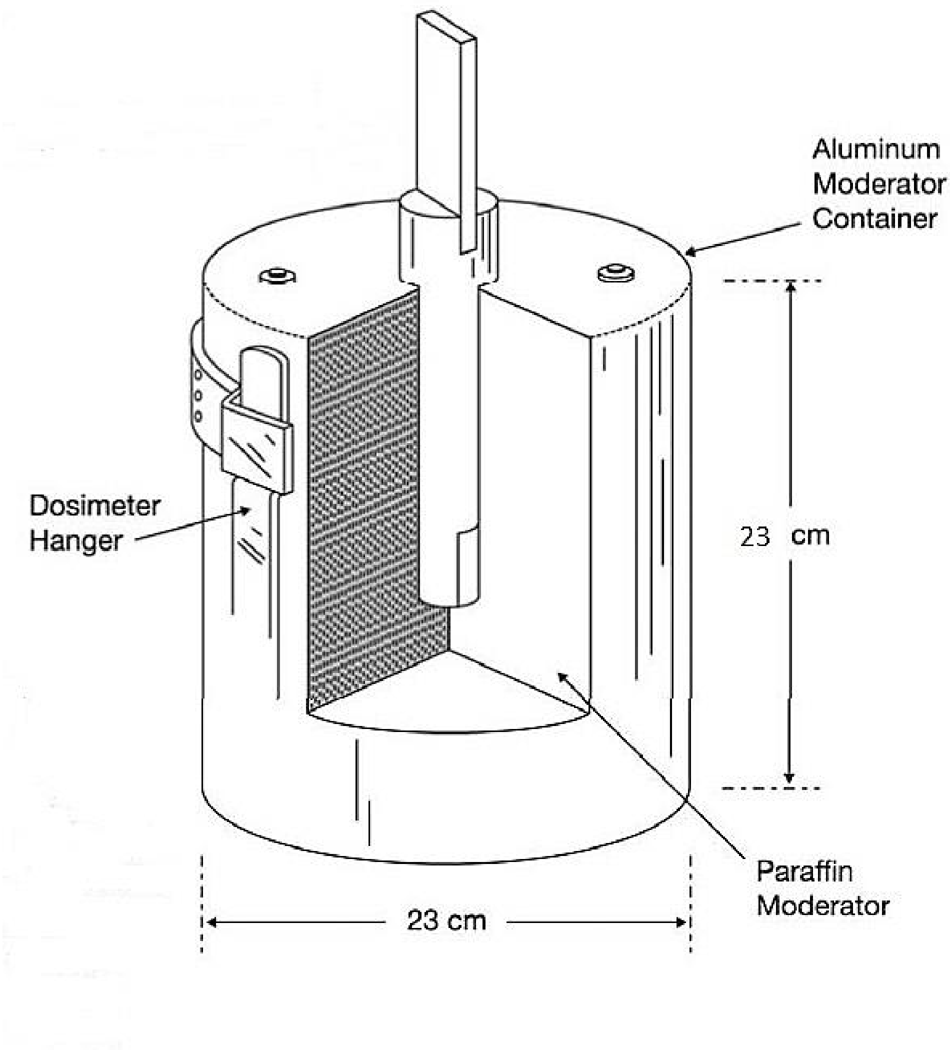

Figure B.5 PNNL FNAD Cylindrical Moderator Dimensions

Table B.1 PNNL FNAD Component Dimensions and Composition

Drawing	Component Name	Component Position	Composition	Outer Dimensions (nominal)				Attenuation Thickness[1] (cm)	Nominal density (g/cm^3)	Nominal Mass (g)	Nominal density thickness (g/cm^2)
				Length (cm)	Width (cm)	Thickness (cm)	Diameter (cm)				
Outer Dosimetry Package	sulfur pellet 7 pack	A	S	4.8	4.1	0.191	1.27	0.191	1.8	3.07	0.343
	copper foil (B1)	B1	Cu	n/a	n/a	0.025	1.27	0.025	8.96	0.281	0.228
	large cadmium cup	B1	Cd	n/a	n/a	0.051	1.68	0.051	8.69	1.22	0.441
	small cadmium cup	B1	Cd	n/a	n/a	0.051	1.52	0.051	8.69	1.15	0.441
	copper foil (B2)	B2	Cu	n/a	n/a	0.025	1.27	0.025	8.96	0.281	0.228
	large cadmium cup	B2	Cd	n/a	n/a	0.051	1.68	0.051	8.69	1.22	0.441
	small cadmium cup	B2	Cd	n/a	n/a	0.051	1.52	0.051	8.69	1.15	0.441
	indium foil (C)	C	In	n/a	n/a	0.025	1.27	0.025	7.31	0.236	0.186
	large cadmium cup	C	Cd	n/a	n/a	0.051	1.68	0.051	8.69	1.22	0.441
	small cadmium cup	C	Cd	n/a	n/a	0.051	1.52	0.051	8.69	1.15	0.441
	Indium foil (D)	D	In	n/a	n/a	0.025	1.27	0.025	7.31	0.236	0.186
	O-ring spacer	D	Buna-N rubber	n/a	n/a	0.178	1.60	0.000	1.3	n/a	n/a
	gold foil (E)	E	Au	1	1	0.013	n/a	0.013	19.3	0.250	0.245
	plastic spacer	E	PET	1	1	0.140	n/a	0.140	1.15	0.161	0.161
	gold foil (F)	F	Au	1	1	0.013	n/a	0.013	19.3	0.250	0.245
	large cadmium cup	F	Cd	n/a	n/a	0.051	1.68	0.051	8.69	1.22	0.441
	small cadmium cup	F	Cd	n/a	n/a	0.051	1.52	0.051	8.69	1.15	0.441
	OSL nanoDot	dot1	ABS + Al_2O_3:C	0.99	1.01	0.191	n/a	0.046	n/a	n/a	n/a
	OSLN nanoDot	dot2	ABS + Al_2O_3:C	0.99	1.01	0.191	n/a	0.046	n/a	n/a	n/a
	nanoDot Cover Plate	dot1, dot2	PET	1.42	3.78	0.229	n/a	0.229	1.15	n/a	0.263
	foil coverpPlate	A, B1, B2, C, D, E, F	PET	13.13	3.78	0.254	n/a	0.254	1.15	n/a	0.292
	detector tray	A, B1, B2, C, F, dot1, dot2	PET	14.71	4.37	0.711	n/a	0.102	1.15	n/a	0.117
	detector tray	D, E	PET	14.71	4.37	0.711	n/a	0.152	1.15	n/a	0.175
Inner Dosimetry Package	gold foil (G)	G	Au	1.00	1.00	0.013	n/a	0.013	19.3	0.250	0.245
	cardboard spacer	G	paper	1.00	1.00	0.058	n/a	0.058	0.75	0.044	0.044
	OSL nanoDot	dot3	ABS + Al_2O_3:C	0.99	1.01	0.191	n/a	0.046	n/a	n/a	n/a
	OSLN nanoDot	dot4	ABS + Al_2O_3:C	0.99	1.01	0.191	n/a	0.046	n/a	n/a	n/a
	OSLN nanoDot	dot5	ABS + Al_2O_3:C	0.99	1.01	0.191	n/a	0.046	n/a	n/a	n/a
	OSLN nanoDot	dot6	ABS + Al_2O_3:C	0.99	1.01	0.191	n/a	0.046	n/a	n/a	n/a
	detector tray	dot3, dot4, dot5, dot6	PET	4.70	2.46	0.208	n/a	0.013	1.15	n/a	0.015
	detector tray	G	PET	4.70	2.46	0.208	n/a	0.076	1.15	n/a	0.088
	detector cover plate	G, dot3, dot4, dot5, dot6	PET	4.70	2.20	0.061	n/a	0.061	1.15	n/a	0.070
Cylindrical Moderator	paraffin moderator	n/a	paraffin filled aluminum can	23.0	n/a	n/a	23.0	10.2	0.93	n/a	9.51
Candle Assembly	polyethylene candlestick	n/a	polyethylene	24.1	n/a	n/a	2.54	1.27	0.94	n/a	1.19

Notes:

1 Attenuation thickness is the thickness of the part material that lies in the path of a normally incident beam of radiation passing through the sensitive volume of the detector. For foils and pellets, this is the same as the foil or pellet thickness. For detector trays, this will be less than the nominal outer dimension thickness.

Appendix C

Irradiation Locations in the DAF

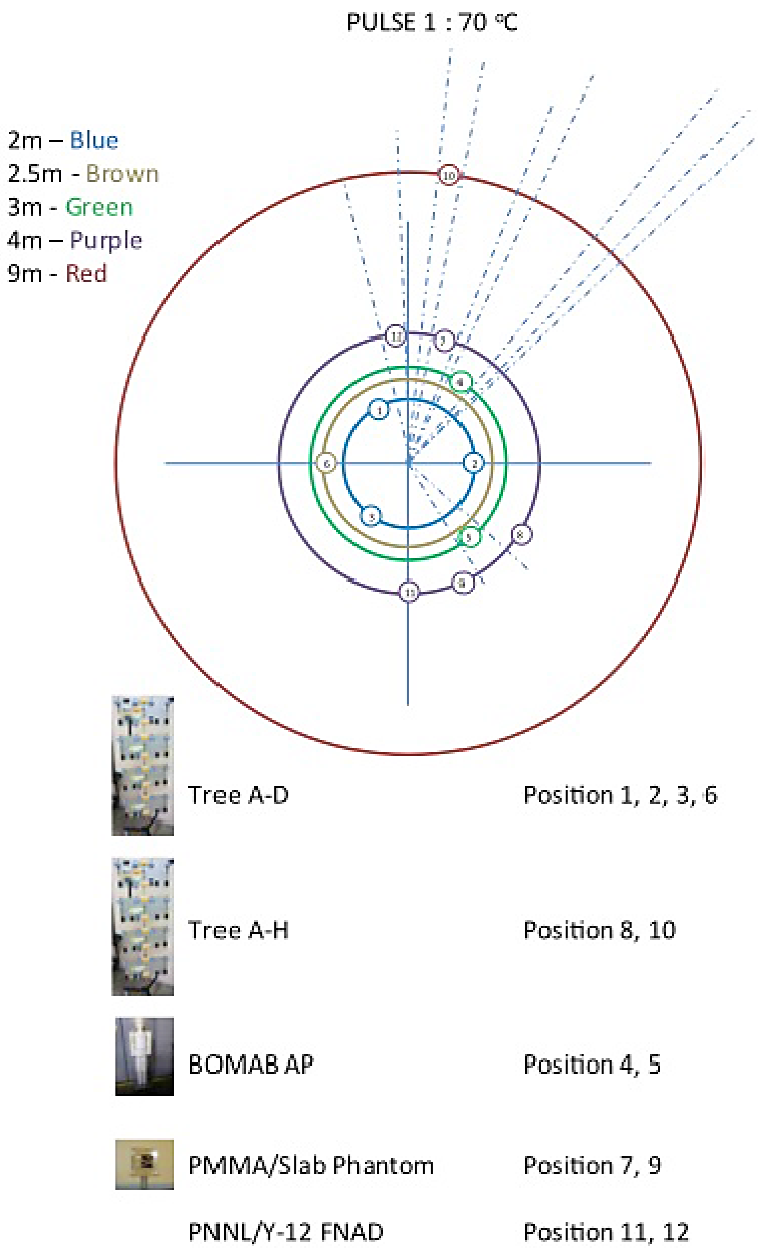

Figure C.1 Irradiation Locations for Pulse 1

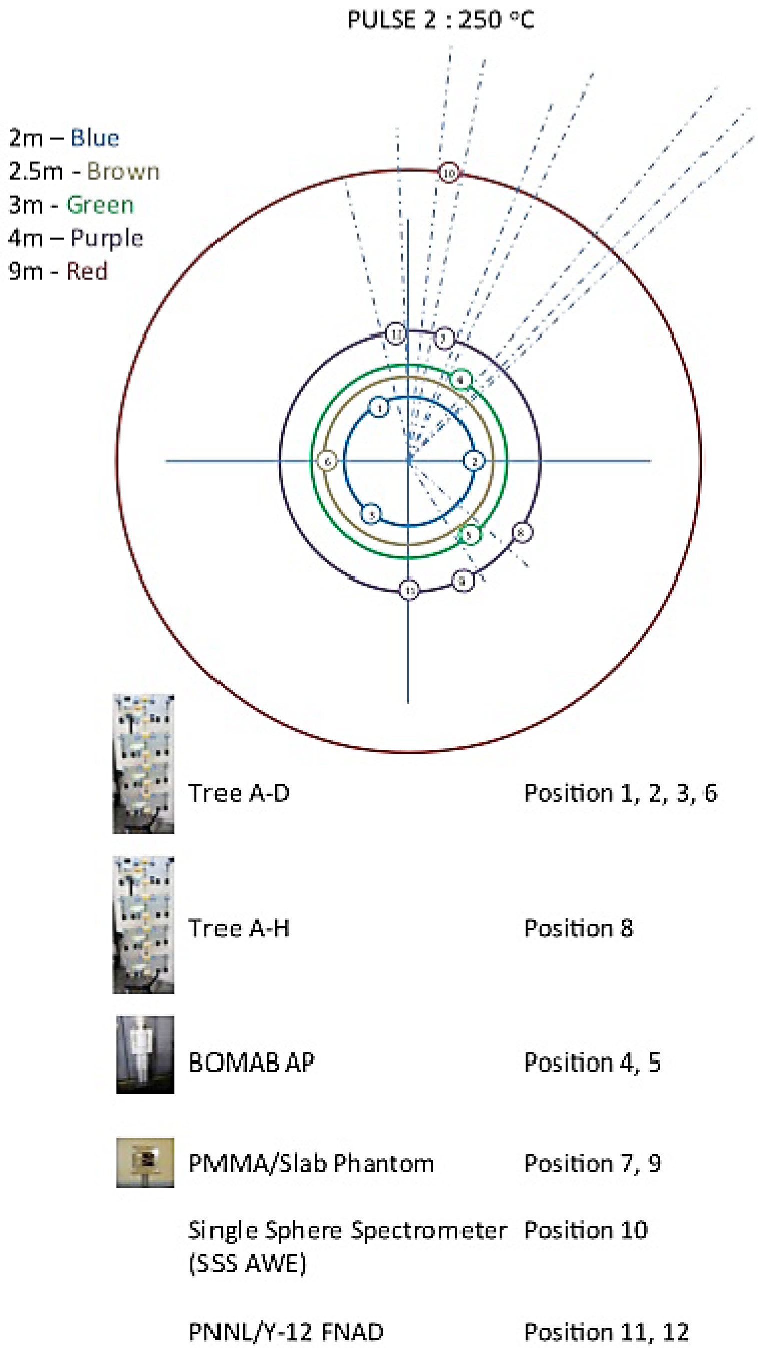

Figure C.2 Irradiation Locations for Pulse 2

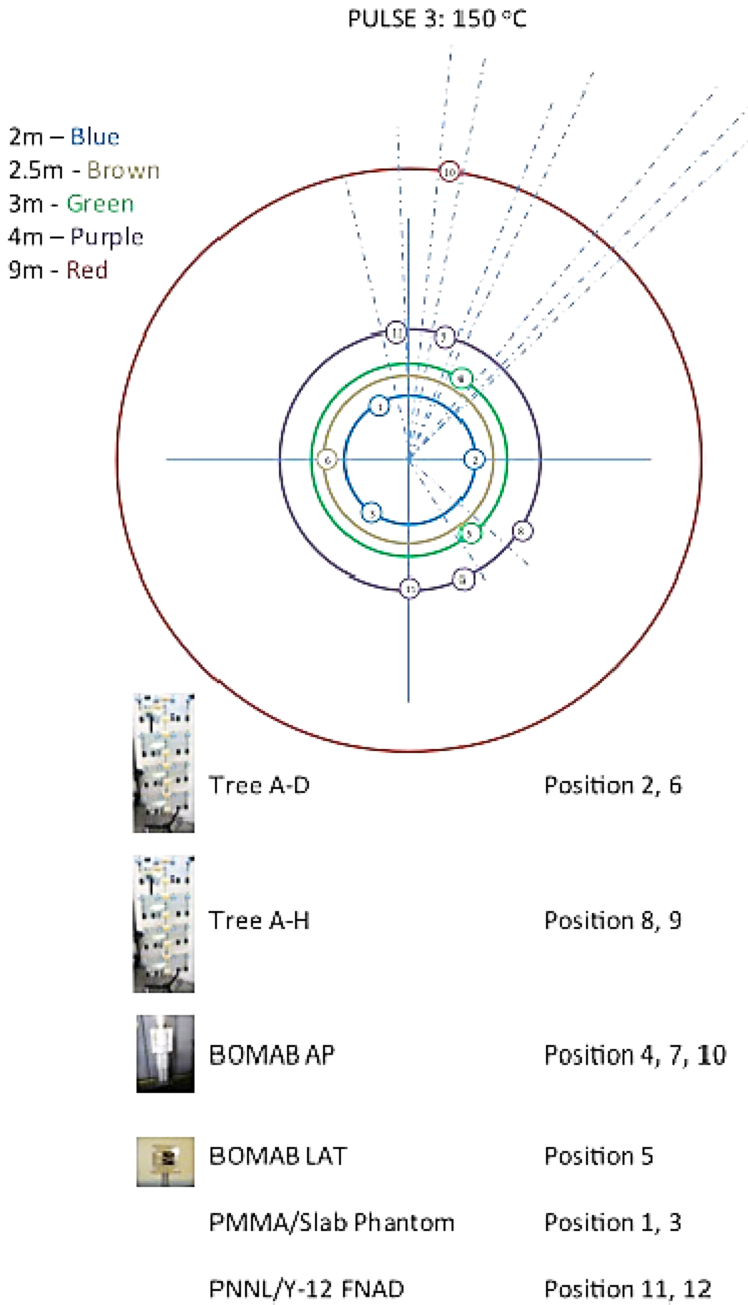

Figure C.3 Irradiation Locations for Pulse 3

Table C.1 Dosimeter Placement at Irradiation Locations for Pulses 1,2 and 3

Pulse #	Position #	distance (m)	phantom type	PNNL PNADs (InLight shell)			Hanford PNADs (flat plate assembly)			EPDs					FNADS	RadWatch Dosimeters
				front	back	total	5mil	10 mil	total	Thermo Mark 2.5	Mirion-MGP DMC3000	Mirion-MGP DMC2000	Miron-MGP DMC3000	Total		
1	1	2	Tree A-D	PNAD1, PNAD2		2			0					0		
	2	2	Tree A-D	PNAD3, PNAD4		2	PNAD61	PNAD62	2					0		
	3	2	Tree A-D			0			0					0		
	4	3	BOMAB	PNAD5	PNAD6	2			0					0		RW1, RW2
	5	3	BOMAB	PNAD7	PNAD8	2			0					0		
	6	2.5	Tree A-D	PNADs 9, 10, 11, 12		4			0					0		
	7	4	PMMA	PNAD13		1			0					0		
	8	4	Tree A-H	PNAD15, PNAD16		2			0					0		
	9	4	PMMA		PNAD 14	1			0					0		
	10	9	Tree A-H			0			0	EPD1	EPD2	EPD3	EPD4	4		
	11	4	FNAD			0			0					0	FNAD71	
	12	4	FNAD			0			0					0		
						16			2					4	1	2
2	1	2	Tree A-D	PNAD17, PNAD18		2			0	EPD5	EPD6			2		
	2	2	Tree A-D			0	PNAD63	PNAD64	2			EPD7		1		
	3	2	Tree A-D	PNAD19, PNAD20		2			0					0		
	4	3	BOMAB	PNAD21	PNAD22	2			0					0		RW3, RW4
	5	3	BOMAB	PNAD23	PNAD24	2			0					0		
	6	2.5	Tree A-D	PNAD27, PNAD28		2			0					0		
	7	4	PMMA	PNAD25		1			0					0		
	8	4	Tree A-H	PNAD29,30	PNAD31, PNAD32	4			0					3		
	9	4	PMMA		PNAD26	1			0					0		
	10	9	SSS-AWE			0			0					0		
	11	4	FNAD			0			0					0	FNAD72	
	12	4	FNAD			0			0					0		
						16			2					6	1	2
3	1	2	PMMA		PNAD44	1			0					0		
	2	2	Tree A-D			0	PNAD65	PNAD66	2					0		
	3	2	PMMA	PNAD45		1			0					0		
	4	3	BOMAB	PNAD34	PNAD35	2			0					0		
	5	3	BOMAB - LAT	PNAD36	PNAD37	2			0					0		
	6	2.5	Tree A-D	PNAD33	PNAD42	2			0					0		
	7	4	BOMAB	PNAD38	PNAD39	2			0					0		RW5, RW6
	8	4	Tree A-H			0			0	EPD8	EPD9	EPD10		3		
	9	4	Tree A-H	PNAD43	PNAD46	2			0					0		
	10	9	BOMAB	PNAD41	PNAD40	2			0					0		
	11	4	FNAD			0			0					0	FNAD73	
	12	4	FNAD			0			0					0		
						14			2					3	1	2
					Exercise Total	46		Exercise Total	6				Exercise Totals	13	3	6

Appendix D

Reference Dose Information for Godiva-IV Exercise

Table D.1.1 Pulse 1 Reference Fluence and Dose Values by Position

Pulse 1

Burst Temperature (°C) :	**68.5**
Burst Date/Time:	**5/24/2016 10:11**

TOTAL NEUTRON DOSES

Distance (m)	Position	Total Fluence (n/cm^2)	Tiss. KERMA Dose (Gy)	ANSI 13.3 Dp(10) (Gy)	ANSI 13.3 D*(10) (Gy)	Auxier et. al. Element 57 (Gy)	IAEA 211 (Gy)	NCRP 38 (Gy)
2	1	1.01E+11	1.60	2.14	2.06	2.04	1.98	2.08
2	2	9.59E+10	1.53	2.05	1.98	1.96	1.89	1.99
2	3	1.01E+11	1.59	2.13	2.05	2.03	1.97	2.07
2.5	6	8.58E+10	1.17	1.59	1.53	1.53	1.47	1.56
3	4	6.55E+10	0.90	1.23	1.19	1.19	1.14	1.21
3	5	6.77E+10	0.92	1.26	1.21	1.21	1.17	1.24
4	7	5.10E+10	0.64	0.89	0.86	0.86	0.83	0.88
4	8	5.33E+10	0.66	0.92	0.88	0.89	0.86	0.91
4	9	5.46E+10	0.66	0.92	0.89	0.90	0.86	0.92
9	10	2.86E+10	0.13	0.39	0.38	0.38	0.38	0.40
4	11	5.30E+10	0.65	0.91	0.88	0.88	0.85	0.90

Position 11 fluence, tissue KERMA and dose values estimated from average of Positions 7,8 and 9.

Table D.1.2 Pulse 1 Reference Fluence Values by Distance

68.5 °C Average Fluence (1.6E-9 to 14 MeV)			
Distance (m)	Total Fluence (n/cm^2)	+/- 1s (%)	Comments
2	9.93E+10	2.78%	@ 156 - 197 cm height to top of 30.5 cm plate(s)
2.5	8.58E+10	NA	@ 169 - 220 cm height to top of plate(s)
3	6.66E+10	2.40%	@ 169 - 220 cm height to top of plate(s)
4	5.30E+10	3.49%	@ 178 - 234 cm height to top of plate(s)
9	2.86E+10	NA	alcove

TableD.1.3 Pulse 1 Reference Tissue Kerma and Gamma Dose Values by Distance

68.5 °C Average Tissue KERMA Doses (1.6E-9 to 14 MeV)						
Distance (m)	Neutron KERMA (Gy)	+/- 1s (%)	Gamma Dose (Gy)	+/- 1s (%)	Total Dose (Gy)	Comments
2	1.57	2.23%	0.22	19%	1.79	@ 156 - 197 cm height to top of 30.5 cm plate(s)
2.5	1.17	NA	0.17	29%	1.34	@ 169 - 220 cm height to top of plate(s)
3	0.91	1.20%	0.14	43%	1.05	@ 169 - 220 cm height to top of plate(s)
4	0.66	1.62%	0.11	74%	0.77	@ 178 - 234 cm height to top of plate(s)
9	0.13	NA	0.02	NA	0.15	alcove
Gamma dose for 9m distance was estimated from the 4 meter dose using inverse square law.						

Table D.2.1 Pulse 2 Reference Fluence and Dose Values by Position

Pulse 2

Burst Temperature (°C) :	**244.8**
Burst Date/Time:	**5/25/2016 9:42**

TOTAL NEUTRON DOSES								
Distance (m)	Position	Total Fluence (n/cm^2)	Tiss. KERMA Dose (Gy)	ANSI 13.3 Dp(10) (Gy)	ANSI 13.3 D*(10) (Gy)	Auxier et. al. Element 57 (Gy)	IAEA 211 (Gy)	NCRP 38 (Gy)
2	1	3.60E+11	5.70	7.64	7.37	7.29	7.06	7.43
2	2	3.43E+11	5.47	7.32	7.07	6.99	6.77	7.12
2	3	3.60E+11	5.68	7.61	7.34	7.26	7.03	7.40
2.5	6	3.07E+11	4.17	5.70	5.48	5.47	5.26	5.59
3	4	2.34E+11	3.23	4.41	4.24	4.24	4.09	4.33
3	5	2.42E+11	3.29	4.50	4.32	4.32	4.17	4.42
4	7	1.82E+11	2.30	3.19	3.06	3.09	2.97	3.16
4	8	1.91E+11	2.37	3.29	3.16	3.18	3.06	3.26
4	9	1.95E+11	2.37	3.30	3.17	3.20	3.07	3.28
9	10	1.02E+11	0.45	1.41	1.35	1.37	1.35	1.42
4	11	1.89E+11	2.35	3.26	3.13	3.16	3.03	3.23

Position 11 fluence, tissue KERMA and dose values estimated from average of Positions 7,8 and 9.

Table D.2.2 Pulse 2 Reference Fluence Values by Distance

244.8 °C Average Fluence (1.6E-9 to 14 MeV)			
Distance (m)	Total Fluence (n/cm^2)	+/- 1s (%)	Comments
2	3.54E+11	2.78%	@ 156 - 197 cm height to top of 30.5 cm plate(s)
2.5	3.07E+11	NA	@ 169 - 220 cm height to top of plate(s)
3	2.38E+11	2.40%	@ 169 - 220 cm height to top of plate(s)
4	1.89E+11	4.21%	@ 178 - 234 cm height to top of plate(s)
9	1.02E+11	5.50%	alcove

Table D.2.3 Pulse 2 Reference Tissue Kerma and Gamma Dose Values by Distance

244.8 °C Average Tissue KERMA Doses (1.6E-9 to 14 MeV)						
Distance (m)	Neutron KERMA (Gy)	+/- 1s (%)	Gamma Dose (Gy)	+/- 1s (%)	Total Dose (Gy)	Comments
2	5.62	2.23%	0.78	19%	6.40	@ 156 - 197 cm height to top of 30.5 cm plate(s)
2.5	4.17	NA	0.61	29%	4.78	@ 169 - 220 cm height to top of plate(s)
3	3.26	1.20%	0.50	43%	3.76	@ 169 - 220 cm height to top of plate(s)
4	2.35	1.62%	0.40	74%	2.75	@ 178 - 234 cm height to top of plate(s)
9	0.45	NA	0.08	NA	0.53	alcove
Gamma dose for 9m distance was estimated from the 4 meter dose using inverse square law.						

Table D.3.1 Pulse 3 Reference Fluence and Dose Values by Position

Pulse 3								
Burst Temperature (°C) :		**147.7**						
Burst Date/Time:		**5/26/2016 11:35**						
TOTAL NEUTRON DOSES								
Distance (m)	Position	Total Fluence (n/cm^2)	Tiss. KERMA Dose (Gy)	ANSI 13.3 Dp(10) (Gy)	ANSI 13.3 D*(10) (Gy)	Auxier et. al. Element 57 (Gy)	IAEA 211 (Gy)	NCRP 38 (Gy)
2	1	2.17E+11	3.44	4.61	4.45	4.40	4.26	4.48
2	2	2.07E+11	3.30	4.42	4.27	4.22	4.08	4.30
2	3	2.17E+11	3.43	4.59	4.43	4.38	4.24	4.47
2.5	6	1.85E+11	2.52	3.44	3.30	3.30	3.18	3.37
3	4	1.41E+11	1.95	2.66	2.56	2.56	2.47	2.61
3	5	1.46E+11	1.98	2.71	2.61	2.61	2.51	2.67
4	7	1.10E+11	1.39	1.92	1.85	1.86	1.79	1.91
4	8	1.15E+11	1.43	1.99	1.90	1.92	1.84	1.97
4	9	1.18E+11	1.43	1.99	1.91	1.93	1.85	1.98
9	10	6.17E+10	0.27	0.850	0.810	0.83	0.810	0.860
4	11	1.14E+11	1.42	1.97	1.89	1.90	1.83	1.95

Position 11 fluence, tissue KERMA and dose values estimated from average of Positions 7,8 and 9.

Table D.3.2 Pulse 3 Reference Fluence Values by Distance

147.7 °C Average Fluence (1.6E-9 to 14 MeV)			
Distance (m)	Total Fluence (n/cm2)	+/- 1s (%)	Comments
2	2.14E+11	2.78%	@ 156 - 197 cm height to top of 30.5 cm plate(s)
2.5	1.85E+11	NA	@ 169 - 220 cm height to top of plate(s)
3	1.44E+11	2.40%	@ 169 - 220 cm height to top of plate(s)
4	1.14E+11	3.49%	@ 178 - 234 cm height to top of plate(s)
9	6.17E+10	5.50%	alcove

Table D.3.3 Pulse 3 Reference Tissue Kerma and Gamma Dose Values by Distance

147.7 °C Average Tissue KERMA Doses (1.6E-9 to 14 MeV)						
Distance (m)	Neutron KERMA (Gy)	+/- 1s (%)	Gamma Dose (Gy)	+/- 1s (%)	Total Dose (Gy)	Comments
2	3.39	2.23%	0.47	19%	3.86	@ 156 - 197 cm height to top of 30.5 cm plate(s)
2.5	2.52	NA	0.37	29%	2.89	@ 169 - 220 cm height to top of plate(s)
3	1.97	1.20%	0.30	43%	2.27	@ 169 - 220 cm height to top of plate(s)
4	1.42	1.62%	0.24	74%	1.66	@ 178 - 234 cm height to top of plate(s)
9	0.27	NA	0.05	NA	0.32	alcove
Gamma dose for 9m distance was estimated from the 4 meter dose using inverse square law.						

Appendix E

Godiva-IV Neutron Energy Spectra at Dosimeter Irradiation Locations

Table E.1 Neutron Energy Spectra at Dosimeter Irradiation Locations

Energy bin lower bound	Energy bin upper bound	Fluence Normalized to a 70°C Pulse (n/cm^2)								
MeV	MeV	Position 1 (2.0 m)	Position 2 (2.0 m)	Position 3 (2.0 m)	Position 4 (3.0 m)	Position 5 (3.0 m)	Position 6 (2.5 m)	Position 7 (4.0 m)	Position 8 (4.0 m)	Position 9 (4.0 m)
1.00E-09	1.58E-09	3.13E+05	2.81E+05	2.74E+05	2.14E+05	2.27E+05	2.56E+05	1.88E+05	1.98E+05	2.06E+05
1.58E-09	2.51E-09	2.30E+06	2.02E+06	1.88E+06	1.61E+06	1.73E+06	1.85E+06	1.42E+06	1.49E+06	1.57E+06
2.51E-09	3.98E-09	1.64E+07	1.45E+07	1.36E+07	1.15E+07	1.24E+07	1.33E+07	1.01E+07	1.07E+07	1.12E+07
3.98E-09	6.31E-09	8.03E+07	7.12E+07	6.77E+07	5.63E+07	6.02E+07	6.59E+07	4.94E+07	5.20E+07	5.46E+07
6.31E-09	1.00E-08	3.05E+08	2.72E+08	2.62E+08	2.14E+08	2.28E+08	2.53E+08	1.88E+08	1.97E+08	2.07E+08
1.00E-08	1.58E-08	6.99E+08	6.29E+08	6.12E+08	4.92E+08	5.22E+08	5.89E+08	4.31E+08	4.53E+08	4.73E+08
1.58E-08	2.51E-08	1.33E+09	1.20E+09	1.19E+09	9.37E+08	9.92E+08	1.14E+09	8.22E+08	8.63E+08	9.00E+08
2.51E-08	3.98E-08	1.90E+09	1.74E+09	1.74E+09	1.35E+09	1.43E+09	1.66E+09	1.19E+09	1.25E+09	1.30E+09
3.98E-08	6.31E-08	2.09E+09	1.92E+09	1.95E+09	1.50E+09	1.58E+09	1.87E+09	1.32E+09	1.38E+09	1.44E+09
6.31E-08	1.00E-07	2.14E+09	1.98E+09	2.04E+09	1.56E+09	1.64E+09	1.98E+09	1.37E+09	1.43E+09	1.49E+09
1.00E-07	1.58E-07	1.77E+09	1.65E+09	1.72E+09	1.31E+09	1.37E+09	1.68E+09	1.14E+09	1.20E+09	1.25E+09
1.58E-07	2.51E-07	1.15E+09	1.08E+09	1.14E+09	8.68E+08	9.09E+08	1.13E+09	7.58E+08	7.96E+08	8.32E+08
2.51E-07	3.98E-07	7.61E+08	7.17E+08	7.69E+08	5.88E+08	6.15E+08	7.71E+08	5.12E+08	5.39E+08	5.65E+08
3.98E-07	6.31E-07	7.20E+08	6.80E+08	7.35E+08	5.69E+08	5.94E+08	7.52E+08	4.95E+08	5.21E+08	5.48E+08
6.31E-07	1.00E-06	7.46E+08	7.04E+08	7.64E+08	6.01E+08	6.29E+08	7.96E+08	5.22E+08	5.51E+08	5.82E+08
1.00E-06	1.00E-02	2.11E+10	2.01E+10	2.21E+10	1.73E+10	1.82E+10	2.34E+10	1.50E+10	1.60E+10	1.69E+10
1.00E-02	5.04E-02	5.13E+09	4.91E+09	5.33E+09	3.86E+09	4.05E+09	5.36E+09	3.40E+09	3.64E+09	3.76E+09
5.04E-02	5.72E-02	3.28E+08	3.13E+08	3.37E+08	2.40E+08	2.52E+08	3.33E+08	2.02E+08	2.14E+08	2.22E+08
5.72E-02	6.51E-02	4.54E+08	4.34E+08	4.67E+08	3.32E+08	3.50E+08	4.61E+08	2.80E+08	2.96E+08	3.08E+08
6.51E-02	7.39E-02	4.25E+08	4.06E+08	4.37E+08	3.11E+08	3.27E+08	4.32E+08	2.62E+08	2.77E+08	2.88E+08
7.39E-02	8.37E-02	5.08E+08	4.85E+08	5.21E+08	3.68E+08	3.88E+08	5.11E+08	2.92E+08	3.11E+08	3.21E+08
8.37E-02	9.55E-02	4.17E+08	3.98E+08	4.27E+08	3.00E+08	3.16E+08	4.15E+08	2.19E+08	2.34E+08	2.40E+08
9.55E-02	1.08E-01	5.56E+08	5.31E+08	5.69E+08	4.00E+08	4.21E+08	5.54E+08	2.92E+08	3.13E+08	3.21E+08
1.08E-01	1.23E-01	5.46E+08	5.22E+08	5.59E+08	3.93E+08	4.14E+08	5.45E+08	2.87E+08	3.07E+08	3.15E+08
1.23E-01	1.40E-01	7.03E+08	6.71E+08	7.17E+08	4.97E+08	5.25E+08	6.88E+08	3.64E+08	3.91E+08	4.00E+08
1.40E-01	1.58E-01	6.14E+08	5.86E+08	6.25E+08	4.31E+08	4.55E+08	5.95E+08	3.16E+08	3.39E+08	3.46E+08
1.58E-01	2.01E-01	1.69E+09	1.62E+09	1.72E+09	1.19E+09	1.25E+09	1.64E+09	8.71E+08	9.35E+08	9.55E+08
2.01E-01	2.22E-01	7.73E+08	7.38E+08	7.82E+08	5.25E+08	5.54E+08	7.23E+08	3.87E+08	4.15E+08	4.22E+08
2.22E-01	2.47E-01	1.12E+09	1.07E+09	1.13E+09	7.58E+08	7.99E+08	1.04E+09	5.59E+08	5.99E+08	6.09E+08
2.47E-01	2.74E-01	9.50E+08	9.07E+08	9.61E+08	6.45E+08	6.81E+08	8.88E+08	4.76E+08	5.10E+08	5.18E+08
2.74E-01	3.05E-01	1.36E+09	1.30E+09	1.38E+09	9.25E+08	9.75E+08	1.27E+09	6.82E+08	7.31E+08	7.43E+08
3.05E-01	3.38E-01	1.23E+09	1.18E+09	1.24E+09	8.10E+08	8.51E+08	1.11E+09	5.99E+08	6.39E+08	6.47E+08
3.38E-01	3.78E-01	1.79E+09	1.71E+09	1.80E+09	1.16E+09	1.22E+09	1.59E+09	8.58E+08	9.14E+08	9.25E+08
3.78E-01	4.21E-01	2.00E+09	1.91E+09	2.01E+09	1.30E+09	1.36E+09	1.78E+09	9.60E+08	1.02E+09	1.04E+09
4.21E-01	4.66E-01	1.73E+09	1.66E+09	1.74E+09	1.13E+09	1.18E+09	1.54E+09	8.32E+08	8.87E+08	8.97E+08
4.66E-01	5.18E-01	2.40E+09	2.30E+09	2.41E+09	1.53E+09	1.59E+09	2.08E+09	1.13E+09	1.20E+09	1.21E+09
5.18E-01	6.01E-01	3.19E+09	3.05E+09	3.20E+09	1.96E+09	2.03E+09	2.64E+09	1.44E+09	1.52E+09	1.53E+09
6.01E-01	6.71E-01	2.99E+09	2.87E+09	3.00E+09	1.84E+09	1.90E+09	2.48E+09	1.35E+09	1.42E+09	1.43E+09
6.71E-01	7.41E-01	2.66E+09	2.54E+09	2.66E+09	1.63E+09	1.69E+09	2.20E+09	1.20E+09	1.26E+09	1.27E+09
7.41E-01	8.25E-01	3.27E+09	3.14E+09	3.28E+09	1.97E+09	2.02E+09	2.63E+09	1.44E+09	1.51E+09	1.51E+09
8.25E-01	9.16E-01	3.02E+09	2.90E+09	3.02E+09	1.73E+09	1.77E+09	2.29E+09	1.25E+09	1.30E+09	1.30E+09
9.16E-01	1.02E+00	2.65E+09	2.55E+09	2.65E+09	1.52E+09	1.56E+09	2.01E+09	1.10E+09	1.14E+09	1.14E+09
1.02E+00	1.13E+00	3.65E+09	3.51E+09	3.65E+09	2.10E+09	2.14E+09	2.77E+09	1.52E+09	1.57E+09	1.57E+09
1.13E+00	1.26E+00	3.40E+09	3.27E+09	3.40E+09	1.96E+09	1.99E+09	2.58E+09	1.41E+09	1.46E+09	1.46E+09
1.26E+00	1.42E+00	3.37E+09	3.24E+09	3.35E+09	1.84E+09	1.85E+09	2.35E+09	1.30E+09	1.33E+09	1.32E+09
1.42E+00	1.61E+00	2.77E+09	2.67E+09	2.75E+09	1.48E+09	1.49E+09	1.87E+09	1.04E+09	1.06E+09	1.05E+09
1.61E+00	1.85E+00	3.82E+09	3.67E+09	3.79E+09	2.05E+09	2.05E+09	2.58E+09	1.43E+09	1.45E+09	1.44E+09
1.85E+00	2.09E+00	3.48E+09	3.35E+09	3.46E+09	1.85E+09	1.85E+09	2.32E+09	1.29E+09	1.30E+09	1.29E+09
2.09E+00	2.38E+00	1.71E+09	1.65E+09	1.69E+09	8.73E+08	8.65E+08	1.06E+09	5.93E+08	5.89E+08	5.80E+08
2.38E+00	2.69E+00	1.90E+09	1.83E+09	1.87E+09	9.66E+08	9.58E+08	1.17E+09	6.57E+08	6.52E+08	6.42E+08
2.69E+00	3.07E+00	2.58E+09	2.48E+09	2.54E+09	1.31E+09	1.30E+09	1.59E+09	8.92E+08	8.86E+08	8.73E+08
3.07E+00	3.48E+00	1.19E+09	1.15E+09	1.17E+09	6.03E+08	5.98E+08	7.18E+08	4.06E+08	4.02E+08	3.94E+08
3.48E+00	3.96E+00	8.05E+08	7.74E+08	7.89E+08	4.04E+08	4.01E+08	4.76E+08	2.71E+08	2.67E+08	2.61E+08
3.96E+00	4.73E+00	1.51E+09	1.45E+09	1.48E+09	7.57E+08	7.51E+08	8.91E+08	5.07E+08	5.00E+08	4.89E+08
4.73E+00	5.31E+00	5.47E+08	5.26E+08	5.35E+08	2.75E+08	2.73E+08	3.22E+08	1.84E+08	1.81E+08	1.77E+08
5.31E+00	5.88E+00	1.86E+08	1.79E+08	1.82E+08	9.38E+07	9.36E+07	1.08E+08	6.23E+07	6.14E+07	5.98E+07
5.88E+00	6.43E+00	2.02E+08	1.94E+08	1.97E+08	1.02E+08	1.01E+08	1.17E+08	6.75E+07	6.65E+07	6.47E+07
6.43E+00	6.98E+00	2.25E+08	2.17E+08	2.20E+08	1.13E+08	1.13E+08	1.31E+08	7.54E+07	7.43E+07	7.23E+07
6.98E+00	7.52E+00	1.83E+08	1.76E+08	1.79E+08	9.22E+07	9.20E+07	1.06E+08	6.12E+07	6.04E+07	5.87E+07
7.52E+00	8.04E+00	1.26E+08	1.21E+08	1.23E+08	6.36E+07	6.35E+07	7.35E+07	4.23E+07	4.17E+07	4.06E+07
8.04E+00	8.56E+00	0.00E+00	0.00E+00	0.00E+00	0.00E+00	0.00E+00	0.00E+00	0.00E+00	0.00E+00	0.00E+00
8.56E+00	9.07E+00	0.00E+00	0.00E+00	0.00E+00	0.00E+00	0.00E+00	0.00E+00	0.00E+00	0.00E+00	0.00E+00
9.07E+00	9.57E+00	0.00E+00	0.00E+00	0.00E+00	0.00E+00	0.00E+00	0.00E+00	0.00E+00	0.00E+00	0.00E+00
9.57E+00	1.06E+01	0.00E+00	0.00E+00	0.00E+00	0.00E+00	0.00E+00	0.00E+00	0.00E+00	0.00E+00	0.00E+00
1.06E+01	1.16E+01	0.00E+00	0.00E+00	0.00E+00	0.00E+00	0.00E+00	0.00E+00	0.00E+00	0.00E+00	0.00E+00
1.16E+01	1.45E+01	0.00E+00	0.00E+00	0.00E+00	0.00E+00	0.00E+00	0.00E+00	0.00E+00	0.00E+00	0.00E+00

Appendix F

Activity Measurement Results for PNAD and FNAD Components

Table F.1 Specific Activity per Unit Fluence and per Unit Dose in PNAD Foils Grouped by Distance and Exposure Geometry

					Measured Specific Activity per Unit Fluence A_o / ϕ_{tot} $(cm^2\ g^{-1}\ min^{-1})$						Measured Specific Activity per Unit Absorbed Dose $A_o / D_p(10)_n$ $(cGy^{-1}\ g^{-1}\ min^{-1})$					
					A	B	C		D		A	B	C		D	
					S	Cu (Cd)	In (Cd)		In		S	Cu (Cd)	In (Cd)		In	
distance (m)	phantom type	location on phantom	mounting on phantom	Foil Thickness (mil)	P-32	Cu-64	In-115m	In-116m	In-115m	In-116m	P-32	Cu-64	In-115m	In-116m	In-115m	In-116m
2.0	Tree A-D	air	normal	10	1.38E-08	4.70E-07	1.04E-06	3.70E-04	1.03E-06	1.04E-03	6.48E+00	2.21E+02	4.90E+02	1.74E+05	4.83E+02	4.87E+05
2.0	Tree A-D	air	normal	5	1.34E-08	5.07E-07	1.01E-06	4.79E-04	1.04E-06	1.38E-03	6.27E+00	2.37E+02	4.75E+02	2.24E+05	4.89E+02	6.48E+05
2.5	Tree A-D	air	normal	10	1.12E-08	5.61E-07	8.57E-07	4.79E-04	8.46E-07	1.33E-03	6.03E+00	3.02E+02	4.62E+02	2.58E+05	4.56E+02	7.19E+05
4.0	Tree A-H	air	normal	10	7.87E-09	6.52E-07	6.46E-07	6.00E-04	6.30E-07	1.79E-03	4.58E+00	3.79E+02	3.76E+02	3.49E+05	3.67E+02	1.04E+06
3.0	BOMAB	front	normal	10	9.99E-09	6.98E-07	7.33E-07	6.56E-04	7.61E-07	3.00E-03	5.33E+00	3.73E+02	3.91E+02	3.50E+05	4.06E+02	1.60E+06
4.0	BOMAB	front	normal	10	9.27E-09	7.35E-07	6.95E-07	7.46E-04	6.44E-07	3.58E-03	5.31E+00	4.21E+02	3.98E+02	4.28E+05	3.69E+02	2.05E+06
2.0	PMMA	front	normal	10	1.45E-08	7.34E-07	1.10E-06	6.14E-04	1.12E-06	2.85E-03	6.88E+00	3.47E+02	5.18E+02	2.90E+05	5.29E+02	1.35E+06
4.0	PMMA	front	normal	10	9.10E-09	7.65E-07	6.89E-07	7.24E-04	6.65E-07	3.11E-03	5.20E+00	4.37E+02	3.94E+02	4.14E+05	3.80E+02	1.78E+06
3.0	BOMAB - LAT	side	normal	10	5.27E-09	5.13E-07	4.26E-07	5.08E-04	4.02E-07	2.45E-03	2.84E+00	2.76E+02	2.30E+02	2.74E+05	2.17E+02	1.32E+06
3.0	BOMAB	back	normal	10	1.58E-09	3.30E-07	1.13E-07	3.53E-04	1.22E-07	1.76E-03	8.45E-01	1.76E+02	6.05E+01	1.88E+05	6.49E+01	9.37E+05
4.0	BOMAB	back	normal	10	1.52E-09	3.53E-07	1.09E-07	3.19E-04	1.08E-07	1.58E-03	8.69E-01	2.02E+02	6.25E+01	1.83E+05	6.20E+01	9.06E+05
9.0	BOMAB	back	normal	10	3.86E-10	5.23E-08	2.62E-08	5.72E-05	3.58E-08	9.85E-04	2.80E-01	3.80E+01	1.90E+01	4.15E+04	2.60E+01	7.15E+05
2.0	PMMA	back	normal	10	2.19E-09	3.35E-07	1.78E-07	3.73E-04	1.75E-07	1.71E-03	1.03E+00	1.58E+02	8.36E+01	1.76E+05	8.23E+01	8.04E+05
4.0	PMMA	back	normal	10	1.84E-09	4.61E-07	1.49E-07	5.02E-04	1.49E-07	2.45E-03	1.09E+00	2.73E+02	8.80E+01	2.97E+05	8.81E+01	1.45E+06

Table F.2 Specific Activity per Unit Fluence and per Unit Dose in FNAD Foils

				Measured Specific Activity per Unit Fluence A_o / ϕ_{tot} ($cm^2\ g^{-1}\ min^{-1}$)									
				Outer Dosimetry Package								Inner Package
				A	B	C		D		E	F	G
				S	Cu (Cd)	In (Cd)	In (Cd)	In	In	Au	Au (Cd)	Au
Pulse #	distance (m)	Position #	Given Fluence (n/cm^2)	P-32	Cu-64	I-115m	I-116m	I-115m	I-116m	Au-198	Au-198	Au-198
1	4.0	11	5.30E+10	7.60E-09	7.14E-07	7.44E-07	N/A	6.07E-07	N/A	1.32E-05	4.73E-06	2.75E-05
2	4.0	11	1.89E+11	7.84E-09	7.96E-07	6.61E-07	6.24E-04	6.87E-07	2.00E-03	1.18E-05	5.00E-06	2.83E-05
3	4.0	11	1.14E+11	7.57E-09	7.53E-07	6.26E-07	5.69E-04	6.66E-07	2.00E-03	1.28E-05	4.95E-06	2.73E-05

				Measured Specific Activity per Unit Ambient Absorbed Dose $A_o / D^*(10)_n$ ($cGy^{-1}\ g^{-1}\ min^{-1}$)								
				Outer Dosimetry Package								Inner Package
				A	B	C		D		E	F	G
				S	Cu (Cd)	In (Cd)	In (Cd)	In	In	Au	Au (Cd)	Au
Pulse #	distance (m)	Position #	Given Dose, $D^*(10)_n$ (cGy)	P-32	Cu-64	I-115m	I-116m	I-115m	I-116m	Au-198	Au-198	Au-198
1	4.0	11	88	4.59E+00	4.31E+02	4.49E+02	N/A	3.66E+02	N/A	7.96E+03	2.86E+03	1.66E+04
2	4.0	11	313	4.74E+00	4.82E+02	4.00E+02	3.78E+05	4.15E+02	1.21E+06	7.15E+03	3.03E+03	1.71E+04
3	4.0	11	189	4.59E+00	4.56E+02	3.79E+02	3.45E+05	4.04E+02	1.21E+06	7.76E+03	3.00E+03	1.65E+04

Table F.3 Specific Activity per Unit Fluence in Foils Exposed Under Normal AP Geometry

Irradiaton Geometry	Irradiation Distance	Average Specific Activity Per Unit Fluence A_o / Φ_{tot} ($cm^2\ g^{-1}\ min^{-1}$)										
		A	B	C-115	C-116	D-115	D-116	D-116 - C-116	E	F	E - F	G
		S	Cu (Cd)	In (Cd)	In (Cd)	In (bare)	In (bare)	In (bare) - In (Cd)	Au (bare)	Au (Cd)	Au (bare) - Au (Cd)	Au (bot)
		P-32	Cu-64	I-115m	I-116m	I-115m	I-116m	I-116m	Au-198	Au-198	Au-198	Au-198
on phantom	2.0 m	1.45E-08	7.34E-07	1.10E-06	6.14E-04	1.12E-06	2.85E-03	2.24E-03				
	2.5 m											
	3.0 m	9.99E-09	6.98E-07	7.33E-07	6.56E-04	7.61E-07	3.00E-03	2.34E-03				
	4.0 m	9.18E-09	7.50E-07	6.92E-07	7.35E-04	6.54E-07	3.35E-03	2.61E-03				
in air	2.0 m	1.38E-08	4.70E-07	1.04E-06	3.70E-04	1.03E-06	1.04E-03	6.66E-04				
	2.5 m	1.12E-08	5.61E-07	8.57E-07	4.79E-04	8.46E-07	1.33E-03	8.55E-04				
	3.0 m											
	4.0 m	7.87E-09	6.52E-07	6.46E-07	6.00E-04	6.30E-07	1.79E-03	1.19E-03	1.26E-05	4.90E-06	7.71E-06	2.77E-05

Appendix G

Averaged Neutron Energy Spectra at Each Irradiation Distance

Table G.1 Normalized Fluence at 2.0 m, 2.5 m, 3.0 m, and 4.0 m Distances

Energy bin lower bound	Energy bin upper bound	Normalized Fluence (n/cm^2)			
MeV	MeV	2.0 m	2.5 m	3.0 m	4.0 m
1.00E-09	2.15E-09	1.55E-05	1.56E-05	1.82E-05	1.68E-05
2.15E-09	4.64E-09	3.71E-04	3.77E-04	4.35E-04	4.82E-04
4.64E-09	1.00E-08	3.06E-03	3.12E-03	3.54E-03	3.92E-03
1.00E-08	2.15E-08	1.37E-02	1.41E-02	1.57E-02	1.74E-02
2.15E-08	4.64E-08	2.67E-02	2.81E-02	3.04E-02	3.37E-02
4.64E-08	1.00E-07	3.15E-02	3.39E-02	3.59E-02	3.98E-02
1.00E-07	2.15E-07	2.29E-02	2.55E-02	2.64E-02	2.93E-02
2.15E-07	4.64E-07	1.27E-02	1.47E-02	1.49E-02	1.65E-02
4.64E-07	1.00E-06	1.13E-02	1.36E-02	1.37E-02	1.52E-02
1.00E-06	2.15E-06	1.63E-02	2.05E-02	2.01E-02	2.25E-02
2.15E-06	4.64E-06	1.64E-02	2.06E-02	2.02E-02	2.26E-02
4.64E-06	1.00E-05	1.64E-02	2.05E-02	2.01E-02	2.25E-02
1.00E-05	2.15E-05	1.63E-02	2.05E-02	2.01E-02	2.25E-02
2.15E-05	4.64E-05	1.64E-02	2.06E-02	2.02E-02	2.26E-02
4.64E-05	1.00E-04	1.64E-02	2.05E-02	2.01E-02	2.25E-02
1.00E-04	2.15E-04	1.63E-02	2.05E-02	2.01E-02	2.25E-02
2.15E-04	4.64E-04	1.64E-02	2.06E-02	2.02E-02	2.26E-02
4.64E-04	1.00E-03	1.64E-02	2.05E-02	2.01E-02	2.25E-02
1.00E-03	2.15E-03	1.63E-02	2.05E-02	2.01E-02	2.25E-02
2.15E-03	4.64E-03	1.64E-02	2.06E-02	2.02E-02	2.26E-02
4.64E-03	1.00E-02	1.64E-02	2.05E-02	2.01E-02	2.25E-02
1.00E-02	1.25E-02	6.58E-03	7.77E-03	7.44E-03	8.41E-03
1.25E-02	1.58E-02	6.91E-03	8.16E-03	7.81E-03	8.83E-03
1.58E-02	1.99E-02	6.80E-03	8.03E-03	7.69E-03	8.69E-03
1.99E-02	2.51E-02	6.84E-03	8.08E-03	7.74E-03	8.75E-03
2.51E-02	3.16E-02	6.79E-03	8.02E-03	7.67E-03	8.68E-03
3.16E-02	3.98E-02	6.80E-03	8.03E-03	7.69E-03	8.69E-03
3.98E-02	5.01E-02	6.79E-03	8.01E-03	7.67E-03	8.67E-03
5.01E-02	6.30E-02	6.35E-03	7.33E-03	7.03E-03	7.54E-03
6.30E-02	7.94E-02	7.71E-03	8.86E-03	8.50E-03	8.93E-03
7.94E-02	1.00E-01	7.76E-03	8.82E-03	8.47E-03	8.07E-03
1.00E-01	1.25E-01	9.07E-03	1.03E-02	9.87E-03	9.20E-03
1.25E-01	1.58E-01	1.13E-02	1.26E-02	1.21E-02	1.13E-02
1.58E-01	1.99E-01	1.50E-02	1.65E-02	1.60E-02	1.49E-02
1.99E-01	2.51E-01	1.94E-02	2.07E-02	2.01E-02	1.88E-02
2.51E-01	3.16E-01	2.38E-02	2.53E-02	2.45E-02	2.30E-02
3.16E-01	3.98E-01	3.26E-02	3.33E-02	3.23E-02	3.03E-02
3.98E-01	5.01E-01	4.06E-02	4.09E-02	3.97E-02	3.73E-02
5.01E-01	6.30E-01	4.80E-02	4.58E-02	4.48E-02	4.17E-02
6.30E-01	7.94E-01	5.95E-02	5.58E-02	5.47E-02	5.08E-02
7.94E-01	1.00E+00	5.83E-02	5.11E-02	5.07E-02	4.63E-02
1.00E+00	1.25E+00	6.70E-02	5.81E-02	5.77E-02	5.25E-02
1.25E+00	1.58E+00	5.48E-02	4.34E-02	4.44E-02	3.91E-02
1.58E+00	1.99E+00	5.79E-02	4.47E-02	4.60E-02	4.02E-02
1.99E+00	2.51E+00	3.61E-02	2.62E-02	2.77E-02	2.35E-02
2.51E+00	3.16E+00	3.59E-02	2.54E-02	2.71E-02	2.27E-02
3.16E+00	3.98E+00	1.61E-02	1.11E-02	1.21E-02	9.96E-03
3.98E+00	5.01E+00	1.58E-02	1.08E-02	1.18E-02	9.71E-03
5.01E+00	6.30E+00	5.62E-03	3.79E-03	4.22E-03	3.44E-03
6.30E+00	7.94E+00	5.08E-03	3.40E-03	3.82E-03	3.10E-03
7.94E+00	1.00E+01	2.16E-04	1.45E-04	1.62E-04	1.31E-04
1.00E+01	1.58E+01	0.00E+00	0.00E+00	0.00E+00	0.00E+00
1.58E+01	2.00E+01	0.00E+00	0.00E+00	0.00E+00	0.00E+00
1.00E-09	2.00E+01	1.00E+00	1.00E+00	1.00E+00	1.00E+00

Appendix H

Physical Data Used for Calculation of Effective Cross Sections

Table H.1 Physical Data for Foils

Target Element			Target Atom		Reaction	Product Atom		n	A.N.
Element Symbol	Atomic Number, Z	Atomic Weight, A.W. (g/mole)	Isotope Symbol	Atom Percent Abundance[1], χ (isotope atoms / element atoms)		Isotope Symbol	Decay Constant, λ (min^{-1})	Target atoms per gram of foil (g^{-1})	Avogadro's number (atoms per mole) ($mole^{-1}$)
In	49	114.82	^{115}In	0.9571	^{115}In(n,γ)^{116m}In	^{116m}In	1.279E-02	5.0198494E+21	
In	49	114.82	^{115}In	0.9571	^{115}In(n,n′)^{115m}In	^{115m}In	2.575E-03	5.0198494E+21	
Cu	29	63.546	^{63}Cu	0.6917	^{63}Cu(n,γ)^{64}Cu	^{64}Cu	9.096E-04	6.5551173E+21	
S	16	32.066	^{32}S	0.9493	^{32}S(n,p)^{32}P	^{32}P	3.368E-05	1.7828287E+22	
Au	79	196.97	^{197}Au	1.0000	^{197}Au(n,γ)^{198}Au	^{198}Au	1.785E-04	3.0573899E+21	
									6.0221409E+23
1. Chart of the Nuclides, Knolls Atomic Power Laboratory, Naval Reactors, U.S. Department of Energy, 16th Edition-Revised to 2002									

Appendix I

microStar® Reader Calibration Factors

Table I.1 PNAD Reader Calibration Factors (example)

PNAD InLight									
Reader Serial Number	Reader Type	Reader Environment	Calibration ID	Calibraton Name	Dose Range	Badge Type	Calibration Date/Time	Calibration Factor (counts / unit of dose)	Dose Units
11040683	Protection Level	PNAD LD	51	Co-60 (strong beam)	0.005 cGy - 10 cGy	InLight	1/5/2016 7:10 PM	12268	cGy
11040683	Protection Level	PNAD LD	52	Co-60 (weak beam)	10 cGy - 1000 cGy	InLight	1/5/2016 7:54 PM	895	cGy
14240805	Accident Level	PNAD HD	69	Co-60 (strong beam)	0.1 cGy - 75 cGy	InLight	1/4/2016 2:43 PM	639	cGy
14240805	Accident Level	PNAD HD	71	Co-60 (weak beam)	75 cGy - 10,000 cGy	InLight	1/4/2016 5:03 PM	35	cGy

Table I.2 FNAD Reader Calibration Factors (example)

FNAD nanoDot									
Reader Serial Number	Reader Type	Reader Environment	Calibration ID	Calibraton Name	Dose Range	Badge Type	Calibration Date/Time	Calibration Factor (counts / unit of dose)	Dose Units
11040683	Protection Level	FNAD LD	68	Co-60 (strong beam)	0.005 cGy - 10 cGy	nanoDot	1/10/2016 7:14 PM	8420	cGy
11040683	Protection Level	FNAD LD	69	Co-60 (weak beam)	10 cGy - 1000 cGy	nanoDot	1/10/2016 7:30 PM	679	cGy
14240805	Accident Level	FNAD HD	73	Co-60 (strong beam)	0.1 cGy - 75 cGy	nanoDot	1/12/2016 1:30 PM	409	cGy
14240805	Accident Level	FNAD HD	72	Co-60 (weak beam)	75 cGy - 10,000 cGy	nanoDot	1/11/2016 9:17 PM	25	cGy

Appendix J

OSL/OSLN Dose Response Linearity Corrections

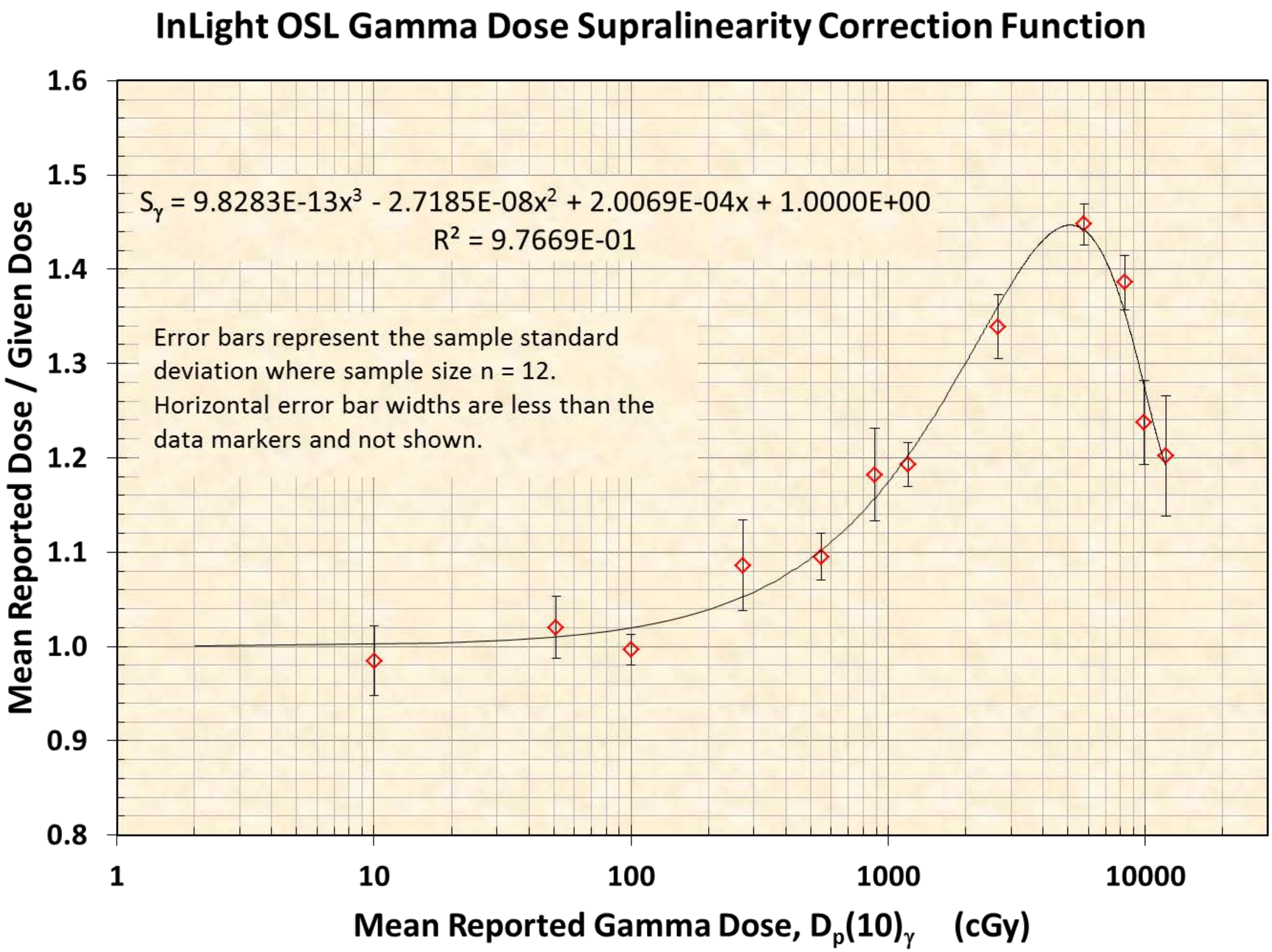

Figure J.1 OSL Gamma Dose Supralinearity Correction Function for InLight® Dosimeters

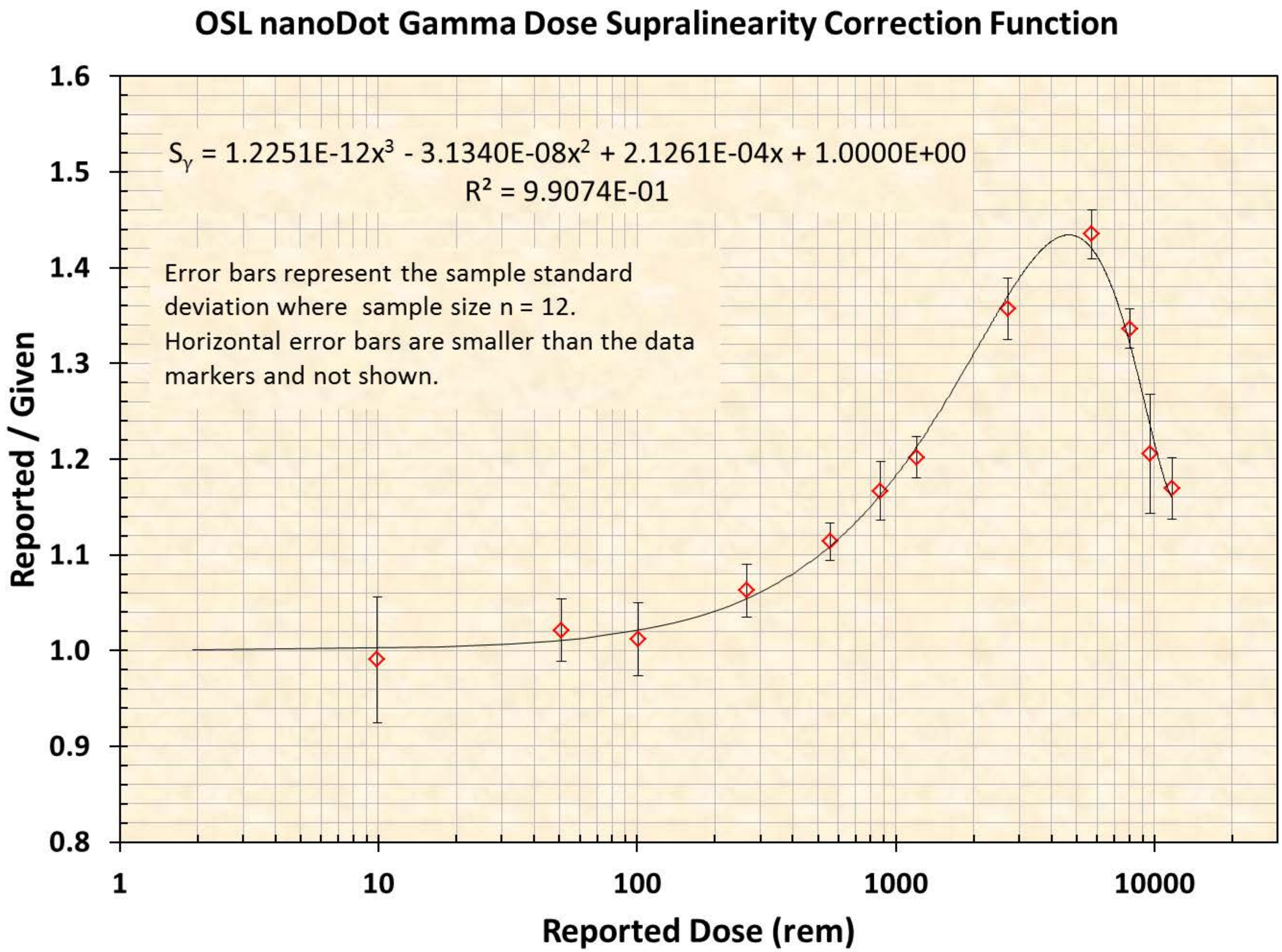

Figure J.2 OSL gamma dose supralinearity correction function for nanoDot® dosimeters.

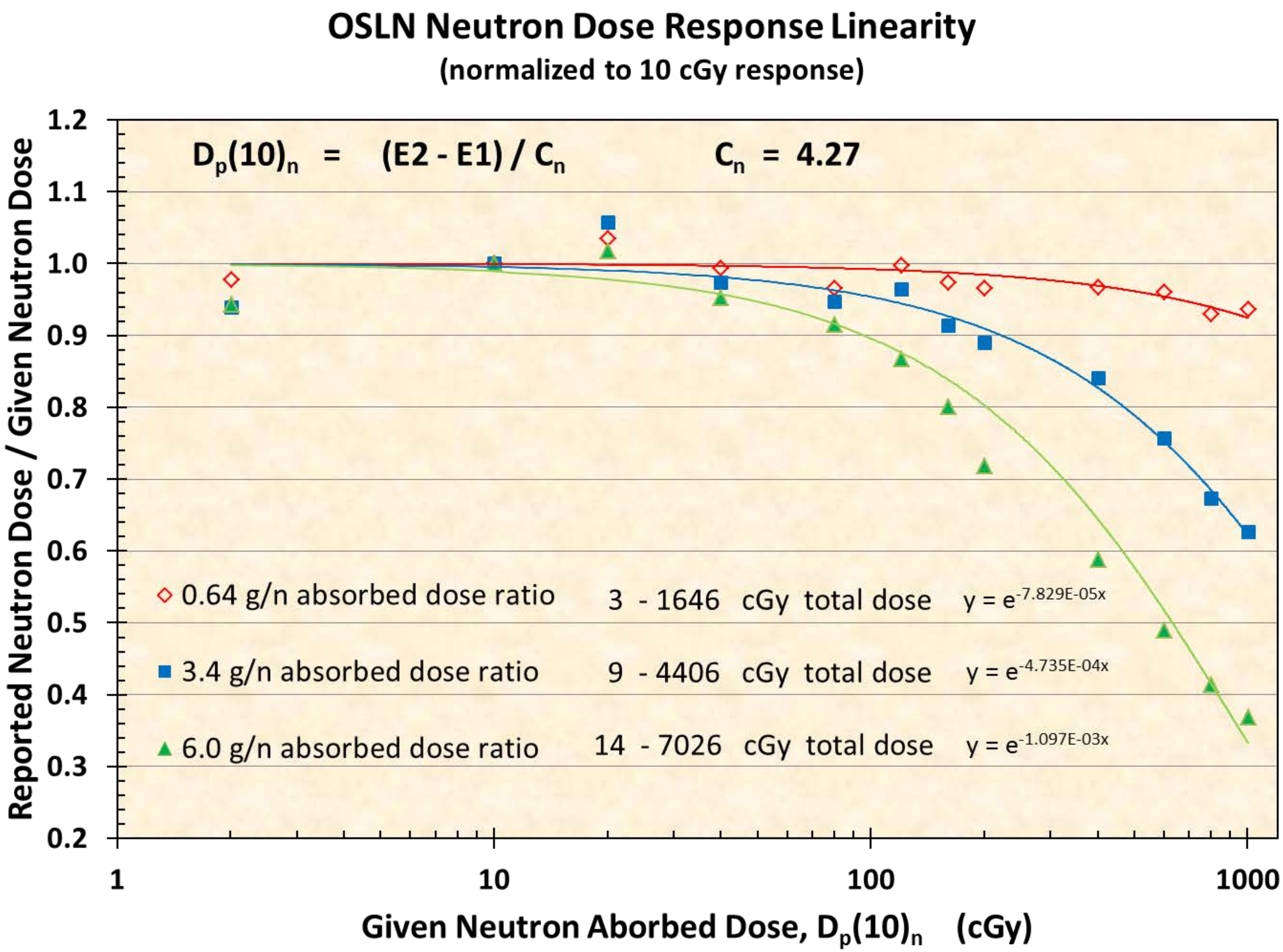

Figure J.3 OSLN neutron dose response in unmoderated ^{252}Cf neutron / ^{60}Co gamma mixed fields

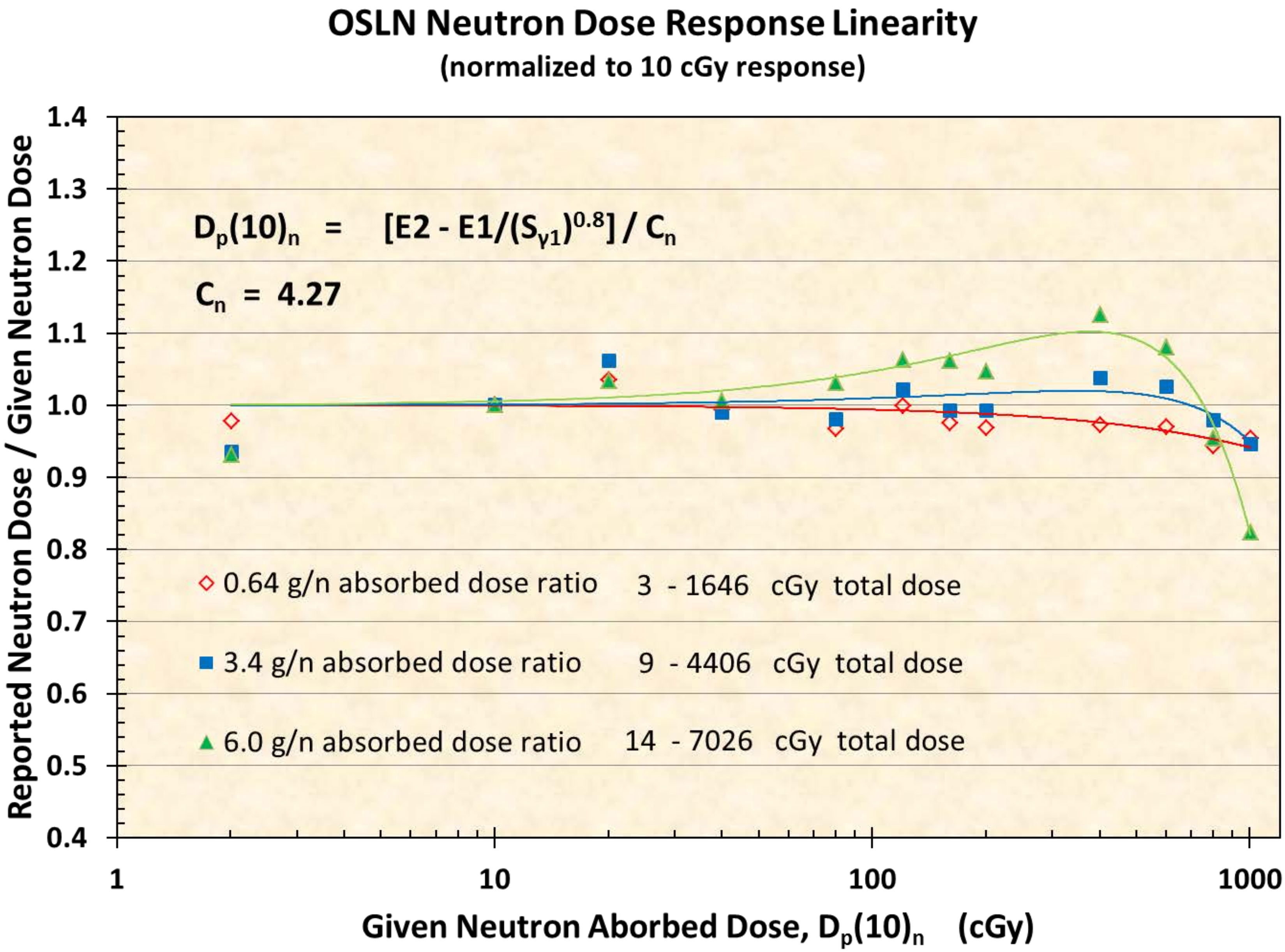

Figure J.4 OSLN neutron dose response with correction for non-linearity applied

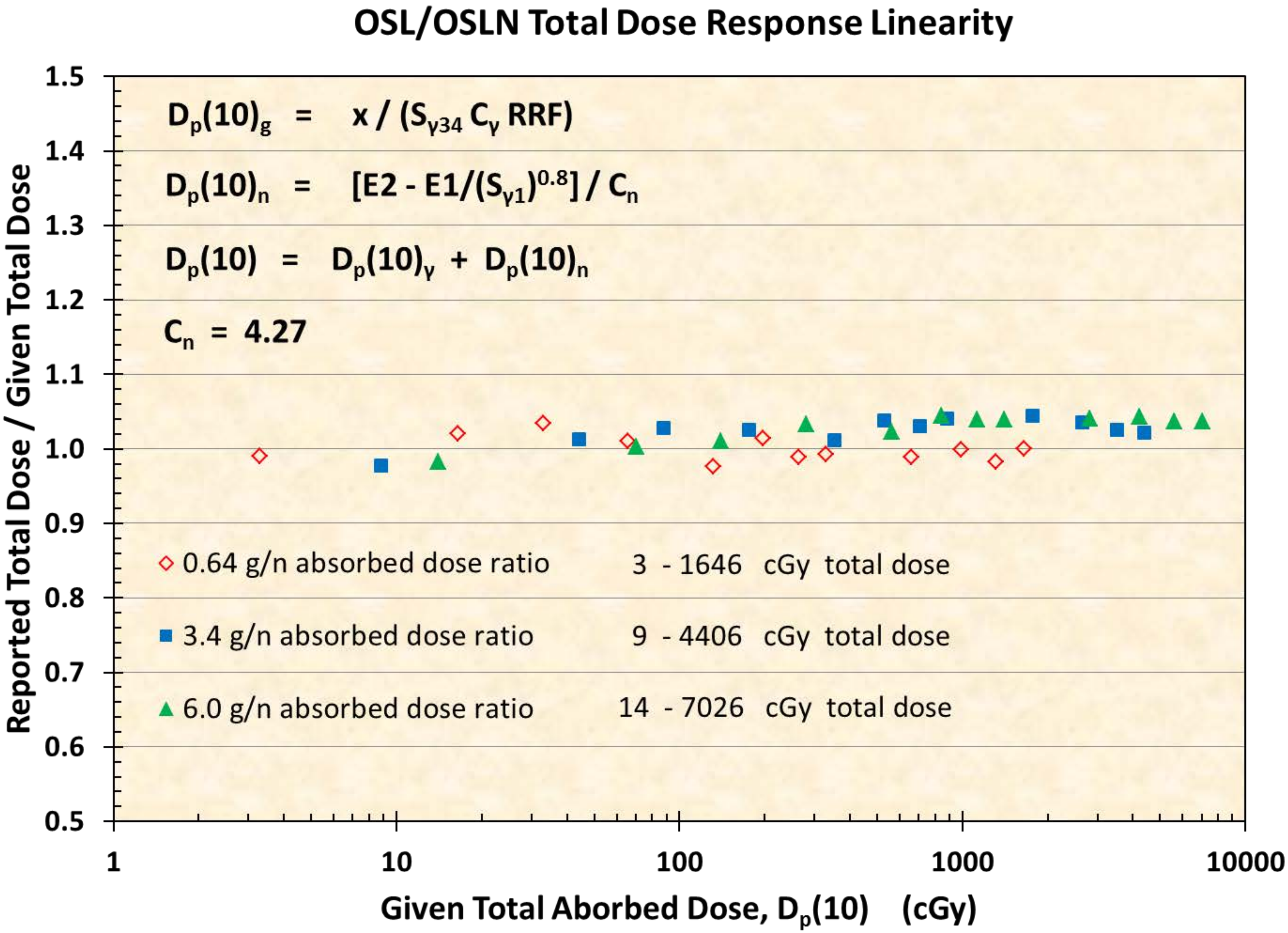

Figure J.5 Total dose response of InLight® dosimeter with corrections for gamma and neutron dose non-linearity applied.

Appendix K

Accuracy of Foil Measured Fluence and Dose Within NAD Energy Regions

Table K.1 Accuracy of PNAD Fluence and Dose Measurements <u>in Air</u>

dosimeter #	pulse #	position #	distance (m)	dosimeter orientation WRT source	Given Φ_{tot} (cm^{-2})	Measured Φ_{bin} /Given Φ_{bin}: Φ_{th} 0.001 eV - 0.464 eV	Φ_{Cu} 0.464 eV - 100 keV	Φ_a 100 keV - 1.25 MeV	Φ_{In} 1.25 MeV - 20 MeV	Φ_b 1.25 MeV - 3.16 MeV	Φ_S 3.16 MeV - 20 MeV	Φ_{total} 0.001 eV - 20 MeV	Given D_{tot} $D_p(10)_n$ (cGy)	Reported D_{bin} / Given D_{bin}: D_{th} 0.001 eV - 0.464 eV	D_{Cu} 0.464 eV - 100 keV	D_a 100 keV - 1.25 MeV	D_b 1.25 MeV - 3.16 MeV	D_S 3.16 MeV - 20 MeV	D_{total} 0.001 eV - 20 MeV	Reported Dose, $D_p(10)_n$ (cGy)	P_i
1	1	1	2.0	AP	1.01E+11	0.87	0.97	0.97	0.96	0.98	0.86	0.96	214	0.84	0.93	0.92	0.94	0.83	0.91	196	-0.09
2	1	1	2.0	AP	1.01E+11	0.77	0.95	0.97	0.97	0.97	0.98	0.94	214	0.74	0.91	0.92	0.93	0.95	0.92	197	-0.08
3	1	2	2.0	AP	9.59E+10	0.77	0.99	0.95	0.92	0.90	0.97	0.93	205	0.74	0.94	0.89	0.86	0.93	0.88	181	-0.12
4	1	2	2.0	AP	9.59E+10	0.74	0.94	1.03	1.06	1.08	0.99	0.98	205	0.71	0.89	0.97	1.03	0.94	0.98	200	-0.02
*62	1	2	2.0	AP	9.59E+10	0.83	0.95	1.06	1.10	1.13	0.96	1.01	205	0.79	0.90	0.99	1.08	0.92	1.01	206	0.01
17	2	1	2.0	AP	3.60E+11	0.86	1.11	1.06	1.01	1.02	0.99	1.04	764	0.83	1.06	1.00	0.98	0.95	0.98	752	-0.02
18	2	1	2.0	AP	3.60E+11	0.97	1.01	1.01	1.00	1.00	0.97	1.00	764	0.93	0.96	0.95	0.96	0.94	0.96	730	-0.04
19	2	3	2.0	AP	3.60E+11	0.90	1.03	1.10	1.13	1.13	1.10	1.06	761	0.87	0.98	1.04	1.09	1.06	1.06	804	0.06
20	2	3	2.0	AP	3.60E+11	0.96	0.97	1.08	1.12	1.11	1.13	1.04	761	0.93	0.93	1.02	1.07	1.09	1.04	791	0.04
*64	2	2	2.0	AP	3.43E+11	0.85	1.01	1.03	1.03	1.03	1.03	1.01	732	0.81	0.96	0.97	0.98	0.99	0.97	713	-0.03
*66	3	2	2.0	AP	2.07E+11	0.86	1.06	1.04	1.01	1.03	0.96	1.02	442	0.82	1.01	0.97	0.98	0.92	0.97	428	-0.03
					mean	**0.85**	**1.00**	**1.03**	**1.03**	**1.04**	**1.00**	**1.00**	**mean**	**0.82**	**0.95**	**0.97**	**0.99**	**0.96**	**0.97**	**B**	**-0.03**
					C.V.	**0.09**	**0.05**	**0.05**	**0.07**	**0.07**	**0.07**	**0.04**	**C.V.**	**0.09**	**0.05**	**0.05**	**0.07**	**0.07**	**0.05**	**S**	**0.05**
					n	**11**	**11**	**11**	**11**	**11**	**11**	**11**	**n**	**11**	**11**	**11**	**11**	**11**	**11**	**n**	**11**
**61	1	2	2.0	AP	9.59E+10	0.03	1.00	1.00	1.00	0.99	1.01	0.89	205	0.03	0.95	0.94	0.94	0.96	0.93	191	-0.07
**63	2	2	2.0	AP	3.43E+11	1.10	1.11	1.05	1.01	1.01	0.98	1.06	732	1.06	1.06	0.99	0.96	0.94	0.98	716	-0.02
**65	3	2	2.0	AP	2.07E+11	1.14	1.12	1.05	1.00	1.02	0.91	1.07	442	1.09	1.06	0.98	0.97	0.87	0.97	429	-0.03
					mean	**0.76**	**1.08**	**1.03**	**1.00**	**1.01**	**0.97**	**1.01**	**mean**	**0.73**	**1.02**	**0.97**	**0.96**	**0.92**	**0.96**	**B**	**-0.04**
					C.V.	**0.83**	**0.06**	**0.02**	**0.01**	**0.01**	**0.05**	**0.10**	**C.V.**	**0.83**	**0.06**	**0.03**	**0.01**	**0.05**	**0.03**	**S**	**0.03**
					n	**3**	**3**	**3**	**3**	**3**	**3**	**3**	**n**	**3**	**3**	**3**	**3**	**3**	**3**	**n**	**3**
9	1	6	2.5	AP	8.58E+10	0.96	0.90	0.93	1.05	1.04	1.12	0.94	159	0.90	0.85	0.89	0.98	1.06	0.93	148	-0.07
10	1	6	2.5	AP	8.58E+10	0.92	0.94	0.98	1.11	1.08	1.24	0.98	159	0.87	0.88	0.93	1.03	1.17	0.98	156	-0.02
11	1	6	2.5	AP	8.58E+10	1.10	0.94	0.93	1.01	0.99	1.12	0.97	159	1.04	0.89	0.89	0.94	1.06	0.92	147	-0.08
12	1	6	2.5	AP	8.58E+10	0.91	0.94	0.99	1.11	1.11	1.11	0.98	159	0.86	0.89	0.94	1.06	1.05	0.98	156	-0.02
27	2	6	2.5	AP	3.07E+11	0.99	1.03	1.10	1.25	1.26	1.20	1.09	570	0.93	0.98	1.04	1.19	1.13	1.09	622	0.09
28	2	6	2.5	AP	3.07E+11	1.05	1.00	1.07	1.24	1.24	1.23	1.07	570	0.99	0.94	1.02	1.17	1.16	1.07	613	0.07
33	3	6	2.5	AP	1.85E+11	1.03	0.97	1.02	1.15	1.13	1.23	1.03	344	0.97	0.92	0.97	1.07	1.16	1.01	349	0.01
42	3	6	2.5	AP	1.85E+11	1.13	1.03	1.06	1.19	1.18	1.25	1.08	344	1.06	0.97	1.01	1.11	1.18	1.06	364	0.06
					mean	**1.01**	**0.97**	**1.01**	**1.14**	**1.13**	**1.19**	**1.02**	**mean**	**0.95**	**0.91**	**0.96**	**1.07**	**1.12**	**1.01**	**B**	**0.01**
					C.V.	**0.08**	**0.05**	**0.06**	**0.07**	**0.08**	**0.05**	**0.06**	**C.V.**	**0.08**	**0.05**	**0.06**	**0.08**	**0.05**	**0.06**	**S**	**0.06**
					n	**8**	**8**	**8**	**8**	**8**	**8**	**8**	**n**	**8**	**8**	**8**	**8**	**8**	**8**	**n**	**8**
15	1	8	4.0	AP	5.33E+10	1.06	1.01	1.04	1.00	1.02	0.93	1.03	92	1.00	0.95	0.99	0.96	0.87	0.96	89	-0.04
16	1	8	4.0	AP	5.33E+10	N/A	0.95	1.02	1.02	1.01	1.03	0.85	92	N/A	0.90	0.96	0.95	0.97	0.93	85	-0.07
29	2	8	4.0	AP	1.91E+11	1.09	1.10	1.06	0.95	0.95	0.98	1.06	329	1.03	1.04	1.01	0.90	0.92	0.97	319	-0.03
30	2	8	4.0	AP	1.91E+11	1.16	1.00	1.01	0.95	0.94	0.97	1.02	329	1.09	0.95	0.96	0.89	0.92	0.93	307	-0.07
31	2	8	4.0	PA	1.91E+11	1.24	1.08	1.12	1.08	1.11	0.94	1.12	329	1.17	1.02	1.06	1.04	0.88	1.04	341	0.04
32	2	8	4.0	PA	1.91E+11	1.13	1.01	1.03	0.98	0.99	0.92	1.03	329	1.06	0.95	0.98	0.94	0.87	0.95	314	-0.05
43	3	9	4.0	AP	1.15E+11	1.35	1.11	1.02	0.86	0.87	0.82	1.08	199	1.27	1.05	0.97	0.82	0.77	0.92	182	-0.08
46	3	9	4.0	AP	1.18E+11	1.30	1.03	0.95	0.80	0.80	0.82	1.01	199	1.25	1.00	0.92	0.77	0.79	0.88	175	-0.12
					mean	**1.19**	**1.03**	**1.03**	**0.96**	**0.96**	**0.93**	**1.02**	**mean**	**1.13**	**0.98**	**0.98**	**0.91**	**0.87**	**0.95**	**B**	**-0.05**
					C.V.	**0.09**	**0.05**	**0.05**	**0.09**	**0.10**	**0.08**	**0.08**	**C.V.**	**0.10**	**0.05**	**0.04**	**0.10**	**0.08**	**0.05**	**S**	**0.05**
					n	**7**	**8**	**8**	**8**	**8**	**8**	**8**	**n**	**7**	**8**	**8**	**8**	**8**	**8**	**n**	**8**

* Hanford PNAD with 10 mil foils

** Hanford PNAD with 5 mil foils

Table K.2 Accuracy of PNAD Fluence and Dose Measurements <u>on Phantom</u>

dosimeter #	pulse #	position #	distance (m)	phantom type	dosimeter location on phantom	dosimeter orientation WRT source	Given Φ_{tot} (cm^{-2})	Measured Φ_{bin} /Given Φ_{bin}: Φ_{th}	Φ_{Cu}	Φ_a	Φ_{In}	Φ_b	Φ_S	Φ_{total}	Given D_{tot} $D_p(10)_n$ (cGy)	Reported D_{bin} / Given D_{bin}: D_{th}	D_{Cu}	D_a	D_b	D_S	D_{total}	Reported Dose, $D_p(10)_n$ (cGy)	P_i
								0.001 eV - 0.464 eV	0.464 eV - 100 keV	100 keV - 1.25 MeV	1.25 MeV - 20 MeV	1.25 MeV - 3.16 MeV	3.16 MeV - 20 MeV	0.001 eV - 20 MeV		0.001 eV - 0.464 eV	0.464 eV - 100 keV	100 keV - 1.25 MeV	1.25 MeV - 3.16 MeV	3.16 MeV - 20 MeV	0.001 eV - 20 MeV		
5	1	4	3.0	BOMAB	front	AP	6.55E+10	2.55	1.19	1.04	0.93	0.94	0.89	1.26	123	2.41	1.13	0.99	0.89	0.84	0.99	121	-0.01
7	1	5	3.0	BOMAB	front	AP	6.77E+10	2.37	1.17	0.98	0.84	0.83	0.91	1.20	126	2.27	1.12	0.94	0.79	0.87	0.93	117	-0.07
21	2	4	3.0	BOMAB	front	AP	2.34E+11	2.91	1.28	1.11	0.98	0.97	1.04	1.37	441	2.74	1.21	1.05	0.92	0.98	1.05	463	0.05
23	2	5	3.0	BOMAB	front	AP	2.42E+11	2.68	1.30	1.06	0.89	0.88	0.95	1.32	450	2.56	1.24	1.02	0.84	0.91	1.00	451	0.00
34	3	4	3.0	BOMAB	front	AP	1.41E+11	2.57	1.22	1.08	0.98	0.98	1.02	1.30	266	2.42	1.15	1.02	0.92	0.96	1.02	272	0.02
							mean	**2.61**	**1.23**	**1.05**	**0.93**	**0.92**	**0.96**	**1.29**	**mean**	**2.48**	**1.17**	**1.00**	**0.87**	**0.91**	**1.00**	**B**	**0.00**
							C.V.	**0.08**	**0.05**	**0.05**	**0.07**	**0.07**	**0.07**	**0.05**	**C.V.**	**0.07**	**0.05**	**0.04**	**0.06**	**0.06**	**0.05**	**S**	**0.05**
							n	**5**	**5**	**5**	**5**	**5**	**5**	**5**	**n**	**5**	**5**	**5**	**5**	**5**	**5**	**n**	**5**
38	3	7	4.0	BOMAB	front	AP	1.10E+11	2.85	1.17	1.14	1.03	1.01	1.09	1.37	192	2.65	1.09	1.06	0.94	1.01	1.07	205	0.07
45	3	3	2.0	PMMA	front	AP	2.17E+11	2.86	1.56	1.26	1.08	1.09	1.05	1.48	459	2.77	1.50	1.19	1.05	1.01	1.16	534	0.16
13	1	7	4.0	PMMA	front	AP	5.10E+10	2.26	1.13	1.12	1.02	1.02	1.03	1.27	89	2.10	1.06	1.05	0.95	0.96	1.04	93	0.04
25	2	7	4.0	PMMA	front	AP	1.82E+11	2.55	1.29	1.20	1.01	0.99	1.11	1.40	319	2.36	1.20	1.12	0.92	1.03	1.09	348	0.09
							mean	**2.40**	**1.21**	**1.16**	**1.02**	**1.01**	**1.07**	**1.33**	**mean**	**2.23**	**1.13**	**1.08**	**0.94**	**0.99**	**1.07**	**B**	**0.07**
							C.V.	**0.09**	**0.09**	**0.05**	**0.01**	**0.02**	**0.05**	**0.07**	**C.V.**	**0.08**	**0.09**	**0.04**	**0.02**	**0.05**	**0.03**	**S**	**0.04**
							n	**2**	**2**	**2**	**2**	**2**	**2**	**2**	**n**	**2**	**2**	**2**	**2**	**2**	**2**	**n**	**2**
36	3	5	3.0	BOMAB	side	LAT	1.46E+11	1.72	0.59	0.35	0.16	0.16	0.14	0.57	271	1.65	0.57	0.33	0.16	0.13	0.30	83	-0.70
37	3	5	3.0	BOMAB	side	LAT	1.46E+11	2.62	1.22	1.04	0.92	0.93	0.88	1.28	271	2.51	1.17	1.00	0.89	0.84	1.00	270	0.00
							mean	**2.17**	**0.91**	**0.70**	**0.54**	**0.55**	**0.51**	**0.93**	**mean**	**2.08**	**0.87**	**0.67**	**0.52**	**0.49**	**0.65**	**B**	**-0.35**
							C.V.	**0.29**	**0.49**	**0.71**	**1.00**	**0.99**	**1.03**	**0.54**	**C.V.**	**0.29**	**0.49**	**0.71**	**0.99**	**1.03**	**0.75**	**S**	**0.49**
							n	**2**	**2**	**2**	**2**	**2**	**2**	**2**	**n**	**2**	**2**	**2**	**2**	**2**	**2**	**n**	**2**
6	1	4	3.0	BOMAB	back	PA	6.55E+10	1.33	0.57	0.34	0.16	0.16	0.16	0.51	123	1.26	0.54	0.32	0.15	0.16	0.29	35	-0.71
8	1	5	3.0	BOMAB	back	PA	6.77E+10	1.79	0.57	0.33	0.15	0.14	0.17	0.56	126	1.71	0.54	0.32	0.14	0.16	0.29	37	-0.71
22	2	4	3.0	BOMAB	back	PA	2.34E+11	1.47	0.55	0.32	0.14	0.13	0.16	0.51	441	1.39	0.52	0.30	0.12	0.15	0.27	119	-0.73
24	2	5	3.0	BOMAB	back	PA	2.42E+11	1.65	0.62	0.35	0.15	0.15	0.14	0.57	450	1.58	0.59	0.34	0.14	0.13	0.30	136	-0.70
35	3	4	3.0	BOMAB	back	PA	1.41E+11	1.58	0.60	0.34	0.13	0.12	0.14	0.55	266	1.49	0.57	0.32	0.12	0.13	0.28	75	-0.72
							mean	**1.56**	**0.58**	**0.34**	**0.14**	**0.14**	**0.15**	**0.54**	**mean**	**1.49**	**0.55**	**0.32**	**0.13**	**0.14**	**0.29**	**B**	**-0.71**
							C.V.	**0.11**	**0.05**	**0.04**	**0.08**	**0.09**	**0.09**	**0.05**	**C.V.**	**0.12**	**0.05**	**0.04**	**0.10**	**0.09**	**0.04**	**S**	**0.02**
							n	**5**	**5**	**5**	**5**	**5**	**5**	**5**	**n**	**5**	**5**	**5**	**5**	**5**	**5**	**n**	**2**
39	3	7	4.0	BOMAB	back	PA	1.10E+11	1.27	0.56	0.38	0.16	0.16	0.18	0.54	192	1.18	0.52	0.35	0.15	0.17	0.31	60	-0.69
44	3	1	2.0	PMMA	back	PA	2.17E+11	1.71	0.71	0.36	0.18	0.18	0.16	0.57	461	1.64	0.68	0.34	0.17	0.15	0.30	138	-0.70
14	1	9	4.0	PMMA	back	PA	5.46E+10	1.90	0.71	0.48	0.21	0.21	0.21	0.72	92	1.83	0.68	0.47	0.20	0.21	0.42	39	-0.58
26	2	9	4.0	PMMA	back	PA	1.95E+11	2.02	0.75	0.52	0.23	0.23	0.22	0.77	330	1.94	0.73	0.50	0.22	0.21	0.45	148	-0.55
							mean	**1.96**	**0.73**	**0.50**	**0.22**	**0.22**	**0.22**	**0.75**	**mean**	**1.88**	**0.71**	**0.48**	**0.21**	**0.21**	**0.43**	**B**	**-0.57**
							C.V.	**0.04**	**0.05**	**0.05**	**0.06**	**0.07**	**0.02**	**0.05**	**C.V.**	**0.04**	**0.04**	**0.05**	**0.07**	**0.02**	**0.05**	**S**	**0.02**
							n	**2**	**2**	**2**	**2**	**2**	**2**	**2**	**n**	**2**	**2**	**2**	**2**	**2**	**2**	**n**	**2**

Table K.3 Accuracy of FNAD Fluence and Dose Measurements in Air Within NAD Energy Bins

Φ_{th} based on ^{116m}In Activity in Indium Foils C and D

dosimeter #	pulse #	position #	distance (m)	phantom type	Given Φ_{tot} (cm^{-2})	Measured Φ_{bin} / Given Φ_{bin}: Φ_{th} 0.001 eV - 0.464 eV	Φ_{Cu} 0.464 eV - 100 keV	Φ_a 100 keV - 1.25 MeV	Φ_{In} 1.25 MeV - 20 MeV	Φ_b 1.25 MeV - 3.16 MeV	Φ_S 3.16 MeV - 20 MeV	Φ_{total} 0.001 eV - 20 MeV
71	1	11	2.0	air	5.30E+10	n/a	1.13	1.16	1.10	1.14	0.89	n/a
72	2	11	2.0	air	1.89E+11	1.39	1.26	1.16	0.98	0.99	0.92	1.20
73	3	11	2.0	air	1.14E+11	1.44	1.19	1.10	0.93	0.93	0.89	1.16
					mean	**1.41**	**1.20**	**1.14**	**1.00**	**1.02**	**0.90**	**1.18**
					C.V.	**0.03**	**0.05**	**0.03**	**0.09**	**0.11**	**0.02**	**0.03**
					n	**2**	**3**	**3**	**3**	**3**	**3**	**2**

D_{th} based on ^{116m}In Activity in Indium Foils C and D

dosimeter #	pulse #	position #	distance (m)	phantom type	Given D_{tot} $D^*(10)_n$ (cGy)	Reported D_{bin} / Given D_{bin}: D_{th} 0.001 eV - 0.464 eV	D_{Cu} 0.464 eV - 100 keV	D_a 100 keV - 1.25 MeV	D_b 1.25 MeV - 3.16 MeV	D_S 3.16 MeV - 20 MeV	D_{total} 0.001 eV - 20 MeV	Reported D_{tot} $D^*(10)_n$ (cGy)	P_i
71	1	11	2.0	air	88	n/a	1.07	1.09	1.07	0.84	n/a	n/a	n/a
72	2	11	2.0	air	313	1.30	1.19	1.10	0.93	0.86	1.03	324	0.03
73	3	11	2.0	air	189	1.35	1.13	1.04	0.88	0.84	0.99	186	-0.01
					mean	**1.33**	**1.13**	**1.08**	**0.96**	**0.84**	**1.01**	**B**	**0.01**
					C.V.	**0.03**	**0.06**	**0.03**	**0.11**	**0.02**	**0.03**	**S**	**0.04**
					n	**2**	**3**	**3**	**3**	**3**	**2**	**n**	**2**

Φ_{th} based on ^{198}Au Activity in Gold Foils E and F

dosimeter #	pulse #	position #	distance (m)	phantom type	Given Φ_{tot} (cm^{-2})	Measured Φ_{bin} / Given Φ_{bin}: Φ_{th} 0.001 eV - 0.464 eV	Φ_{Cu} 0.464 eV - 100 keV	Φ_a 100 keV - 1.25 MeV	Φ_{In} 1.25 MeV - 20 MeV	Φ_b 1.25 MeV - 3.16 MeV	Φ_S 3.16 MeV - 20 MeV	Φ_{total} 0.001 eV - 20 MeV
71	1	11	4.0	air	5.30E+10	1.10	1.13	1.16	1.10	1.14	0.89	1.13
72	2	11	4.0	air	1.89E+11	0.88	1.26	1.16	0.98	0.99	0.92	1.13
73	3	11	4.0	air	1.14E+11	1.02	1.19	1.10	0.93	0.93	0.89	1.10
					mean	**1.00**	**1.20**	**1.14**	**1.00**	**1.02**	**0.90**	**1.12**
					C.V.	**0.11**	**0.05**	**0.03**	**0.09**	**0.11**	**0.02**	**0.02**
					n	**3**	**3**	**3**	**3**	**3**	**3**	**3**

D_{th} based on ^{198}Au Activity in Gold Foils E and F

dosimeter #	pulse #	position #	distance (m)	phantom type	Given D_{tot} $D^*(10)_n$ (cGy)	Reported D_{bin} / Given D_{bin}: D_{th} 0.001 eV - 0.464 eV	D_{Cu} 0.464 eV - 100 keV	D_a 100 keV - 1.25 MeV	D_b 1.25 MeV - 3.16 MeV	D_S 3.16 MeV - 20 MeV	D_{total} 0.001 eV - 20 MeV	Reported D_{tot} $D^*(10)_n$ (cGy)	P_i
71	1	11	4.0	air	88	1.03	1.07	1.09	1.07	0.84	1.06	93	0.06
72	2	11	4.0	air	313	0.83	1.19	1.10	0.93	0.86	1.02	320	0.02
73	3	11	4.0	air	189	0.96	1.13	1.04	0.88	0.84	0.97	184	-0.03
					mean	**0.94**	**1.13**	**1.08**	**0.96**	**0.84**	**1.02**	**B**	**0.02**
					C.V.	**0.11**	**0.06**	**0.03**	**0.11**	**0.02**	**0.04**	**S**	**0.04**
					n	**3**	**3**	**3**	**3**	**3**	**3**	**n**	**3**

D_{total} based on ^{198}Au Activity in Gold Foil G (inner dosimetry package)

$D^*(10)_n = 5.97 \times 10^{-5} A_o$

dosimeter #	pulse #	position #	distance (m)	phantom type	Given D_{tot} $D^*(10)_n$ (cGy)		Reported D_{tot} / Given D_{tot}	Reported D_{tot} $D^*(10)_n$ (cGy)	P_i
71	1	11	4.0	air	88		1.06	87	-0.01
72	2	11	4.0	air	313		1.02	320	0.02
73	3	11	4.0	air	189		0.97	186	-0.01
						mean	**1.02**	**B**	**0.00**
						C.V.	**0.04**	**S**	**0.02**
						n	**3**	**n**	**3**

Appendix L

PNAD InLight® Readings and Calculated Doses

Table L.1 PNAD InLight® Readings and Calculated Doses Using Default Gamma and Godiva Specific Neutron Calibration Factors

PNAD #	Pulse #	Distance (m)	Position #	phantom type	dosimeter location on phantom	InLight BA Case Serial Number	E1 (cGy)	E2 (cGy)	E3 (cGy)	E4 (cGy)	(E3+E4) / 2 (cGy)	Gamma calibration factor, C_γ	Neutron influence correction factor, R	Corrected gamma dose reading, x	E3 E4 gamma supralinearity factor, $S_{\gamma 34}$	Reported $Dp(10)_\gamma$ (cGy)	Given $Dp(10)_\gamma$ (rad)	R/G	E1 gamma supralinearity factor, $S_{\gamma 1}$	$E2 - E1/(S_{\gamma 1})^{0.8}$	Neutron calibration factor, C_n	Reported Neutron Dose, Dp(10)n (cGy)	Given Dp(10)n (cGy)	R/G	Reported Total Dose Dp(10) (cGy)	Given Total Dose Dp(10) (cGy)	R/G	P_i
45	3	2	3	PMMA	front	BA00088219U	104	2412	118	116	117	1.00	0.165	56	1.01	55	47	1.17	1.02	2310	6.19	373	459	0.81	428	506	0.85	-0.15
5	1	3	4	BOMAB	front	BA00129701B	31	790	36	34	35	1.00	0.165	15	1.00	15	14	1.07	1.01	759	6.19	123	123	1.00	138	137	1.00	0.00
7	1	3	5	BOMAB	front	BA001124983	30	760	35	34	34	1.00	0.165	15	1.00	15	14	1.05	1.01	730	6.19	118	126	0.94	133	140	0.95	-0.05
21	2	3	4	BOMAB	front	BA00098475Q	122	2696	133	131	132	1.00	0.165	63	1.01	63	50	1.25	1.02	2576	6.19	416	441	0.94	479	491	0.98	-0.02
23	2	3	5	BOMAB	front	BA00111098C	121	3054	137	128	132	1.00	0.165	54	1.01	53	50	1.07	1.02	2935	6.19	474	450	1.05	527	500	1.05	0.05
34	3	3	4	BOMAB	front	BA000883712	69	1706	82	80	81	1.00	0.165	37	1.01	37	30	1.24	1.01	1637	6.19	265	266	0.99	302	296	1.02	0.02
13	1	4	7	PMMA	front	BA00094689H	21	693	25	24	24	1.00	0.165	7	1.00	7	11	0.59	1.00	673	6.19	109	89	1.22	115	100	1.15	0.15
25	2	4	7	PMMA	front	BA001138158	74	2212	86	86	86	1.00	0.165	29	1.01	29	40	0.72	1.01	2139	6.19	346	319	1.08	374	359	1.04	0.04
38	3	4	7	BOMAB	front	BA001113697	54	1613	66	66	66	1.00	0.165	25	1.00	24	24	1.02	1.01	1559	6.19	252	192	1.31	276	216	1.28	0.28
36	3	3	5	BOMAB - LAT	side	BA000976012	45	1066	53	50	51	1.00	0.165	24	1.00	24	30	0.80	1.01	1022	6.19	165	271	0.61	189	301	0.63	-0.37
37	3	3	5	BOMAB - LAT	side	BA00097742U	69	1655	78	74	76	1.00	0.165	34	1.01	33	30	1.12	1.01	1587	6.19	256	271	0.95	290	301	0.96	-0.04
6	1	3	4	BOMAB	back	BA00098095W	20	461	23	22	23	1.00	0.165	11	1.00	11	14	0.77	1.00	441	6.19	71	123	0.58	82	137	0.60	-0.40
8	1	3	5	BOMAB	back	BA00098462X	22	570	26	24	25	1.00	0.165	10	1.00	10	14	0.73	1.00	549	6.19	89	126	0.70	99	140	0.71	-0.29
14	1	4	9	PMMA	back	BA00093799F	16	555	20	20	20	1.00	0.165	5	1.00	5	11	0.49	1.00	539	6.19	87	92	0.95	92	103	0.90	-0.10
22	2	3	4	BOMAB	back	BA00098722V	72	1561	85	80	83	1.00	0.165	43	1.01	43	50	0.85	1.01	1490	6.19	241	441	0.55	283	491	0.58	-0.42
24	2	3	5	BOMAB	back	BA000923154	75	1711	84	83	84	1.00	0.165	40	1.01	40	50	0.79	1.01	1637	6.19	264	450	0.59	304	500	0.61	-0.39
26	2	4	9	PMMA	back	BA00098366R	54	1898	68	67	68	1.00	0.165	19	1.00	19	40	0.47	1.01	1845	6.19	298	330	0.90	317	370	0.86	-0.14
35	3	3	4	BOMAB	back	BA00098318S	44	1004	52	49	51	1.00	0.165	25	1.01	25	30	0.83	1.01	960	6.19	155	266	0.58	180	296	0.61	-0.39
39	3	4	7	BOMAB	back	BA00097925M	33	737	41	39	40	1.00	0.165	21	1.00	21	24	0.89	1.01	704	6.19	114	192	0.59	135	216	0.63	-0.37
44	3	2	1	PMMA	back	BA00114014P	63	1553	71	70	71	1.00	0.165	31	1.01	31	47	0.65	1.01	1491	6.19	241	461	0.52	271	508	0.53	-0.47
1	1	2	1	Tree A-D	air	BA00098569H	29	414	34	33	34	1.00	0.165	23	1.00	23	22	1.06	1.01	385	6.19	62	214	0.29	86	236	0.36	-0.64
2	1	2	1	Tree A-D	air	BA00099010D	29	410	33	31	32	1.00	0.165	22	1.00	22	22	0.99	1.01	381	6.19	61	214	0.29	83	236	0.35	-0.65
3	1	2	2	Tree A-D	air	BA00097638L	29	381	32	31	32	1.00	0.165	22	1.00	22	22	1.01	1.01	352	6.19	57	205	0.28	79	227	0.35	-0.65
4	1	2	2	Tree A-D	air	BA00130036J	30	379	32	32	32	1.00	0.165	23	1.00	23	22	1.04	1.01	349	6.19	56	205	0.28	79	227	0.35	-0.65
17	2	2	1	Tree A-D	air	BA00129695W	121	1482	124	122	123	1.00	0.165	87	1.02	85	78	1.09	1.02	1363	6.19	220	764	0.29	306	842	0.36	-0.64
18	2	2	1	Tree A-D	air	BA00129074C	115	1429	125	124	124	1.00	0.165	89	1.02	88	78	1.12	1.02	1316	6.19	213	764	0.28	300	842	0.36	-0.64
19	2	2	3	Tree A-D	air	BA00098763P	114	1500	128	125	127	1.00	0.165	90	1.02	88	78	1.13	1.02	1388	6.19	224	761	0.29	312	839	0.37	-0.63
20	2	2	3	Tree A-D	air	BA00099789A	129	1575	129	127	128	1.00	0.165	90	1.02	88	78	1.13	1.03	1449	6.19	234	761	0.31	322	839	0.38	-0.62
9	1	2.5	6	Tree A-D	air	BA00097716P	25	437	29	29	29	1.00	0.165	18	1.00	18	17	1.06	1.01	411	6.19	66	159	0.42	85	176	0.48	-0.52
10	1	2.5	6	Tree A-D	air	BA00130514F	26	431	29	29	29	1.00	0.165	18	1.00	18	17	1.07	1.01	405	6.19	65	159	0.41	84	176	0.48	-0.52
11	1	2.5	6	Tree A-D	air	BA000931090	25	423	29	27	28	1.00	0.165	17	1.00	17	17	1.02	1.01	398	6.19	64	159	0.40	82	176	0.46	-0.54
12	1	2.5	6	Tree A-D	air	BA000883423	25	434	28	28	28	1.00	0.165	17	1.00	17	17	1.00	1.01	409	6.19	66	159	0.42	83	176	0.47	-0.53
27	2	2.5	6	Tree A-D	air	BA00111119G	99	1519	107	107	107	1.00	0.165	69	1.01	68	61	1.12	1.02	1421	6.19	230	570	0.40	298	631	0.47	-0.53
28	2	2.5	6	Tree A-D	air	BA00111701L	101	1544	108	108	108	1.00	0.165	69	1.01	68	61	1.12	1.02	1444	6.19	233	570	0.41	302	631	0.48	-0.52
33	3	2.5	6	Tree A-D	air	BA00098209T	62	943	68	66	67	1.00	0.165	43	1.01	43	37	1.16	1.01	882	6.19	142	344	0.41	185	381	0.49	-0.51
42	3	2.5	6	Tree A-D	air	BA00094794O	58	907	66	62	64	1.00	0.165	42	1.01	41	37	1.12	1.01	849	6.19	137	344	0.40	178	381	0.47	-0.53
15	1	4	8	Tree A-H	air	BA00112043Q	17	368	19	18	18	1.00	0.165	9	1.00	9	11	0.80	1.00	352	6.19	57	92	0.62	66	103	0.64	-0.36
16	1	4	8	Tree A-H	air	BA001155475	16	356	19	18	18	1.00	0.165	9	1.00	9	11	0.82	1.00	340	6.19	55	92	0.60	64	103	0.62	-0.38
29	2	4	8	Tree A-H	air	BA00097672T	60	1220	67	64	66	1.00	0.165	35	1.01	35	40	0.86	1.01	1161	6.19	188	329	0.57	222	369	0.60	-0.40
30	2	4	8	Tree A-H	air	BA00097708M	61	1251	66	63	64	1.00	0.165	33	1.01	32	40	0.81	1.01	1191	6.19	192	329	0.58	225	369	0.61	-0.39
31	2	4	8	Tree A-H	air	BA00110981A	58	1226	67	65	66	1.00	0.165	35	1.01	35	40	0.86	1.01	1168	6.19	189	329	0.57	223	369	0.61	-0.39
32	2	4	8	Tree A-H	air	BA00110998V	61	1234	67	67	67	1.00	0.165	36	1.01	36	40	0.89	1.01	1173	6.19	190	329	0.58	225	369	0.61	-0.39
43	3	4	9	Tree A-H	air	BA000884132	34	816	37	38	38	1.00	0.165	17	1.00	17	24	0.69	1.01	782	6.19	126	199	0.64	143	223	0.64	-0.36
46	3	4	9	Tree A-H	air	BA00097796H	35	798	39	36	37	1.00	0.165	17	1.00	17	24	0.71	1.01	763	6.19	123	199	0.62	140	223	0.63	-0.37

Appendix M

Gamma and Neutron Dose Results for FNADs

Calculated from nanoDot® Readings

Table M.1 Gamma Dose Results for FNADs Calculated Using default Calibration Factors

FNAD OSL CALCULATED GAMMA DOSE (OUTER DOSIMETRY PACKAGE)											
FNAD #	Given Gamma dose Dp(10)γ (cGy)	dot1 OSL γ signal (Co-60 cGy)	dot2 OSLN γ + n signal (Co-60 cGy)	dot2 - dot1 OSLN - OSL net neutron signal (Co-60 cGy)	RRF	Gamma calibration factor, Cγ	Neutron influence correction factor, R	Corrected gamma dose reading without supralinearity correction, x	gamma supralinearity correction factor, S_γ	Reported Gamma Dose Dp(10)γ (cGy)	R/G
71	11	14	407	393	1.00	1.00	0.0086	10.2	1.00	10.1	0.92
72	40	55	1429	1375	1.00	1.00	0.0086	42.8	1.01	42.4	1.06
73	24	32	940	908	1.00	1.00	0.0086	24.1	1.00	24.0	1.00

Table M.2 Neutron Dose Results for FNADs Calculated Using default Calibration Factors

FNAD OSLN CALCULATED NEUTRON DOSE (INNER DOSIMETRY PACKAGE)									
FNAD #	Given Neutron dose D*(10)n (cGy)	dot3 OSL γ signal (Co-60 cGy)	(dot4+dot5+dot6)/3 OSLN γ + n signal (Co-60 cGy)	OSLN - OSL net neutron signal (Co-60 cGy)	gamma supralinearity correction factor, S_γ	OSLN - OSL / $(S_\gamma)^{0.8}$	Neutron calibration factor, C_n	Reported Neutron Dose Dp(10)n (cGy)	R/G
71	88	17	1193	1176	1.00	1176	12.89	91.2	1.04
72	313	67	3896	3829	1.01	3830	12.89	297	0.95
73	189	39	2444	2405	1.01	2406	12.89	187	0.99

Appendix N

PNAD Performance

Table N.1 PNAD Performance with Foil Calculated Neutron Dose

Irradiation Data				ANSI/HPS N13.3 $D_p(10)$ Reference Doses			PNAD Performance with foil calculated neutron dose							
PNAD No.	Distance (m)	phantom type	dosimeter location on phantom	Given Gamma dose $D_p(10)_\gamma$ (cGy)	Given Neutron dose $D_p(10)_n$ (cGy)	Given Total dose $D_p(10)$ (cGy)	OSL Gamma Dose (cGy)	OSL Gamma R/G	Foil Neutron Dose (cGy)	Foil Neutron R/G	PNAD γ + n Dose (cGy)	PNAD γ + n R/G	P_i	Pass or Fail
45	2	PMMA	front	47	459	506	55	1.17	534	1.16	589	1.16	0.16	Pass
5	3	BOMAB	front	14	123	137	15	1.07	121	0.99	136	0.99	-0.01	Pass
7	3	BOMAB	front	14	126	140	15	1.05	117	0.93	132	0.94	-0.06	Pass
21	3	BOMAB	front	50	441	491	63	1.25	463	1.05	526	1.07	0.07	Pass
23	3	BOMAB	front	50	450	500	53	1.07	451	1.00	504	1.01	0.01	Pass
34	3	BOMAB	front	30	266	296	37	1.24	272	1.02	309	1.05	0.05	Pass
13	4	PMMA	front	11	89	100	7	0.59	93	1.04	99	0.99	-0.01	Pass
25	4	PMMA	front	40	319	359	29	0.72	348	1.09	377	1.05	0.05	Pass
38	4	BOMAB	front	24	192	216	24	1.02	205	1.07	230	1.06	0.06	Pass
36	3	BOMAB - LAT	side	30	271	301	24	0.80	83	0.30	107	0.35	-0.65	Fail
37	3	BOMAB - LAT	side	30	271	301	33	1.12	270	1.00	304	1.01	0.01	Pass
6	3	BOMAB	back	14	123	137	11	0.77	35	0.29	46	0.34	-0.66	Fail
8	3	BOMAB	back	14	126	140	10	0.73	37	0.29	47	0.34	-0.66	Fail
14	4	PMMA	back	11	92	103	5	0.49	39	0.42	44	0.43	-0.57	Fail
22	3	BOMAB	back	50	441	491	43	0.85	119	0.27	162	0.33	-0.67	Fail
24	3	BOMAB	back	50	450	500	40	0.79	136	0.30	176	0.35	-0.65	Fail
26	4	PMMA	back	40	330	370	19	0.47	148	0.45	167	0.45	-0.55	Fail
35	3	BOMAB	back	30	266	296	25	0.83	75	0.28	99	0.34	-0.66	Fail
39	4	BOMAB	back	24	192	216	21	0.89	60	0.31	81	0.38	-0.62	Fail
44	2	PMMA	back	47	461	508	31	0.65	138	0.30	169	0.33	-0.67	Fail
1	2	Tree A-D	air	22	214	236	23	1.06	196	0.91	219	0.93	-0.07	Pass
2	2	Tree A-D	air	22	214	236	22	0.99	197	0.92	219	0.93	-0.07	Pass
3	2	Tree A-D	air	22	205	227	22	1.01	181	0.88	204	0.90	-0.10	Pass
4	2	Tree A-D	air	22	205	227	23	1.04	200	0.98	223	0.98	-0.02	Pass
17	2	Tree A-D	air	78	764	842	85	1.09	752	0.98	838	1.00	0.00	Pass
18	2	Tree A-D	air	78	764	842	88	1.12	730	0.96	818	0.97	-0.03	Pass
19	2	Tree A-D	air	78	761	839	88	1.13	804	1.06	892	1.06	0.06	Pass
20	2	Tree A-D	air	78	761	839	88	1.13	791	1.04	880	1.05	0.05	Pass
9	2.5	Tree A-D	air	17	159	176	18	1.06	148	0.93	166	0.95	-0.05	Pass
10	2.5	Tree A-D	air	17	159	176	18	1.07	156	0.98	174	0.99	-0.01	Pass
11	2.5	Tree A-D	air	17	159	176	17	1.02	147	0.92	164	0.93	-0.07	Pass
12	2.5	Tree A-D	air	17	159	176	17	1.00	156	0.98	173	0.98	-0.02	Pass
27	2.5	Tree A-D	air	61	570	631	68	1.12	622	1.09	691	1.09	0.09	Pass
28	2.5	Tree A-D	air	61	570	631	68	1.12	613	1.07	681	1.08	0.08	Pass
33	2.5	Tree A-D	air	37	344	381	43	1.16	349	1.01	392	1.03	0.03	Pass
42	2.5	Tree A-D	air	37	344	381	41	1.12	364	1.06	405	1.06	0.06	Pass
15	4	Tree A-H	air	11	92	103	9	0.80	89	0.96	98	0.95	-0.05	Pass
16	4	Tree A-H	air	11	92	103	9	0.82	85	0.93	94	0.92	-0.08	Pass
29	4	Tree A-H	air	40	329	369	35	0.86	319	0.97	353	0.96	-0.04	Pass
30	4	Tree A-H	air	40	329	369	32	0.81	307	0.93	340	0.92	-0.08	Pass
31	4	Tree A-H	air	40	329	369	35	0.86	341	1.04	376	1.02	0.02	Pass
32	4	Tree A-H	air	40	329	369	36	0.89	314	0.95	349	0.95	-0.05	Pass
43	4	Tree A-H	air	24	199	223	17	0.69	182	0.92	199	0.89	-0.11	Pass
46	4	Tree A-H	air	24	199	223	17	0.71	175	0.88	192	0.86	-0.14	Pass

Table N.2 PNAD Performance with InLight® Calculated Neutron Dose

Irradiation Data				ANSI/HPS N13.3 $D_p(10)$ Reference Doses			PNAD Performance with InLight calculated neutron dose (C_n = 6.19)							
PNAD No.	**Distance (m)**	**phantom type**	**dosimeter location on phantom**	**Given Gamma dose $D_p(10)_\gamma$ (cGy)**	**Given Neutron dose $D_p(10)_n$ (cGy)**	**Given Total dose $D_p(10)$ (cGy)**	**OSL Gamma Dose (cGy)**	**OSL Gamma R/G**	**OSLN Neutron Dose (cGy)**	**OSLN Neutron R/G**	**PNAD γ + n Dose (cGy)**	**PNAD γ + n R/G**	**P_i**	**Pass or Fail**
45	2	PMMA	front	47	459	506	55	1.17	373	0.81	428	0.85	-0.15	Pass
5	3	BOMAB	front	14	123	137	15	1.07	123	1.00	138	1.00	0.00	Pass
7	3	BOMAB	front	14	126	140	15	1.05	118	0.94	133	0.95	-0.05	Pass
21	3	BOMAB	front	50	441	491	63	1.25	416	0.94	479	0.98	-0.02	Pass
23	3	BOMAB	front	50	450	500	53	1.07	474	1.05	527	1.05	0.05	Pass
34	3	BOMAB	front	30	266	296	37	1.24	265	0.99	302	1.02	0.02	Pass
13	4	PMMA	front	11	89	100	7	0.59	109	1.22	115	1.15	0.15	Pass
25	4	PMMA	front	40	319	359	29	0.72	346	1.08	374	1.04	0.04	Pass
38	4	BOMAB	front	24	192	216	24	1.02	252	1.31	276	1.28	0.28	Fail
36	3	BOMAB - LAT	side	30	271	301	24	0.80	165	0.61	189	0.63	-0.37	Fail
37	3	BOMAB - LAT	side	30	271	301	33	1.12	256	0.95	290	0.96	-0.04	Pass
6	3	BOMAB	back	14	123	137	11	0.77	71	0.58	82	0.60	-0.40	Fail
8	3	BOMAB	back	14	126	140	10	0.73	89	0.70	99	0.71	-0.29	Fail
14	4	PMMA	back	11	92	103	5	0.49	87	0.95	92	0.90	-0.10	Pass
22	3	BOMAB	back	50	441	491	43	0.85	241	0.55	283	0.58	-0.42	Fail
24	3	BOMAB	back	50	450	500	40	0.79	264	0.59	304	0.61	-0.39	Fail
26	4	PMMA	back	40	330	370	19	0.47	298	0.90	317	0.86	-0.14	Pass
35	3	BOMAB	back	30	266	296	25	0.83	155	0.58	180	0.61	-0.39	Fail
39	4	BOMAB	back	24	192	216	21	0.89	114	0.59	135	0.63	-0.37	Fail
44	2	PMMA	back	47	461	508	31	0.65	241	0.52	271	0.53	-0.47	Fail
1	2	Tree A-D	air	22	214	236	23	1.06	62	0.29	86	0.36	-0.64	Fail
2	2	Tree A-D	air	22	214	236	22	0.99	61	0.29	83	0.35	-0.65	Fail
3	2	Tree A-D	air	22	205	227	22	1.01	57	0.28	79	0.35	-0.65	Fail
4	2	Tree A-D	air	22	205	227	23	1.04	56	0.28	79	0.35	-0.65	Fail
17	2	Tree A-D	air	78	764	842	85	1.09	220	0.29	306	0.36	-0.64	Fail
18	2	Tree A-D	air	78	764	842	88	1.12	213	0.28	300	0.36	-0.64	Fail
19	2	Tree A-D	air	78	761	839	88	1.13	224	0.29	312	0.37	-0.63	Fail
20	2	Tree A-D	air	78	761	839	88	1.13	234	0.31	322	0.38	-0.62	Fail
9	2.5	Tree A-D	air	17	159	176	18	1.06	66	0.42	85	0.48	-0.52	Fail
10	2.5	Tree A-D	air	17	159	176	18	1.07	65	0.41	84	0.48	-0.52	Fail
11	2.5	Tree A-D	air	17	159	176	17	1.02	64	0.40	82	0.46	-0.54	Fail
12	2.5	Tree A-D	air	17	159	176	17	1.00	66	0.42	83	0.47	-0.53	Fail
27	2.5	Tree A-D	air	61	570	631	68	1.12	230	0.40	298	0.47	-0.53	Fail
28	2.5	Tree A-D	air	61	570	631	68	1.12	233	0.41	302	0.48	-0.52	Fail
33	2.5	Tree A-D	air	37	344	381	43	1.16	142	0.41	185	0.49	-0.51	Fail
42	2.5	Tree A-D	air	37	344	381	41	1.12	137	0.40	178	0.47	-0.53	Fail
15	4	Tree A-H	air	11	92	103	9	0.80	57	0.62	66	0.64	-0.36	Fail
16	4	Tree A-H	air	11	92	103	9	0.82	55	0.60	64	0.62	-0.38	Fail
29	4	Tree A-H	air	40	329	369	35	0.86	188	0.57	222	0.60	-0.40	Fail
30	4	Tree A-H	air	40	329	369	32	0.81	192	0.58	225	0.61	-0.39	Fail
31	4	Tree A-H	air	40	329	369	35	0.86	189	0.57	223	0.61	-0.39	Fail
32	4	Tree A-H	air	40	329	369	36	0.89	190	0.58	225	0.61	-0.39	Fail
43	4	Tree A-H	air	24	199	223	17	0.69	126	0.64	143	0.64	-0.36	Fail
46	4	Tree A-H	air	24	199	223	17	0.71	123	0.62	140	0.63	-0.37	Fail

Appendix O

FNAD Performance

Table O.1 FNAD Performance with Foil Calculated Neutron Dose

Irradiation Data					ANSI/HPS N13.3 D*(10) Reference Doses			FNAD Performance with foil calculated neutron dose (C_γ = 1.00)							
FNAD No.	Pulse No.	Distance (m)	Location No.	Given Neutron Fluence (n/cm^2)	Given Gamma dose $D^*(10)_\gamma$ (cGy)	Given Neutron dose $D^*(10)_n$ (cGy)	Given Total dose D*(10) (cGy)	OSL Gamma Dose (cGy)	OSL Gamma R/G	Foil Neutron Dose (cGy)	Foil Neutron R/G	FNAD γ + n Dose (cGy)	FNAD γ + n R/G	P_i	Pass or Fail
71	1	4	11	5.30E+10	11	88	99	10	0.92	87	0.99	97	0.98	-0.02	Pass
72	2	4	11	1.89E+11	40	313	353	42	1.06	320	1.02	362	1.03	0.03	Pass
73	3	4	11	1.14E+11	24	189	213	24	1.00	186	0.99	210	0.99	-0.01	Pass

Table O.2 FNAD Performance with OSLN Calculated Neutron Dose Using Default Calibration Factors

Irradiation Data					ANSI/HPS N13.3 D*(10) Reference Doses			FNAD Performance with OSLN calculated neutron dose (C_γ = 1.00, C_n = 12.89)							
FNAD No.	Pulse No.	Distance (m)	Location No.	Given Neutron Fluence (n/cm^2)	Given Gamma dose $D^*(10)_\gamma$ (cGy)	Given Neutron dose $D^*(10)_n$ (cGy)	Given Total dose D*(10) (cGy)	OSL Gamma Dose (cGy)	OSL Gamma R/G	OSLN Neutron Dose (cGy)	OSLN Neutron R/G	PNAD γ + n Dose (cGy)	PNAD γ + n R/G	P_i	Pass or Fail
71	1	4	11	5.30E+10	11	88	99	10	0.92	91.2	1.04	101	1.03	0.03	Pass
72	2	4	11	1.89E+11	40	313	353	42	1.06	297	0.95	340	0.96	-0.04	Pass
73	3	4	11	1.14E+11	24	189	213	24	1.00	187	0.99	211	0.99	-0.01	Pass

This page intentionally left blank

Pacific Northwest
NATIONAL LABORATORY

Proudly Operated by **Battelle** *Since 1965*

902 Battelle Boulevard
P.O. Box 999
Richland, WA 99352
1-888-375-PNNL (7665)

U.S. DEPARTMENT OF
ENERGY